TECHNICAL REPORT STANDARD PAGE

1. Report No. **FHWA/LA.10/470**	2. Government Accession No.	3. Recipient's Catalog No.
4. Title and Subtitle **Calibration of Resistance Factors Needed in the LRFD Design of Drilled Shafts**	5. Report Date **September 2010** 6. Performing Organization Code	
7. Author(s) **Murad Y. Abu-Farsakh, Xinbao Yu, Sungmin Yoon, and Ching Tsai**	8. Performing Organization Report No. **470**	
9. Performing Organization Name and Address **Louisiana Transportation Research Center** **4101 Gourrier Avenue** **Baton Rouge, LA 70808**	10. Work Unit No. 11. Contract or Grant No. **LTRC Number: 07-2GT** **State Project Number: 736-99-1408**	
12. Sponsoring Agency Name and Address **Louisiana Transportation Research Center** **4101 Gourrier Avenue** **Baton Rouge, LA 70808**	13. Type of Report and Period Covered **Final Report** **November 2006–August 2010** 14. Sponsoring Agency Code	

15. Supplementary Notes
Conducted in Cooperation with the U.S. Department of Transportation, Federal Highway Administration

16. Abstract

The first report on Load and Resistance Factor Design (LRFD) calibration of driven piles in Louisiana (LTRC Final Report 449) was completed in May 2009. As a continuing effort to implement the LRFD design methodology for deep foundations in Louisiana, this report will present the reliability based analyses for the calibration of the resistance factor for LRFD design of axially loaded drilled shafts. A total of 16 cases of drilled shaft load tests were available to authors from Louisiana Department of Transportation and Development (LADOTD) archives. Out of those, only 11 met the Federal Highway Administration (FHWA) "5%B" settlement criterion. Due to the limited number of available drilled shaft cases in Louisiana, additional drilled shaft cases were collected from state of Mississippi that has subsurface soil conditions similar to Louisiana soils. A total of 15 drilled shafts from Mississippi were finally selected from 50 available cases, based on selection criteria of subsurface soil conditions and final settlement. As a result, a database of 26 drilled shaft tests representing the typical design practice in Louisiana was created for statistical reliability analyses. The predictions of total, side, and tip resistance versus settlement behavior of drilled shafts were established from soil borings using the FHWA O'Neill and Reese design method via the SHAFT computer program. The measured drilled shaft axial nominal resistance was determined from either the Osterberg cell (O-cell) test or the conventional top-down static load test. For the 22 drilled shafts that were tested using O-cells, the tip and side resistances were deduced separately from test results. Statistical analyses were performed to compare the predicted total, tip, and side drilled shaft nominal axial resistance with the corresponding measured nominal resistance. Results of this showed that the selected FHWA design method significantly underestimates measured drilled shaft resistance. The Monte Carlo simulation method was selected to perform the LRFD calibration of resistance factors of drilled shaft under strength I limit state. The total resistance factors obtained at different reliability index (β) were determined and compared with those available in literature. Results of reliability analysis, corresponding to a target reliability index (β) of 3.0, reveals resistance factors for side (ϕ_{side}), tip (ϕ_{tip}), and total resistance factor (ϕ_{total}) are 0.20, 0.75, and 0.5, respectively.

17. Key Words	18. Distribution Statement
LRFD, Reliability Analysis, Drilled shafts, O'Neill and Reese method, O-cell test, top-down static load test.	**Unrestricted. This document is available through the National Technical Information Service, Springfield, VA 21161.**

19. Security Classif. (of this report)	20. Security Classif. (of this page)	21. No. of Pages	22. Price
Unclassified	**Unclassified**	**110**	

Project Review Committee

Each research project will have an advisory committee appointed by the LTRC Director. The Project Review Committee is responsible for assisting the LTRC Administrator or Manager in the development of acceptable research problem statements, requests for proposals, review of research proposals, oversight of approved research projects, and implementation of findings.

The dedication and work effort of the following Project Review Committee members to guide this research study to fruition are acknowledged and appreciated.

LTRC Administrator

Zhongjie "Doc" Zhang, Ph.D., P.E.
Pavement and Geotechnical Research Administrator

Members

Kim Garlington, DOTD
Arthur D'Andrea, DOTD
Jenny Fu, DOTD
Arturo Aguirre, FHWA
Gavin Gautreau, LTRC

Directorate Implementation Sponsor

Richard Savoie, DOTD Chief Engineer

Calibration of Resistance Factors Needed in the LRFD Design of Drilled Shafts

by

Murad Y. Abu-Farsakh, Ph.D., P.E.
Xinbao Yu, Ph.D.
Sungmin Yoon, Ph. D., P.E.
Ching Tsai, Ph.D., P.E.

Louisiana Transportation Research Center
4101 Gourrier Avenue
Baton Rouge, LA 70808

LTRC Project No. 07-2GT
State Project No. 736-99-1408

conducted for

Louisiana Department of Transportation and Development
Louisiana Transportation Research Center

September 2010

ABSTRACT

The first report on Load and Resistance Factor Design (LRFD) calibration of driven piles in Louisiana (LTRC Final Report 449) was completed in May 2009. As a continuing effort to implement the LRFD design methodology for deep foundations in Louisiana, this report will present the reliability based analyses for the calibration of the resistance factor for LRFD design of axially loaded drilled shafts. A total of 16 cases of drilled shaft load tests were available to authors from Louisiana Department of Transportation and Development (LADOTD) archives. Out of those, only 11 met the Federal Highway Administration (FHWA) "5%B" settlement criterion. Due to the limited number of available drilled shaft cases in Louisiana, additional drilled shaft cases were collected from state of Mississippi that has subsurface soil conditions similar to Louisiana soils. A total of 15 drilled shafts from Mississippi were finally selected from 50 available cases, based on selection criteria of subsurface soil conditions and final settlement. As a result, a database of 26 drilled shaft tests representing the typical design practice in Louisiana was created for statistical reliability analyses. The predictions of total, side, and tip resistance versus settlement behavior of drilled shafts were established from soil borings using the FHWA O'Neill and Reese design method via the SHAFT computer program. The measured drilled shaft axial nominal resistance was determined from either the Osterberg cell (O-cell) test or the conventional top-down static load test. For the 22 drilled shafts that were tested using O-cells, the tip and side resistances were deduced separately from test results. Statistical analyses were performed to compare the predicted total, tip, and side drilled shaft nominal axial resistance with the corresponding measured nominal resistance. Results of this showed that the selected FHWA design method significantly underestimates measured drilled shaft resistance. The Monte Carlo simulation method was selected to perform the LRFD calibration of resistance factors of drilled shaft under strength I limit state. The total resistance factors obtained at different reliability index (β) were determined and compared with those available in literature. Results of reliability analysis, corresponding to a target reliability index (β) of 3.0, reveals resistance factors for side (ϕ_{side}), tip (ϕ_{tip}), and total resistance factor (ϕ_{total}) are 0.20, 0.75, and 0.5, respectively.

ACKNOWLEDGMENTS

This research project was funded by the LADOTD (State Project No. 736-99-1408) and Louisiana Transportation Research Center (LTRC Project No. 07-2GT). Sean Ferguson with Mississippi Department of Transportation contributed the Mississippi drilled shaft load test database. The comments and suggestions of Mark Morvant and Zhongjie Zhang of LTRC are gratefully acknowledged.

IMPLEMENTATION STATEMENT

The Federal Highway Administration and American Association of Highway Transportation Officials (AASHTO) set a transition date of October 1, 2007, after which all new federal-funded bridges shall be designed using LRFD design methodology to ensure a consistent level of reliability in design of both substructure and superstructure. Researchers understand that the current AASHTO specifications recommended resistance factors for use in the design of drilled shaft foundation, which is somewhat conservative for Louisiana soils, thereby increasing the cost of deep foundations. In order to secure federal funds and to provide an efficient and consistent design, it becomes necessary to calibrate the resistance factors for drilled shaft design using the local drilled shaft tests and soil databases. Therefore this research study focused on LRFD calibration of resistance factors for O'Neill and Reese design method commonly used by LADOTD engineers based on a local database. The resistance factors based on a reliability index of 3.0 recommended in this study will be available for immediate implementation of the LRFD methodology in the design of all future drilled shaft foundations. In addition, the calibration effort in this study is documented; therefore the calibration process becomes a heritage for LADOTD users and thereby enhances future LRFD research and development. As experience is gained in the application of LRFD to design, the role of past Allowable Stress Design (ASD) practice will become less important; all the advantages of the LRFD design described in the problem statement can be fully addressed. Based on this research, the reliability indices and resistance factors for the O'Neill and Reese design method used in LADOTD is recommended. These recommendations are expected to be used in the design of future state projects involved drilled shafts.

This project is a continuation of the previous project entitled "Calibration of Resistance Factors Needed in the LRFD Design of Driven Piles" *[1]*. This project will complete the effort of implementing the LRFD design for deep foundations in Louisiana.

TABLE OF CONTENTS

LIST OF TABLES

LIST OF FIGURES

INTRODUCTION

LRFD has been used increasingly and become mandatory for design of all bridge projects funded by FHWA. Compared to the ASD method, LRFD can achieve a compatible reliability between the bridge superstructure and substructure. The uncertainty of load and resistance are quantified separately and reasonably incorporated into the design process. Therefore, this reliability-based design approach will generally produce a more efficient and consistent design than the traditional ASD factor of safety approach *[2]*. To achieve these goals, many researchers have been working to develop a reasonable way to implement the LRFD method in bridge substructure design and to determine appropriate resistance factors for different regional soil conditions *[3, 4, 5, 6, 7, 8, 9,* and *10]*.

Although the AASHTO LRFD specifications were approved for use in 1994, the implementation of these specifications for bridge design has been slow *[11, 12]*. The resistance factors (ϕ) proposed in the AASHTO specifications were derived from ASD safety factors to maintain a consistent level of reliability with past practice. As a result, little improvement has been made toward a more efficient design. One outstanding problem with the resistance factor calibration is the lack of good database *[4*, *13]*. Even in the latest edition of the AASHTO specifications, a significant number of resistance factors in the foundation design were still selected based on the calibration with ASD *[14]*. Several research efforts have been carried out to calibrate the resistance factors for drilled shafts from case histories available nationally and locally *[4, 12, 13*, and *15]*.

Paikowsky et al. calibrated resistance factors for drilled shafts based on a database developed by the University of Florida, the FHWA, and O'Neill et al. *[4, 16]*. Resistance factors for total nominal resistance and side resistance were calibrated for drilled shafts in different types of soils considering the effect of construction methods. To reflect the change of load factors and design method in the AASHTO LRFD specifications, Allen recalibrated resistance factors for drilled shafts based on the databases in the previous literature by fitting to ASD as well as using the Monte Carlo method *[4, 15, 17, 18* and *19]*. Yang et al. calibrated resistance factors for side resistance estimated by the O'Neill and Reese method based on 19 Osterberg cell (O-cell) test data in Kansas, Colorado, and Missouri *[17, 20]*. Based on the top-down test data of drilled shaft collected in the NCHRP Project 24-17, Liang and Li calibrated resistance factors of drilled shafts designed using the O'Neill and Reese method via the Monte Carlo approach *[13, 17]*.

The use of single drilled shafts to support individual columns in bridges and buildings is widely practiced. When superstructures are sensitive to foundation movements, the

settlement of a drill shaft is important to the normal operation of supported superstructures. According to the FHWA drilled shaft design method, the nominal resistance of drilled shafts is defined as the load carried by the shaft at the head displacement equal to 5 percent of the shaft diameter, if the shaft has not plunged prior to this displacement *[17, 21]*.

Currently, AASHTO specifications recommend using total resistance factors (ϕ_t) for single drilled shafts in an axial compression range from 0.40 to 0.60 at the reliability index (β) of 3.0 depending on different soil conditions *[14]*. The recommended resistance factors, however, were calibrated based on a drilled shaft database that was collected from various sites and does not necessarily reflect the local soil condition or local design practice of individual states. As a result, the resistance factors recommended by the existing AASHTO LRFD design code should be verified and recalibrated to account for local soil conditions and design practice in Louisiana.

OBJECTIVE

The main objective of this study was to calibrate the resistance factors (ϕ_{total}, ϕ_{side}, and ϕ_{tip}) of axially loaded drilled shafts installed in Louisiana soils at strength I limit state based on the available drilled shaft load test database collected from Louisiana and Mississippi Departments of Transportation (DOTs) and LADOTD design experience. The findings of this research effort will help Louisiana geotechnical engineers implement the LRFD design methodology for the design of all drilled shafts in future Louisiana projects as mandated by AASHTO.

SCOPE

To reach the objectives of this study, 66 drilled shaft cases with different lengths and diameters that were tested using the Osterberg cell (O-cell) method or conventional top-down static load test were collected from LADOTD and Mississippi DOTs. Out of those, 26 drilled shaft tests were finally selected based on specific screening criterion; among those cases, 22 drilled shafts were tested using O-cells and 4 drilled shafts were tested using the conventional top-down static load test. The SHAFT program was used to predict the load settlement curves of drilled shaft from soil borings. Statistical analyses were conducted on the collected data to evaluate the O'Neill and Reese (FHWA) design method. A target reliability index of 3.0 was selected. Based on the collected database, LRFD calibration of drilled shaft was performed to determine resistance factors (tip, side, and total) using the Monte Carlo simulation method.

METHODOLOGY

As discussed earlier, the main objective of this research study was to calibrate the resistance factors for FHWA design method needed in the LRFD design of drilled shafts based on Louisiana database and experience. Background information on current drilled shaft design methodology and LRFD calibration are introduced first. Then, a total of 26 drilled shaft load tests and their corresponding soil borings were identified and collected from LADOTD and MSDOT files. The collected drilled shaft load test data and soil properties were compiled and analyzed. The methodology of collecting, compiling, and analyzing the drilled shaft load test database is presented in this section.

Background

Prediction of Ultimate Resistance of Drilled Shafts

The ultimate axial resistance (Q_u) of a drilled shaft consists of the end-bearing resistance (Q_b) and the skin frictional resistance (Q_s). The ultimate drilled shaft resistance can then be calculated using the following equation

$$Q_u = Q_b + Q_s = q_b.A_b + \sum_{i=1}^{n} f_i A_{si} \quad (1)$$

where, q_b is the unit tip bearing resistance, A_b is the cross-section area of the drilled shaft base, f_i is the average unit skin friction of the soil layer i, A_{si} is the area of the drilled shaft interfacing with layer i, and n is the number of soil layers along the drilled shaft.

In this research, the load-settlement behavior and ultimate drilled shaft resistance were determined according to FHWA suggestions based on the O'Neill and Reese method *[17]*.

Skin Friction in Cohesive Soil. The skin friction for drilled shafts is calculated based on the static α-method as described by O'Neill and Reese [*16*]. The undrained shear strength, S_u, is used in the following equation to compute the ultimate load transfer in skin friction (f_{sz}) at any given depth (z) below the ground surface:

$$f_{sz} = \alpha_z S_{uz} \quad (2)$$

where, α_z is shear strength reduction factor at depth z, S_{uz} is the undrained shear strength at depth z, and f_{sz} is then used to calculate the total load Q_s in skin friction as:

$$Q_s = \int_0^L f_{sz} dA \quad (3)$$

where, dA is the differential area of the perimeter along the sides of the drilled shaft over the penetration depth, and L is the penetration of the drilled shaft below ground surface.
The α-value used in the equations is shown in Table 1.

Table 1
α-value used to determine side resistance [*14*]

Location along drilled shaft	α-value	Value of S_{uz}/P_a*
From ground surface to depth of 1.5 m (5 ft)	0	—
Bottom one diameter or one shaft diameter above the bell (if any)	0	—
All others	0.55	$S_{uz}/P_a \leq 1.5$
	$0.55 - 0.1\ (S_{uz}/P_a - 1.5)$	$1.5 \leq S_{uz}/P_a \leq 2.5$

*P_a: atmospheric pressure
S_{uz}: undrained shear strength at depth z

End Bearing in Cohesive Soil. Load transfer in end bearing is computed by the following equation, which was developed by O'Neill and Reese and other investigators, and has proven to be fairly effective *[17]*.

$$q_b = N_c S_{ub},\ S_{ub} \leq 0.25\ \text{MPa}\ (2.6\ \text{tsf}) \tag{4}$$

where,

$$N_c = 1.33\,(\ln I_r + 1) \tag{5}$$

In equations (4) and (5), S_{ub} is the average undrained shear strength of the clay between the base and a depth of 2B below base, and I_r is the rigidity index of the soil, which is expressed by the following equation:

$$I_r = \frac{E_s}{3S_{ub}} \tag{6}$$

where, E_s is the Young's modulus of the soil.

If the average undrained shear strength (S_{ub}) is higher than 96 kPa (1 tsf), N_c of 9 can be assumed with sufficient accuracy *[17]*. If L is less than 3B, the following equation for q_b is recommended for use *[17]*.

$$q_b = 0.667\,(1 + 0.1667\,(L/B))\,N_c S_{ub} \tag{7}$$

Skin Friction in Cohesionless Soil. In cohesionless soil, the β-method is usually used to compute the ultimate unit side resistance, f_{sz}, at depth z as follows *[17]*:

$$f_{SZ} = \beta\,\sigma'_z \le 190 \text{ kPa (2.0 tsf)} \tag{8}$$

$$Q_s = \int_0^L \beta\,\sigma'_z\,dA \tag{9}$$

$$\beta = 1.5 - 0.135\,z^{0.5} \tag{10}$$

$$f_{SZ} = \text{constant for } z \ge 18.3 \text{ m (60 ft)} \tag{11}$$

where, σ'_z is the vertical effective stress in soil at depth z, and z is depth below the ground surface.

In cases where the interface friction angle (δ) between concrete and soil is known, the above equations are exchanged as follows:

$$f_{SZ} = K\,\sigma'_z \tan\delta \tag{12}$$

$$Q_s = \int_0^L K\,\sigma'_z \tan\delta\,dA \tag{13}$$

where, K is the parameter that combines the lateral pressure coefficient and a correlation factor.

End Bearing in Cohesionless Soil. The value of q_b in cohesionless soil is based on the N_{SPT} (uncorrected SPT N value) value that is defined by the average blow count from standard penetration tests (SPT) in the zone between the base and a depth of 2B.

If N_{SPT} is less than 50 blows/0.3 m (50 blows/ft.), the following equations can be used to calculate q_b *[17]*:

$$q_b = 0.0575\,N_{SPT} \text{ (MPa)} \tag{14}$$

$$q_b = 0.60\,N_{SPT} \text{ (tsf)} \tag{15}$$

when N_{SPT} is greater than 50 blows/0.3 m (50 blows/ft.), q_b can be calculated using the method for cohesionless intermediate geomaterial (IGM) described later in this section.

Skin Friction in Cohesionless IGM. In cohesionless IGM, the load transfer in skin friction can be estimated using the friction theory as follows *[17]*:

$$f_{SZ} = \sigma'_z K_{oz} \tan\phi_z \tag{16}$$

where, K_{oz} is the earth pressure coefficient at rest at depth z, and ϕ_z is the internal friction angle at depth z.

End Bearing in Cohesionless IGM. If N_{SPT} exceeds 50 blows/0.3 m (50 blows/ft.), the soils can be classified as cohesionless IGM and q_b can be calculated using following equation:

$$q_b = 0.59 \left(N_{60} \frac{p_a}{\sigma'_z} \right)^{0.8} \sigma'_z \tag{17}$$

where, N_{60} is the average corrected SPT blow count between the base of the drilled shaft and 2B below the base for the condition in which 60 percent of the potential energy of the hammer is transferred to the top of the drive string, and p_a is the atmospheric pressure.

Prediction of Load-Settlement Behavior of Drilled Shaft

The load-settlement behavior of a drilled shaft under short-term compression loading can be calculated using the normalized relations proposed by O'Neill and Reese *[17]*. The normalized average trend curves for cohesive and cohesionless soils are shown in Figure 1. The side friction resistance (R_s) developed for each layer i at a specific settlement can be calculated using the ratio of the average deflection along the sides of a drilled shaft (w_s) to the shaft diameter (B). The average deflection along the side of a drilled shaft can be calculated using the following equation:

$$w_s = w_T - \delta_s/2 \tag{18}$$

where, δ_s is the approximate elastic compression of the drilled shaft, and w_T is the estimated deflection of the head of the drilled shaft.

The developed side friction resistance (R_s) can be obtained from the vertical axis of Figure 1 (a) and (c) for cohesive soils and cohesionless soils, respectively.

The same procedure can be applied to calculate the base resistance developed at a specific settlement. The deflection at the base of a drilled shaft (w_b) can be computed using:

$$w_b = w_T - \delta_s \tag{19}$$

Using the ratio of the deflection at the base to the base diameter (w_b/B_b), the developed base resistance (R_B) can be calculated from the vertical axis of Figure 1 (b) and (d) for cohesive soils and cohesionless soils, respectively.

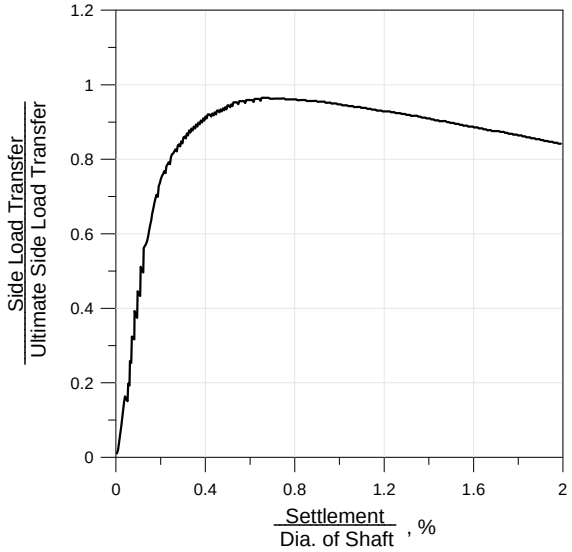

(a) Side load transfer in cohesive soil

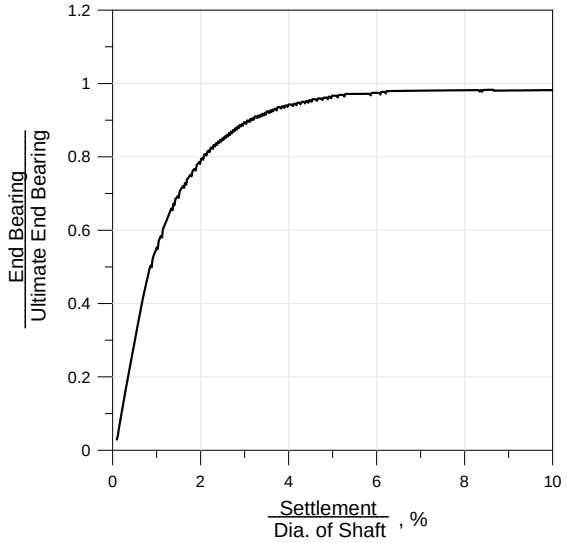

(b) Base load transfer in cohesive soil

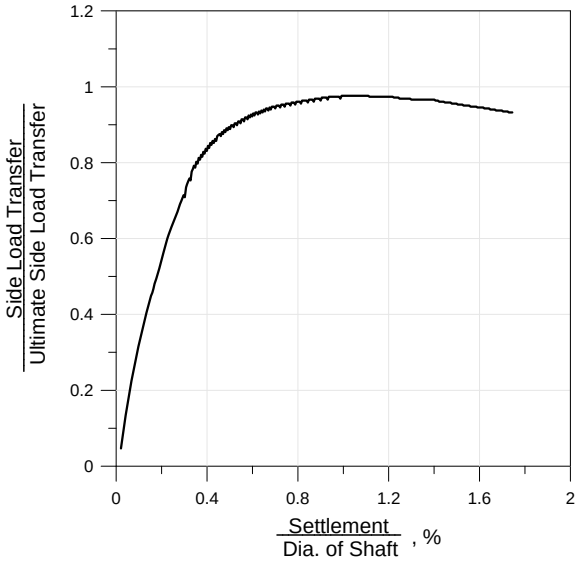

(c) Side load transfer in cohesionless soil

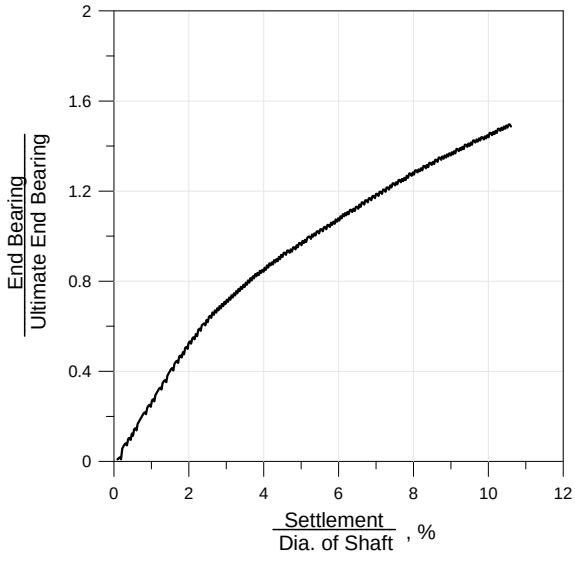

(d) Base load transfer in cohesionless soil

Figure 1
Normalized load transfer representing the average trend value for drilled shaft (after O'Neill and Reese *[17]*)

The developed load (Q_T) at a specific settlement can then be calculated as follows:

$$Q_T = R_B \text{ (developed)} + R_s \text{ (developed)} \quad (20)$$

In this study, the load-settlement behavior was calculated using the program SHAFT 5.0, which is commercially available. An example of a predicted load-settlement curve is shown in Figure 2 *[22]*.

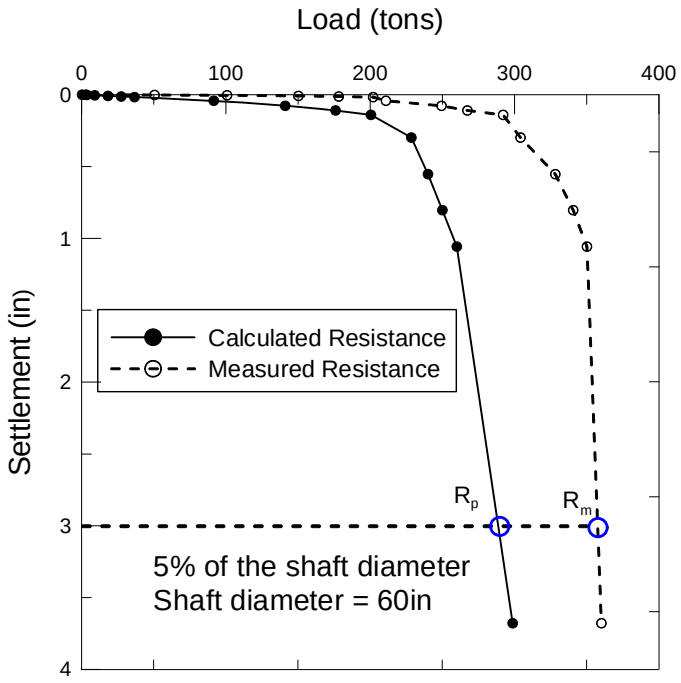

Figure 2
Example of load-settlement analysis and measured value

Measured Load-Settlement Behavior of Drilled Shafts

The O-cell test has been widely used in the United States to determine resistance of drilled shafts. Unlike the conventional top-down load test, the load in an O-cell test is applied at the bottom or near the bottom of drilled shafts via a preinstalled hydraulic cell. During an O-cell load test, the shaft above the cell moves upward, and the shaft below the cell moves downward. As a result, both side friction and end bearing can be measured separately from O-cell test as shown in Figure 3. The upward load shown in the figure was the net upward load (the O-cell measured upward load minus buoyant weight of the drilled shaft). An equivalent top-down curve can be constructed from the two component curves to investigate the combined total pile capacity. Construction of the equivalent top-down curve begins by determining the side shear at an arbitrary deflection point on the side shear-deflection curve (the top curve in Figure 3). The shaft is assumed rigid; its top and bottom move together and

have the same movement at this load. Then the end bearing at the same movement can be determined from the downward curve. By adding the side shear to the mobilized end bearing at the chosen displacement, one can determine a single point on the equivalent top-down curve [*23*]. The complete curve can be obtained by repeating this process. Figure 4 shows an example of the construction of an equivalent top-loaded settlement curve from O-cell test results (Figure 3). The solid line in Figure 4 shows the modified top-down curve to include the additional elastic compression of the shaft.

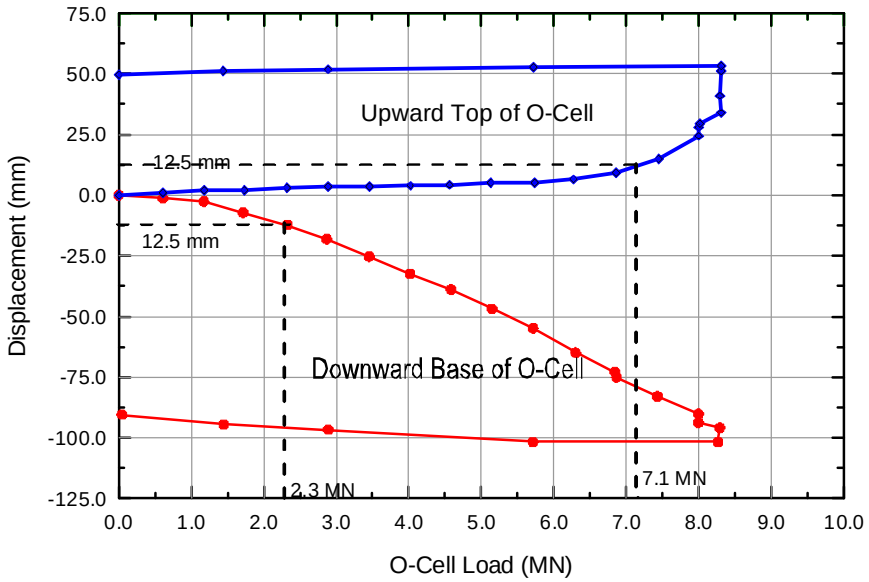

Figure 3
Settlement curves by O-cell

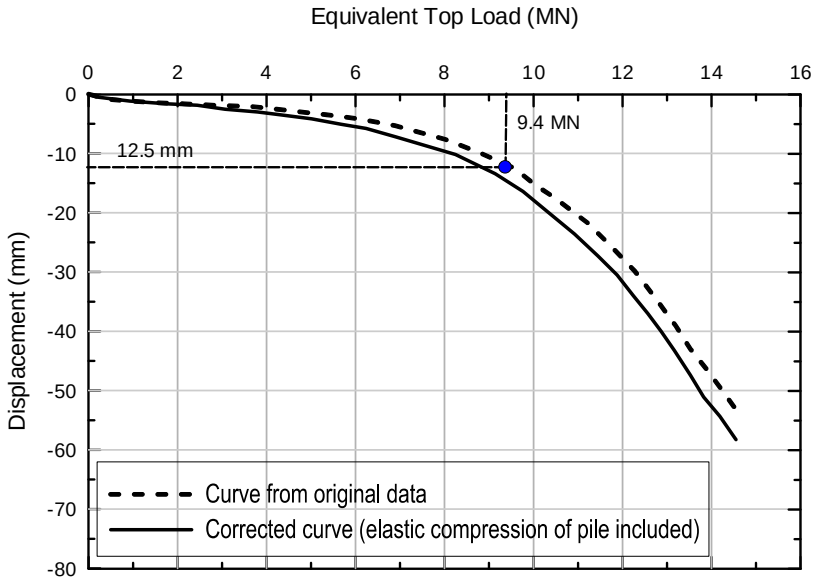

Figure 4
Equivalent top-down settlement curve

According to the comparison study available in literature, the O-cell method has a very close result as the traditional top-down method in terms of measurement of equivalent top-down load-settlement curve [*23*]. Also the number of drilled shafts tested by top-down load tests in this study is small compared to total drilled shaft tests. Therefore, the difference of load test method has a negligible effect on the calibration of resistance factor for drilled shafts.

LRFD Calibration Using Reliability Theory

The basic concept behind LRFD is illustrated in Figures 5 and 6. Here, the distributions of random load (Q) and resistance (R) values are shown as normal distributions. The performance limit state function for the state of the structural system can be described as follows:

$$g(R, Q) = R - Q \tag{21}$$

where, R is the resistance of a given structure, which is a random variable, and Q is the applied load, which is also a random variable.

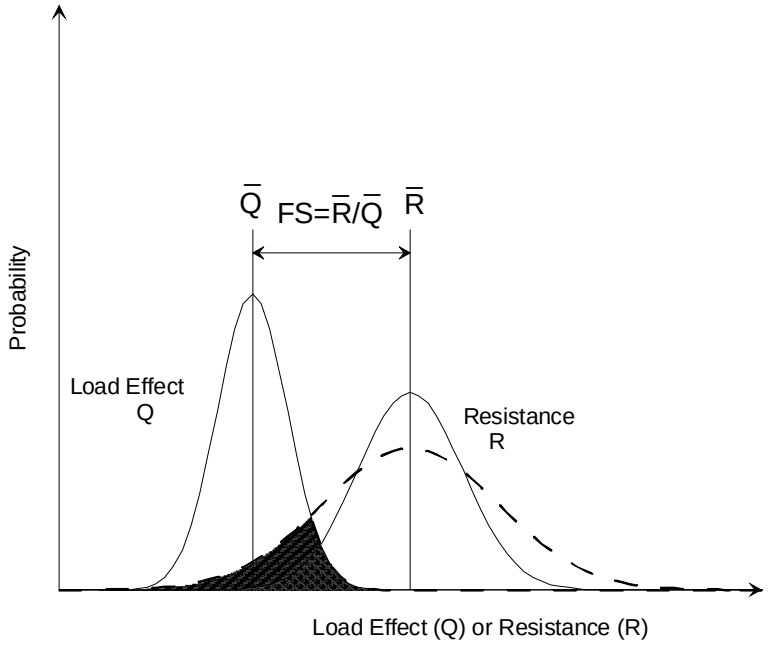

Figure 5
Probability density functions for load effect and resistance

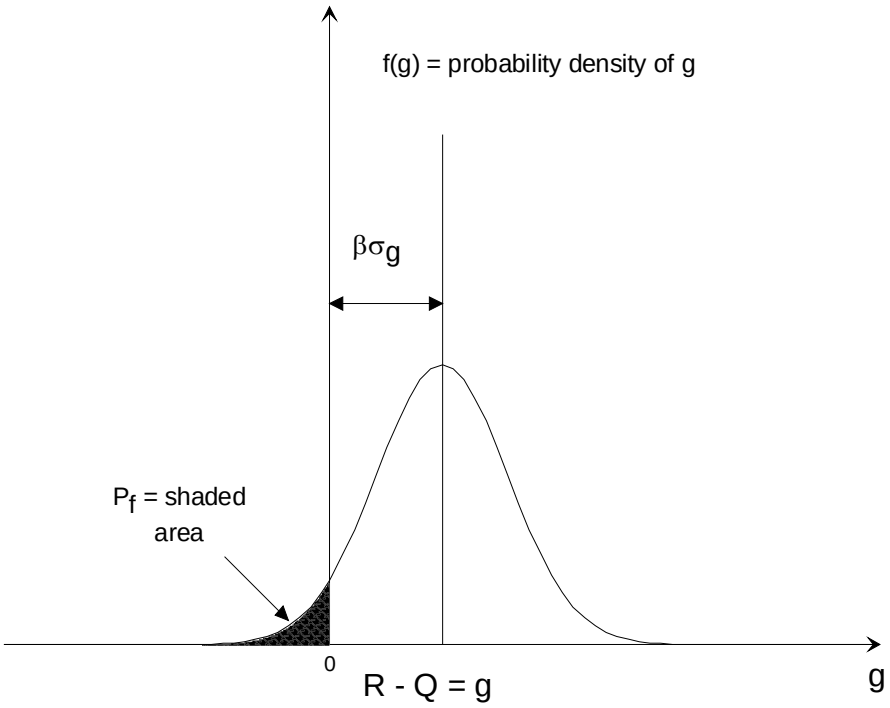

Figure 6
Probability density function of the safety margin *[24]*

The limit state, corresponding to the boundary between desired and undesired performance, would be when g = 0. If $g \geq 0$, the structure is safe (desired performance); if $g < 0$, the structure is unsafe (undesired performance).

The probability of failure is then defined as:

$$p_f = p[g(R,Q) < 0] = p[R < Q] \tag{22}$$

In general terms, if X is a random variable such that $X = (x_1. x_2. x_3 \ldots .x_n)$ with joint probability density function (PDF) $f_x(x)$ and g(x) is a scalar function of input random variable, then $g(x_1. x_2. x_3 \ldots .x_n)$ determines the state of structure such that $g(X) > 0$ means safe domain and $g(X) < 0$ indicates failure domain. Also, there exists a limit state surface at the boundary between the two domains defined as an n-dimensional hyper surface $\{x; g(x) = 0\}$ or the limit state function.

The probability of failure is then given by:

$$P_F = \int_{g(x)_{\leq 0}} f_X(x)dx \tag{23}$$

where, $f_x(x)$ is the probability density function for a random variable X.

Integration is carried out over the failure domain; in other words, the failure probability is the probability of being in the domain of the n-dimensional space bounded by $g(X) \leq 0$.

For a normal distribution of g values, the probability of failure can be equated explicitly to the value of reliability index $\beta = u_g/\sigma_g$, where u_g is the mean value of g and σ_g is the standard deviation of g. The relationship between probability of failure and reliability index can be calculated using the following function.

$$p_f = 1 - NORMSDIST(\beta) \tag{24}$$

Also, if the load and resistance values are normally distributed and the limit state function is linear, then β can be determined from the following relation:

$$\beta = \frac{\mu_R - \mu_Q}{\sqrt{\sigma_R{}^2 + \sigma_Q{}^2}} \tag{25}$$

where, μ_R and μ_Q are the mean and σ_R, and σ_Q are the standard deviation of resistance and load, respectively.

If both the load and resistance distributions are lognormal and the limit state function is a product of random variables, then β can be calculated using a closed-form solution reported by Withiam et al. and Nowak as follows*[10* and *24]*:

$$\beta = \frac{\ln\left[\mu_R / \mu_Q \sqrt{\left(1 + COV_Q^2\right)/\left(1 + COV_R^2\right)}\right]}{\sqrt{\ln\left[\left(1 + COV_Q^2\right)\left(1 + COV_R^2\right)\right]}} \tag{26}$$

where, μ_R is the mean value of the resistance R, and μ_Q is the mean value of the load Q; COV_R and COV_Q are the coefficients of variation for the resistance and load values, respectively.

The limit state function for LRFD design is given below *[14]*:

$$\phi R_n \geq \sum \gamma_i Q_{ni} \tag{27}$$

where, γ_i is the load factor applicable to specific load, Q_{ni} is the specific nominal load, R_n is the nominal resistance available, and ϕ is the resistance factor.

The main objective of LRFD is to calibrate the resistance factor so that equation (27) is always fulfilled for the targeted reliability index (β_t). Thus, combining equations (21) and (27), the limit state function for LRFD is shown as follows:

$$g(R,Q) = \sum \gamma_i Q_n - \sum \phi R_n \tag{28}$$

The term, bias, is referred as the ratio of individual measured values of load or resistance to the predicted value corresponding to that measured value.

Statistical Characterization of the Collected Data

To perform an LRFD calibration, the performance limit state equations must first be determined. The two limit states that are usually checked in the design of piles and drilled shafts are the ultimate limit state (ULS), or strength limit state, and the serviceability limit state (SLS). Both limit states designs are carried out to satisfy the following criteria *[25]*:

ULS: Factored resistance $\geq$ Factored load effects

SLS: Deformation $\leq$ Tolerable deformation to remain serviceable

It is usually considered that the design of deep foundations is controlled by the strength limit state. Therefore, in the following discussion, only the strength I limit state is considered. The following basic equation is recommended to represent limit states design by AASHTO *[14]*:

$$\phi R_n \geq \sum \eta . \gamma_i . Q_i \tag{29}$$

where, ϕ = resistance factor, R_n = nominal resistance, and η = load modifier to account for effects of ductility, redundancy, and operational importance. The value of η usually is taken as 1.00.The value Q_i = load effect, and γ_i =load factor.

It should be noted the calibrated resistance factors are valid only for the ranges of shaft dimensions (length and diameter) employed in this study.

Considering the load combination of dead load and live load for AASHTO Strength I case, the performance limit equation is as follows *[26]*:

$$\phi R_n = \gamma_D Q_D + \gamma_L Q_L \tag{30}$$

where, Q_D and Q_L are the dead load and live load, respectively; γ_D and γ_L are the load factors for dead load and live load, respectively.

The loads applied to the drilled shafts are traditionally based on superstructure analysis; whereas, the actual loads transfer to substructure is not fully researched. Most researchers employ the load statistics and the load factors from AASHTO LRFD specifications, which were originally recommended by Nowak, to make the deep foundation design consistent with the bridge superstructure design *[9]*. For example, Zhang et al., Kim et al., McVay et al., Abu-Farsakh and Titi, and Abu-Farsakh et al. selected the statistical parameters of dead and live loads, which used in the AASHTO LRFD specifications as follow *[1, 26, 27, 28, 29,* and *30]*:

$$\gamma_L = 1.75 \quad \lambda_L = 1.15 \quad COV_L = 0.18$$
$$\gamma_D = 1.25 \quad \lambda_D = 1.08 \quad COV_D = 0.13$$

where, λ_D and λ_L are the load bias factors (mean ratio of measured over predicted value) for the dead load and live load, respectively. COV_D and COV_L are the coefficient of variation values for the dead load and live load, respectively.

The Q_D/Q_L is the dead load to live load ratio, which varies depending on the span length *[31]*. In this research, Q_D/Q_L of 3 is used for calibration since the calibration is insensitive to Q_D/Q_L ratio above 3.

The resistance statistics were calculated in terms of the bias factors. The bias factor is defined as the ratio of the measured shaft resistance over the predicted shaft resistance, i.e.,

$$\lambda_R = \frac{R_m}{R_p} \tag{31}$$

where R_m = measured resistance and R_p = predicted nominal resistance.

Monte Carlo Simulation Method

For more complicated limit state functions, the application of the general statistical method for the calculation of the reliability index is either extremely difficult or impossible. Under this circumstance, Monte Carlo simulation provides the only feasible way to determine the reliability index or the probability of failure. The procedures of Monte Carlo simulation are described in the following paragraphs.

The Monte Carlo method is a technique by which a random number generator is used to extrapolate cumulative density function (CDF) values for each random variable. Extrapolation of CDF makes estimating β possible; otherwise, a limited quantity of data has restricted the reliable estimate of β. Once reliability index, β, is estimated, the probability of failure can be estimated by assuming the distribution of g(x). The steps of Monte Carlo simulation method are as follows:

1. Select a trial resistance factor (ϕ). Generate random numbers for each set of variables. Here there are three variables (resistance and dead load and live load bias factor), so three sets of random variables have to be generated independently for each case. The number of simulation points required is found using relation:

$$N = \frac{1 - P_{true}}{V_p^{\,2} * (P_{true})} \tag{32}$$

where, P_{true} is the lowest magnitude of probability that is to be determined using Monte Carlo simulation, and V_p is the desired coefficient of variation of the simulation result. For estimating probability as low as 10^{-2} and keeping variance under 10 percent, the number of points to be generated in Monte-Carlo simulation is 9900.

For each lognormal variable, sample value x_i is estimated as:

$$x^*_i = \exp(\mu_{lnx} + z_i \sigma_{lnx}) \tag{33}$$

where, $\sigma^2_{\ln x} = \ln(V_x^2 + 1)$ and $\mu_{\ln x} = \ln(\mu_x) - \frac{1}{2}\sigma^2_{\ln x}$

In the above expressions, μ_x and V_x are the arithmetic mean and variance of x; μ_{lnx} and σ_{lnx} are equivalent lognormal mean and standard deviation of ln(x); and z_i = NORMSINV(RAND()) is the random standard normal variable generated using EXCEL function.

2. Define the limit state function [equation (27)].

3. Find the number of cases where $g(x_i) \leq 0$. The probability of failure is then defined as:

$$Pf = \frac{\text{count}(g \leq 0)}{N} \tag{34}$$

and reliability index β is estimated as:

$$\beta = \Phi^{-1}(Pf) \tag{35}$$

4. If the calculated reliability index (β) is different from the selected target reliability index (β_T), the trial resistance factor (ϕ) in step 1 should be changed and iteration needs to be done until $|\beta-\beta_T| <$ tolerance.

Collecting of Drilled Shaft Load Test Database

An extensive search was conducted on LADOTD's archives to collect all available drilled shaft test data in Louisiana. Only 16 drilled shaft test cases were available in LA. Among those, only 11 cases met the FHWA 5%B settlement criterion. Due to the limited number of available cases in Louisiana, performing statistical reliability analysis of drilled shafts based on the available database is not possible. The geotechnical research team at Louisiana Transportation Research Center (LTRC) decided to search for more drilled shaft cases in neighboring states, i.e., Mississippi and Texas. The authors were able to collect 50 drilled shaft cases in MS. Among these 50 cases provided by MSDOT, 26 cases were selected based on initial screening to identify cases with subsurface soil conditions similar to Louisiana soils. However, only 15 of the initial selected cases met the FHWA settlement criterion were included in the database for statistical reliability analysis. The final combined database has 26 cases in total as shown in Table 2 that represents the typical subsurface soils occurring in LA. The geographical locations of drilled shafts for the final selected database are approximately shown in the maps of Figure 7.

The diameter of drilled shafts included in the database ranges from 2 ft. to 6 ft. and length ranges from 35.1 ft. to 138.1ft. All 15 cases collected from MS and 7 cases collected from LA were tested using O-cell; whereas, only 4 cases in LA were tested using conventional top-down load test. The soils encountered in the investigated database include silty clay, clay, sand, clayey sand, and gravel. Most of the soil strata are not homogenous and contain interlayers. Table 2's soil type description is a brief gross approximation/description for the entire pile length/base.

Table 2
Summary of the characteristics of the investigated drilled shafts

I.D.	Location	Diameter B (ft)	Length L (ft)	Soil Type	Load Test Type	Measured resistance* (ton)	Predicted resistance* (ton)
DS01	Caddo, LA	2.5	53.1	Silty clay, sandy silt base	Top-down	1007	485
DS02	Caddo, LA	2.5	35.1	Silty clay, silty sand base	Top-down	784	382
DS03	E. Baton Rouge, LA	3	54.1	Clayey silt, silty clay, silty sand base	O-cell	344	247
DS04	Ouachita, LA	5.5	76.1	Silty sand, sand, silt, silt base	O-cell	1560	1570
DS05	Calcasieu, LA	6	86.9	Stiff clay, silt, stiff clay base	O-cell	1750	1045
DS06	Winn, LA	2.5	23.6	Sand, clay, dense sand base	O-cell	888	521
DS07	Winn, LA	2.5	65.0	Sand, clay, clay base	O-cell	670	390
DS08	E. Baton Rouge, LA	2.5	49.9	Silt, clay, sandy silt base	O-cell	285	325
DS09	Beauregard, LA	5.5	40.7	Clay, silt, silty sand base	O-cell	531	455
DS10	Caddo, LA	3	44.9	Clay, silty clay, clayey sand base	Top-down	405	270
DS11	Caddo, LA	3	62	Clay, silty clay, clayey sand, silty sand base	Top-down	428	418
DS12	Union, MS	4.5	49.9	sand	O-cell	1230	880
DS13	Union, MS	4	73.1	Sand with clay interlayer, sand base	O-cell	1020	900
DS14	Washington, MS	4	123	Silt clay and sand, sand base	O-cell	1515	920

(continued)

I.D.	Location	Diameter B (ft)	Length L (ft)	Soil Type	Load Test Type	Measured resistance* (ton)	Predicted resistance* (ton)
DS15	Washington, MS	4	138.1	Silt clay and sand, sand base	O-cell	1413	490
DS16	Washington, MS	4	119.1	Silt clay and sand, sand base	O-cell	1277	1610
DS17	Washington, MS	5.5	94.1	Sand, gravel base	O-cell	2145	1630
DS18	Washington, MS	4	96.1	Sand, gravel base	O-cell	1082	860
DS19	Washington, MS	4	82	Sand, gravel base	O-cell	1258	1210
DS20	Washington, MS	4	97.1	Sand with clay interlayer, sand base	O-cell	1109	614
DS21	Washington, MS	4	82	Sand, gravel base	O-cell	875	840
DS22	Lee, MS	4	89	Silty clay, sand base	O-cell	2203	2100
DS23	Forrest, MS	6	47.9	Silty sand and sand with gravel	O-cell	1302	1280
DS24	Perry, MS	4.5	64	Sand, gravels and silty clay, silty clay base	O-cell	498	715
DS25	Wayne, MS	4	64	Sand and clay, clay base	O-cell	445	496
DS26	Madison, MS	2	40	Clay	O-cell	215	262

* The resistance is total resistance based on FHWA 5%B interpretation criterion.

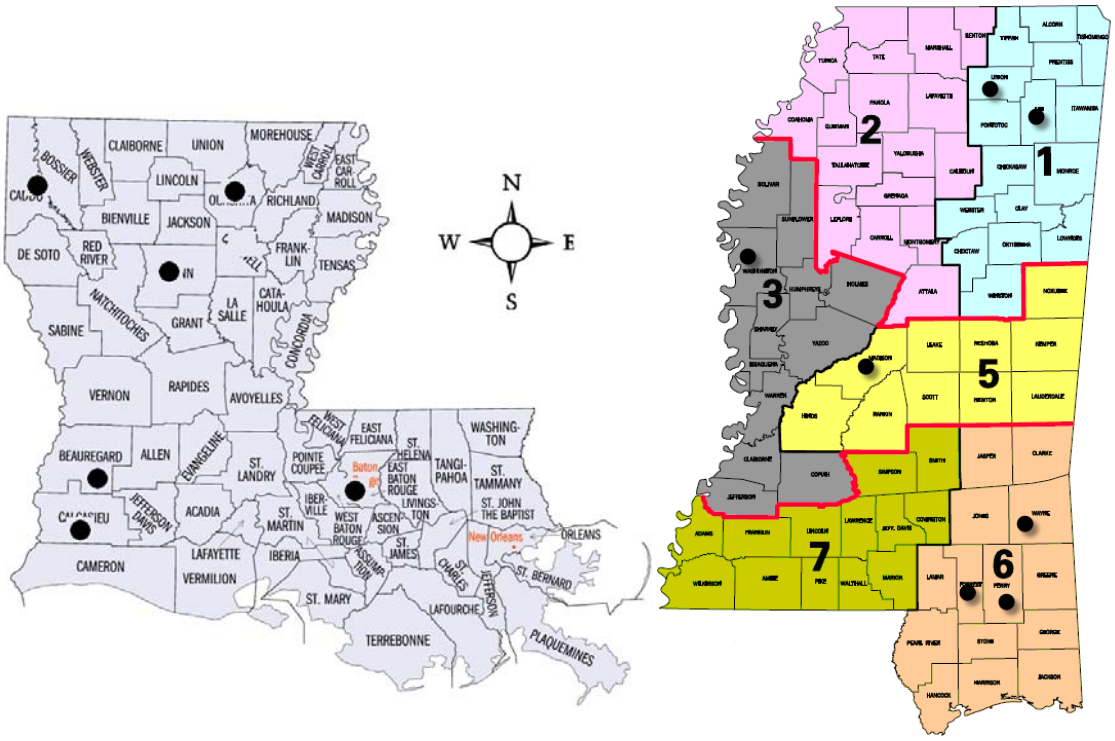

Figure 7
Approximate locations of the investigated drilled shafts

Compilation of Drilled Shaft Test Data

All collected drilled shaft load test reports were compiled along with information and data regarding the project (soil stratification and properties, drilled shaft characteristics, load test data, etc.) and were processed and transferred from each load test report to tables, forms, and graphs. The following data and information were collected and compiled for each drilled shaft load test report.

The soil data consist of information on the soil boring location (station number); soil stratigraphy; unit weight; Atterberg limits; laboratory testing (shear strength, physical properties, etc.); and in-situ test results [e.g., Standard Penetration Test (SPT) for cohesionless soil]. The collected soil data are presented in figures like the example shown in Figure 8. The summary of geotechnical data for all projects investigated in this research is presented in Appendix A.

As shown in Table 2, only a few cases have only sand or clay type of soil. Most soil is layered soils. So the soil type for this database can be classified as mixed soils. The total resistance factor calibrated in this study is therefore considered for mixed soil.

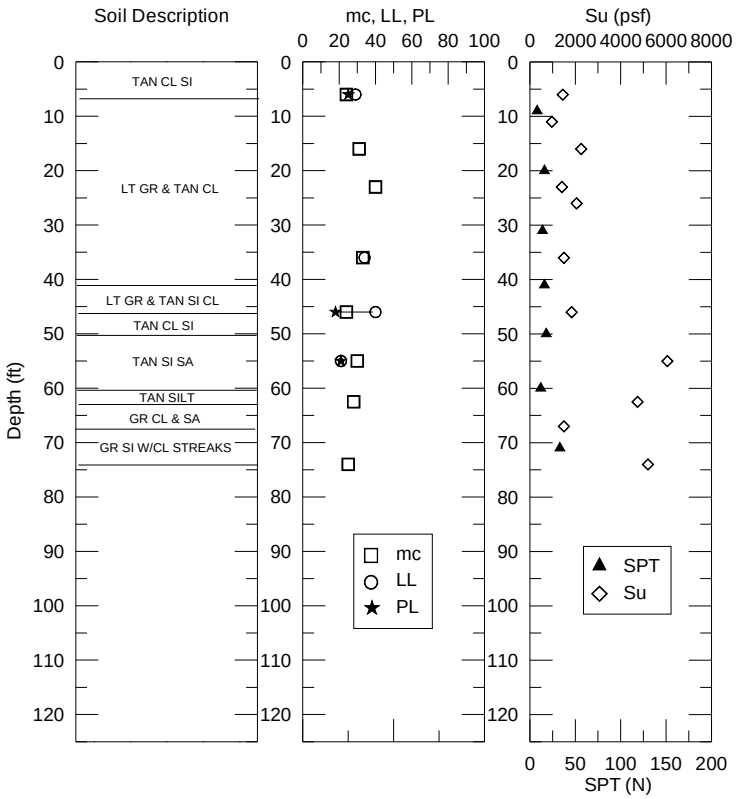

Figure 8
An example summary of geotechnical data for a tested pile (DS03)

Nominal Resistance of Drilled Shafts from Load Test

In this study, a total dataset of 26 drilled shaft cases constructed in silty clay, sand, sand-clay, and mixed soils were collected from the project libraries. The nominal load of drilled shaft was defined as the load corresponding to a settlement of 5% of the shaft diameter or the plunging load whichever occurs first *[16]*. Selection of this criterion was based on recommendation from previous study performed by Paikowsky for LRFD calibration consistency *[3]*. Statistical analysis showed that the FHWA's "5%B" method produced the closest and most consistent capacities with the mean value of the capacities determined by seven methods, which has been further confirmed and used by Zhang et al., Liang and Li, and Abu-Farsakh et al. *[12, 32,* and *33]*.

Nominal resistance of drilled shafts at a settlement of 5% of the shaft diameter can be determined by interpreting the calculation results. The measured nominal resistance can be obtained from measured load-settlement curves by O-cell tests or top-down conventional tests. Figure 2 shows an example of determination of shaft nominal resistance according to the criterion thereof. Some of the measured settlements did not meet the 5% of the shaft

diameter criterion. Therefore, it was necessary to extrapolate the measured load-settlement curves. Extrapolation of the measured load-settlement curves has been carefully performed on some cases that have settlements close to the settlement criterion to determine the estimated load at a settlement of 5% of the shaft diameter. After a comparison study of several extrapolation techniques (hyperbolic, Chin's method, cubic spline, and exponential curve fitting) the exponential curve fitting was chosen as the best method for extrapolation. The extrapolation has been examined to ensure a most reasonable estimation. Figure 9 shows an example of extrapolating the measured load-settlement curve using the proposed exponential curve fitting method. Data that needed large extrapolation were discarded. The final results of drilled shaft test database are summarized earlier in Table 2.

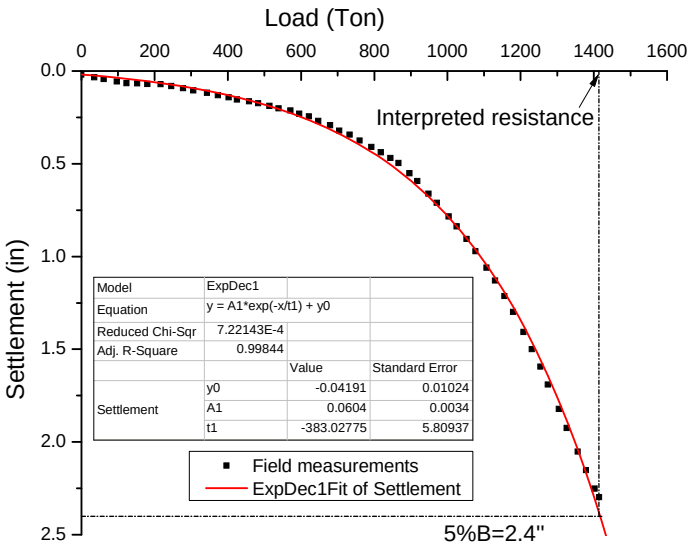

Figure 9
An example of extrapolation of measured top-down load-settlement curve

Separation of Resistance Components

As mentioned earlier, among the selected 26 drilled shaft test cases (referred as dataset 1), 22 drilled shaft cases were tested using O-cells. For those 22 cases (referred as dataset 2), the measured tip and side resistance components for each drilled shaft can be determined separately from O-cell results (Appendix B) using the FHWA interpretation criterion.

The determined measured total resistance of drilled shafts can be determined from the corrected equivalent top-down settlement curve (solid line in Figure 4) using the FHWA interpretation criterion as described in Figure 2. The O-cell test results can provide separate side friction and tip resistance as described in Figure 3. The side friction is the net upward force which equals the friction resistance as in a top-down load test based on O-cell test

assumptions. The interpreted side resistance or tip resistance is determined from the measured curves from O-cell tests at settlement of 5%B minus elastic compression (Figure 4). The elastic compression can be calculated or measured from the plots that are available in load test reports. For drilled shafts that need extrapolation, either the side friction or tip resistance needs to be determined by such an approach. Usually, the component with the larger displacement was preferred to determine the component resistance at 5%B settlement. Once one resistance component is estimated, the other component can be determined as the difference between the total resistance and the known component. This can help minimize the possible errors induced by extrapolation of load-settlement curves if needed. If neither side nor tip displacement reaches 5%B, the component with larger displacement will be extrapolated using hyperbolic method. The interpretation results will be presented in a later section.

Nominal Resistance of Drilled Shafts from Prediction

In this study, the load-settlement behavior was calculated using the program SHAFT v5.0 *[22]*. SHAFT is used to compute the axial capacity and the short-term, load versus settlement curves of drilled shafts in various types of soils. SHAFT v5.0 can analyze drilled-shaft response in six types of strata: (1) clay-cohesive geomaterial, (2) sand-cohesionless geomaterial, (3) clay-shale, (4) strong rock, (5) gravel-cohesionless IGM, and (6) weak rock-cohesive IGM *[22]*. The program allows for any combination of soil layers to be placed in a layered profile. For each soil layer, the program requires input of total unit weight, undrained shear strength for clay, and SPT number for sand. Figure 10 shows an example of input parameters for soil layers. With defined shaft geometry, the program can run the analysis based on FHWA design method described in the early section. The program outputs include: load-settlement curves for total axial load, tip, and side friction. An example of a predicted total load-settlement curve is shown in Figure 4. Separated load-settlement curves are shown in Figure 11. With these predicted load-settlement curves, tip, side, and total resistance at the settlement of 5%B can be easily determined. The interpretation results are shown in a later section.

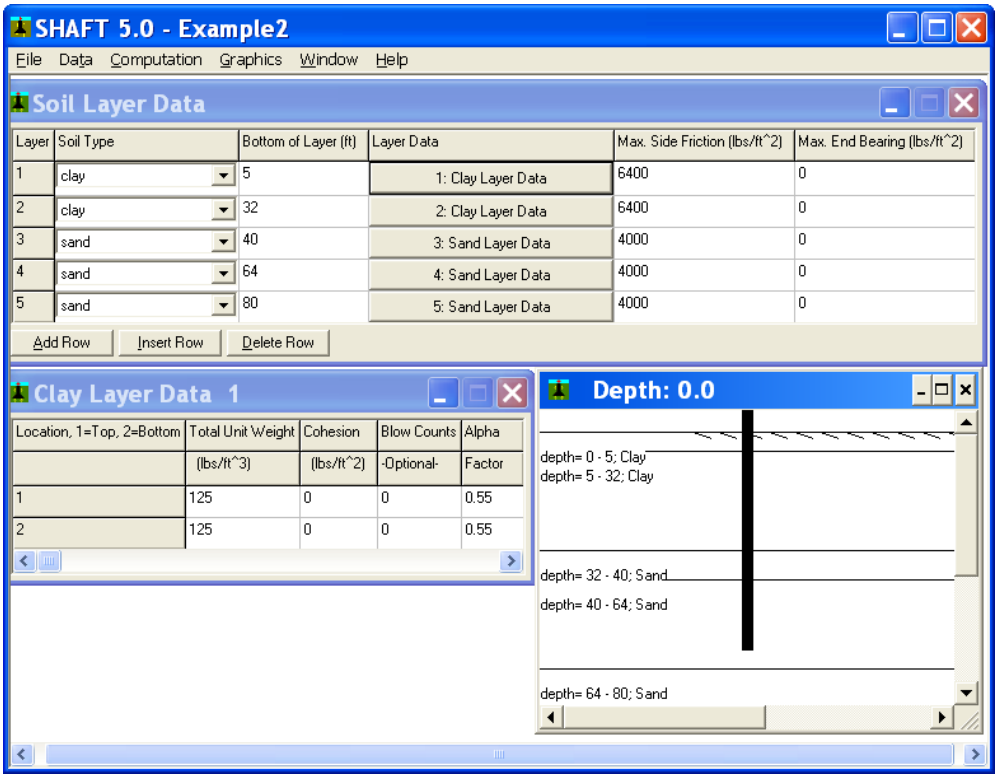

Figure 10
An example of inputs for soil layers

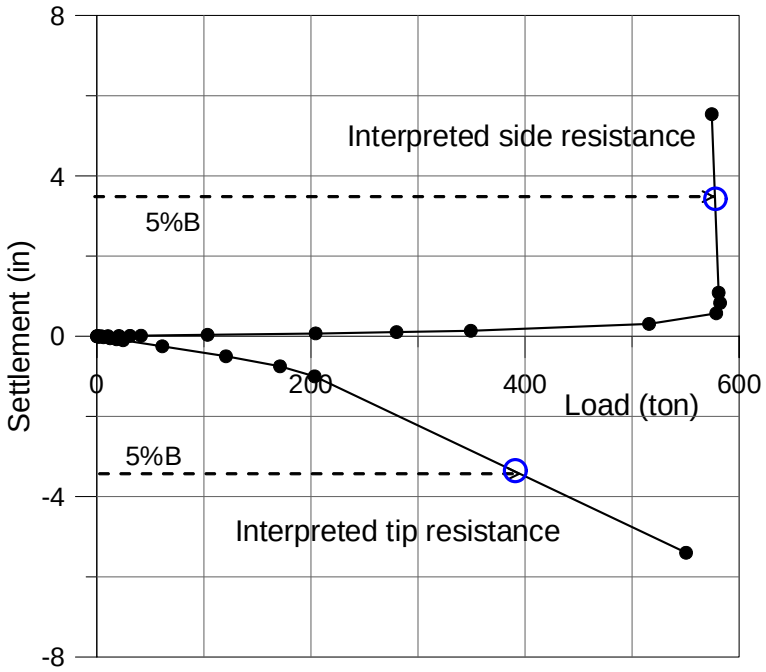

Figure 11
Example of predicted component resistance-settlement curves using SHAFT 5.0

DISCUSSION OF RESULTS

Predicted and Measured Drilled Shaft Resistance

Statistical analyses were performed on two sets of data: total resistance for 26 test cases (dataset 1) including 4 top-down tests and 22 O-cell tests and total separated resistance for 22 O-cell test cases (dataset 2). Total resistance of drilled shafts was analyzed using both datasets to compare the effect of the 4 top-down test cases on the final calibrated resistance factor.

Total Resistance Analyses

From the results of Table 2, a statistical analysis was first conducted on the collected database of 26 drilled shaft cases to evaluate the statistical characteristics of the total nominal drilled shaft resistance. The corresponding resistance bias factor (λ_R), which is the mean ratio between the measured resistance and the predicted resistance (R_m/R_p), was determined. The standard deviation (σ) and the coefficient of variation (COV) of the bias ($\lambda_R=R_m/R_p$) were also calculated and summarized in Table 3.

Table 3
Statistical analysis of drilled shaft design method (26 cases)

Arithmetic calculations				Best fit calculations
R_m/R_p			R_p/R_m	
Mean (λ_R)	σ	COV	Mean	R_{fit}/R_m
1.35	0.50	0.37	0.83	0.79

Figure 12 presents the comparison between the predicted and measured total drilled shaft resistances. A simple regression analysis was also conducted to obtain a line of best fit of the predicted/measured drilled shaft resistances. The slope of the best fit line is 0.79, while the mean ratio of R_p/R_m equals 0.83 and indicates a 21% underestimation of shaft resistance using the FHWA design method in Louisiana soils *[16]*. The COV of R_m/R_p for drilled shaft is 0.37, which agrees well with the COV for the O'Neill and Reese design method (0.27 - 0.74) as reported by Paikowsky *[3]*.

Figure 13 presents the histogram and the normal and lognormal distributions of bias of the drilled shaft (R_m/R_p). Figure 14 illustrates the CDF of the bias values for the FHWA design method [*16*]. As shown in these figures, lognormal distribution matches the histogram and the CDF of drilled shaft data better than the normal distribution; therefore, the lognormal distribution was used here in the reliability calibration analysis. The predicted lognormal distribution obtained by the "best fit to tail" method recommended by Allen et al. is also

shown in Figure 14 *[35]*. The mean and standard deviation of λ_R obtained from the fit-to-tail curve are 1.29 and 0.43, respectively. The mean and standard deviation of λ_R obtained by both methods (statistic calculation and best fit to tail) were used in the LRFD calibration process as will be described in the following section.

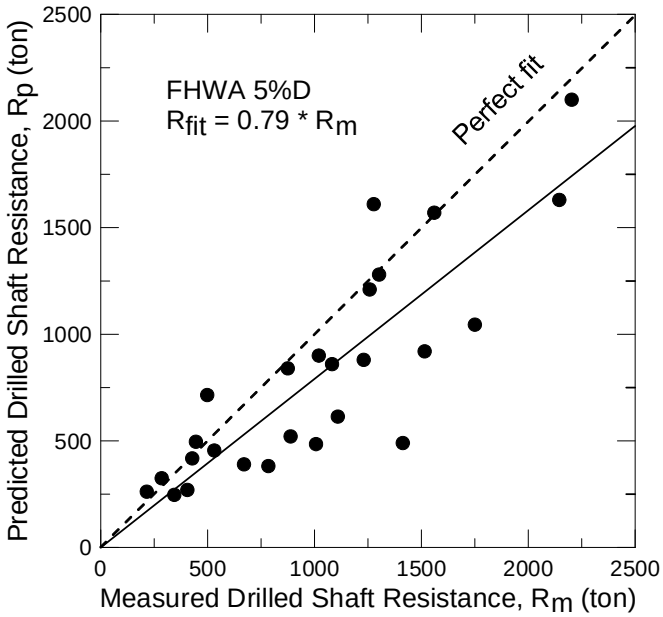

Figure 12
Measured (R_m) versus predicted (R_p) drilled shaft resistance

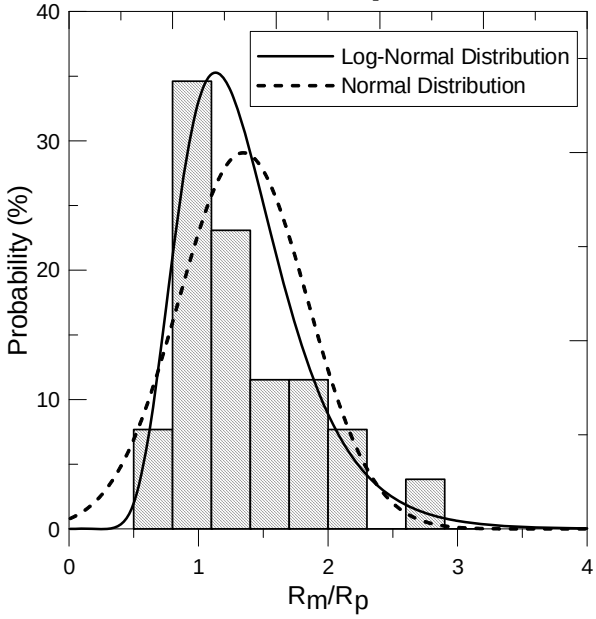

Figure 13
Histogram and probability density function of resistance bias

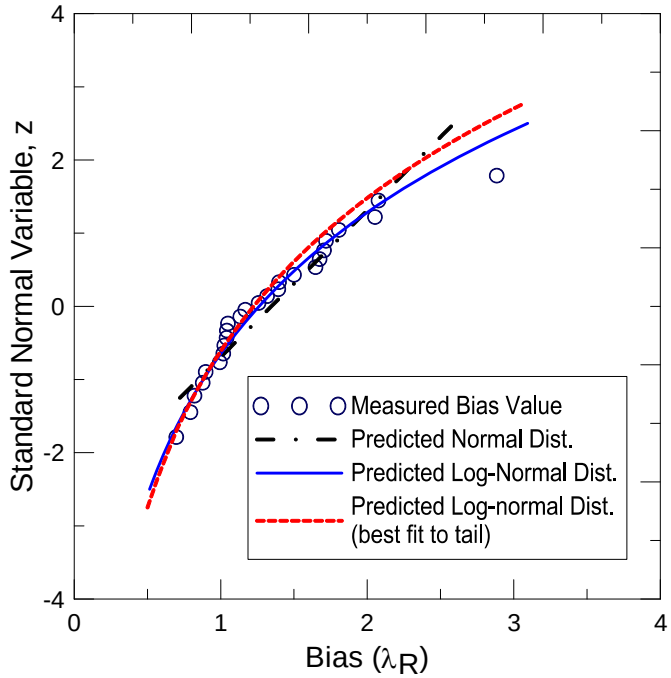

Figure 14
Cumulative distribution function (CDF) of bias values

Separate Resistance Analysis

The tip and side resistance contributions of the investigated 22 O-cell drilled shaft cases are plotted in Figure 15. The average contribution of the side resistance to the total resistance is about 52 percent. Both side resistance and tip resistance contribute significantly to the total resistance of investigated drilled shafts. However, the SHAFT program significantly underestimates tip resistance as indicated in Figure 16. The majority of total resistance (75 percent) comes from side resistance. Tip resistance only contributes 25 percent of total resistance. The interpreted measured resistances are compared to the interpreted predicted resistances as shown in Figures 17 and 18 for tip and side resistances, respectively. The predicted total resistance is only 80 percent of the measured total resistance, which is almost the same as the value fitted using 26 cases. This demonstrates that the four top-down test cases have negligible influence on the statistical analyses. The underestimation is even lower for tip resistance as indicated with predicted resistance of only 35 percent of the measured resistance (Figure 17). The accuracy of side resistance estimation (Figure 18), 118 percent, is better than that of tip resistance. However, the variation of side resistance data is widely scattered.

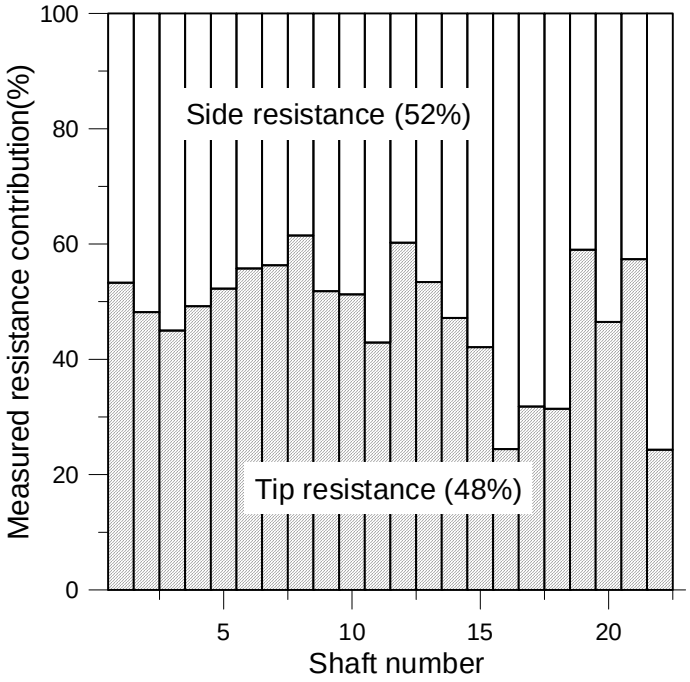

Figure 15
Contribution of measured side and tip resistance

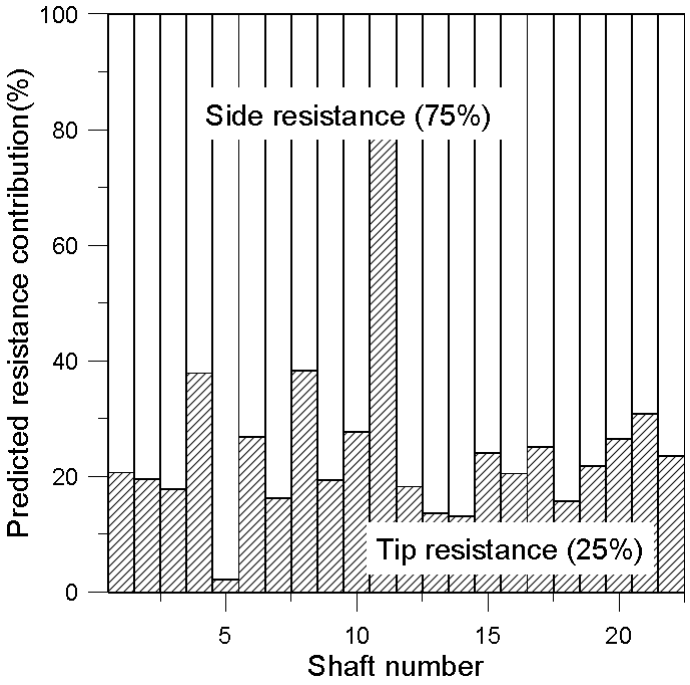

Figure 16
Contribution of predicted side and tip resistance

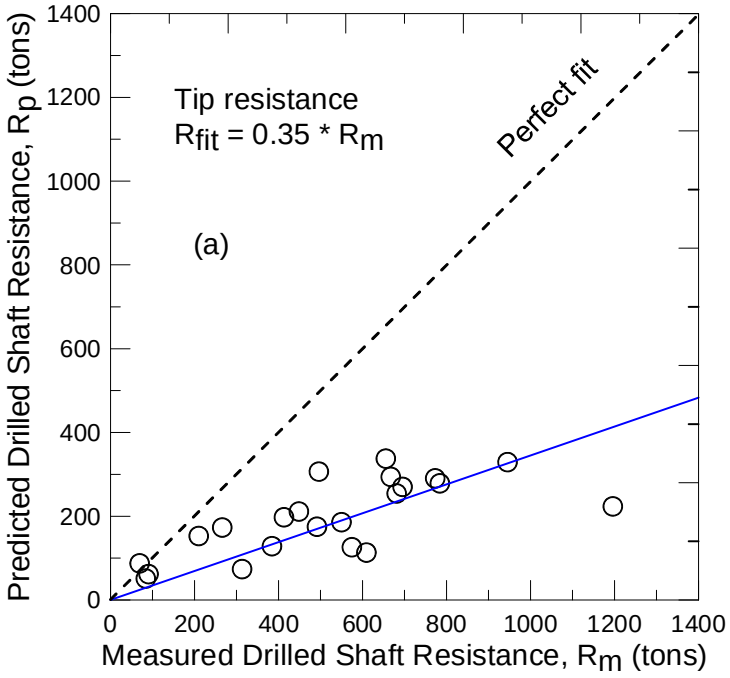

Figure 17
Interpreted measured versus predicted tip resistance of drilled shafts

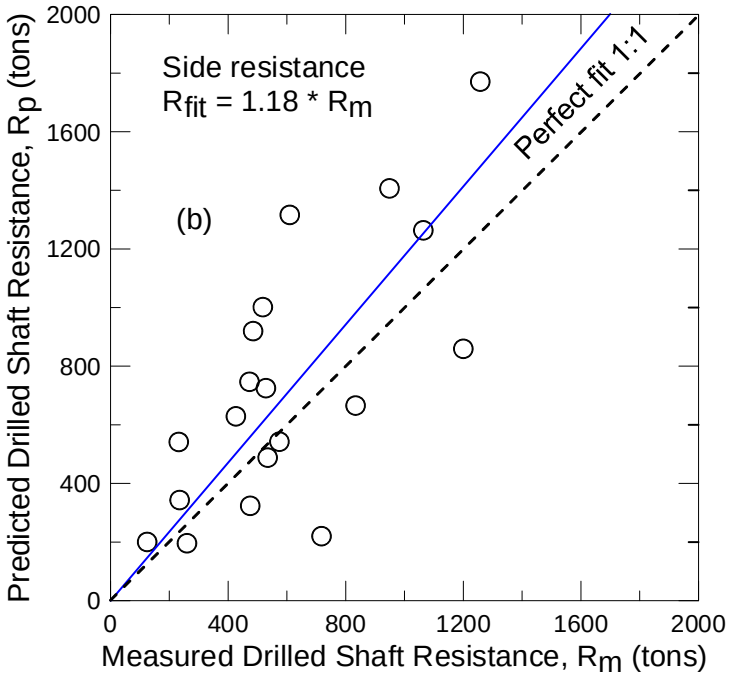

Figure 18
Interpreted measured and predicted side resistance of drilled shafts

A statistical analysis was conducted on the interpreted resistances to evaluate the statistical characteristics of the nominal drilled shaft resistances of different components. The

maximum, minimum, mean (μ), and COV of the bias for different resistance components were calculated and summarized in Table 4. It can be observed that the resistance components have larger variation compared to the total resistance. Prediction of tip resistance is more conservative as the model bias factor is the largest among the three.

Table 4
Summary of bias for drilled shafts tested by O-cell (22 cases)

Statistics	Tip	Side	Total
Max.	5.38	3.26	2.88
Min.	0.79	0.43	0.70
Mean	2.67	0.96	1.29
COV	0.46	0.63	0.38

Figures 19 and 20 present the histogram and the normal and lognormal distributions of the bias of different resistance components. Similar to total resistance condition, the lognormal distribution matches the histogram of bias better than normal distribution; therefore, lognormal distribution was used in reliability calibration analyses.

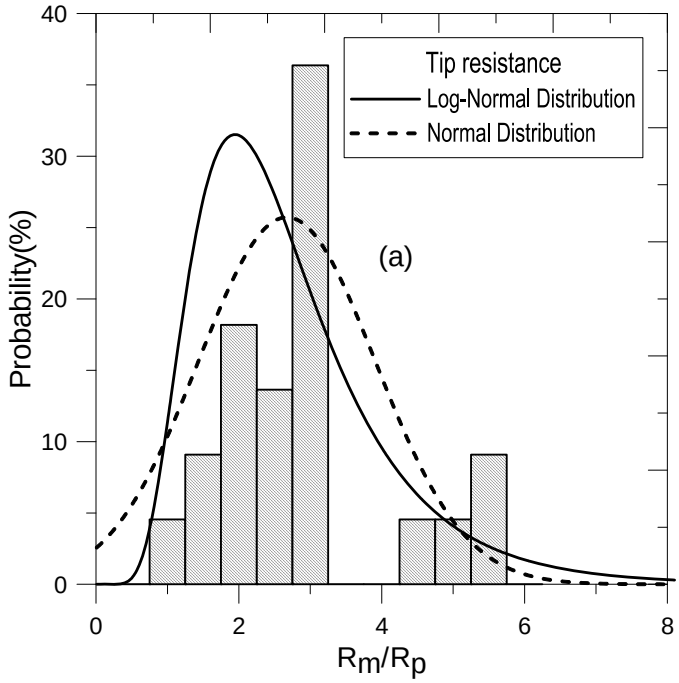

Figure 19
Histograms of bias for tip resistance

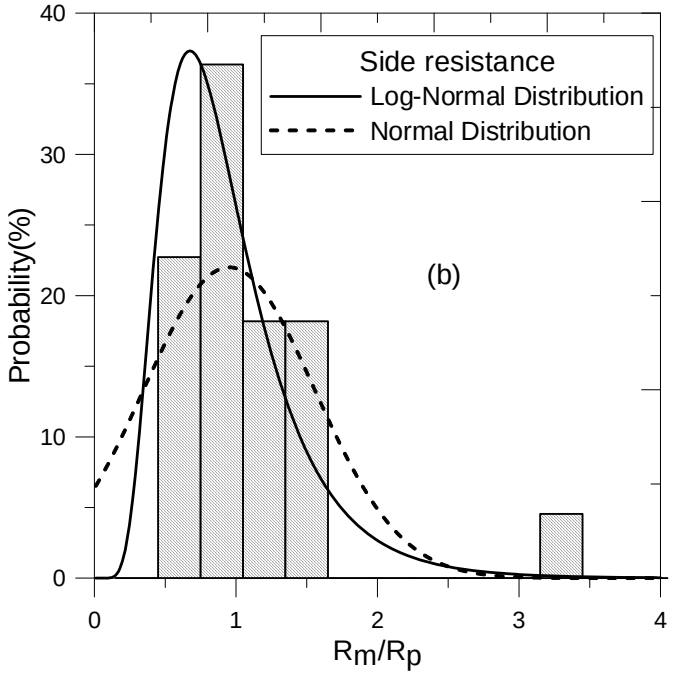

Figure 20
Histograms of bias for side resistance

LRFD Calibration

Total Resistance Factor

This study follows the calibration procedure based on the Monte Carlo simulation method recommended in the Transportation Research Circular E-C079 to determine the total resistance factor of drilled shafts *[35]*. The required number of Monte Carlo trials is based upon achieving a particular confidence level for a specified number of random variables and is not affected by the variability of the random variables *[35, 37,* and *38]*. Using the procedure described by Harr, the number of Monte Carlo trials required for a confidence level of 90 percent is approximately 9,900 *[37]*. For the probabilistic calculations reported in this study, Monte Carlo simulation with 50,000 trials was conducted. The calculated reliability index and the corresponding resistance factor are plotted in Figure 21.

The calibration was conducted with a dead load to live load ratio of 3.0 since it is a typical value used in previous research as discussed previously *[14, 18]*. Paikowsky suggested a required reliability index for the pile foundations of either 2.33 or 3.0 depending on pile redundancy *[4]*. Total resistance factors (ϕ) for the O'Neill and Reese (FHWA) design method corresponding to a target reliability index of 3.0 is 0.55 (0.56 rounded to the nearest 0.05) using "best fit to tail" method and 0.5 (0.52) using the measured bias (Figure 21). The authors believe the resistance factor based on measured bias is more favorable since the

measured bias data can be utilized to its full extent. Total resistance factors from this study as well as reported in previous literature are listed in Table 5. It should be noted that the resistance factors of cohesive and cohesionless soils calibrated by AASHTO and Paikowsky were based on O'Neill and Reese (1988) method *[4, 14,* and *39]*. The work by Liang and Li and current work are based on O'Neill and Reese (1999) method via SHAFT program *[13, 17,* and *22]*. A resistance factor of 0.35 in mixed soils reported by Liang and Li is less than the proposed value of 0.50 in this study*[13]*. This might be due to the difference of soil conditions.

Separated Resistance Factors

The statistical parameters used for the calibration of separated resistance components are listed in Table 4. The side resistance and tip resistance were determined at the same settlement of the shaft top. The bias of side resistance and tip resistance can be considered as independent variables. Therefore, the resistance factor from side and tip can be calibrated separately following the same calibration procedure as for the total resistance. The calculated resistance factors for each resistance component are proposed in Table 6. Only measured bias data were used in this calibration. "Best-fit-to-tail" was not used. It is interesting to notice that the tip resistance factor is higher than the side resistance factor. This may be due to variation of soil type along the shafts. The FHWA design method slightly overestimates the side resistance and yet significantly underestimates the tip resistance. The calibrated total resistance factor using 22 tests (O-cell tests only) is close to the one calibrated using the 26 cases (dataset 1), e.g., total O-cell and top down tests with no separation.

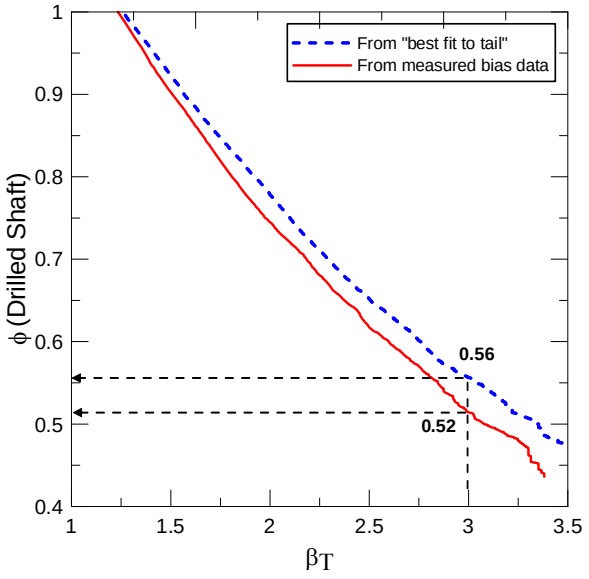

Figure 21
Resistance factors for different reliability indexes

Table 5
Resistance factors (ϕ) for drilled shaft (dataset 1)

$\beta_T = 3.0$	Resistance Factor, ϕ
Current study	0.50 in mixed soils 0.55 in mixed soils (best fit to tail)
Liang and Li *[13]*	0.45 in clay 0.50 in sand 0.35 in mixed soils
Paikowsky *[4]* and AASHTO *[14]*	0.45 in cohesive soils 0.55 in cohesionless soils

Table 6
Separated resistance factors (dataset 2)

Resistance component	Tip	Side	Total
Resistance factor	0.75	0.20	0.50

SUMMARY AND CONCLUSIONS

This study presented the LRFD calibration of the FHWA (O'Neill and Reese) method for drilled shaft design based on the 5% B criterion *[17]*. A drilled shaft load test database of 26 drilled shafts with different sizes and lengths was collected and used to calibrate the total and separated resistance factors. This collected database has four top-down tests and 22 O-cell tests. For each drilled shaft, the load-settlement behavior was estimated using the FHWA method via the SHAFT program. Tip, side, and total resistance factors (ϕ) needed in the LRFD design methodology of drilled shafts in Louisiana were determined at a reliability index (β) of 3.0 and are ready for implementation.

Statistical analyses comparing the predicted and measured drilled shaft resistances were conducted to evaluate the accuracy of the FHWA design method in estimating the measured drilled shaft capacity. Results of the analyses showed that the FHWA method underestimates the total drilled shaft resistance by an average of 21 percent. The prediction of tip resistance is much more conservative than that of side resistance. A large scatter in the prediction of side resistance was observed.

LRFD calibration based on the Monte Carlo simulation method was conducted to determine the resistance factors (ϕ) at different reliability indexes (β) that are needed to implement the LRFD design of axially loaded drilled shafts. Design input parameters for loads were adopted from the AASHTO LRFD design specifications for bridge substructure. Total resistance factor (ϕ_{total}) for mixed soils corresponding to a dead load to live load ratio (Q_D/Q_L) of 3.0 with a target reliability index (β_T) of 3.0 was found to be 0.50. The same total resistance factor was determined from both 26 dataset (top-down + O-cell) and 22 dataset (O-cell) only. This value is slightly different than the value obtained by Paikowsky, recommended by AASHTO, and Liang and Li, probably due to the difference in subsurface soil conditions *[12]*. A tip resistance factor (ϕ_{tip}) of 0.75 and a side resistance factor (ϕ_{side}) of 0.20 were determined based on the 22 O-cell drilled shaft tests. The presented resistance factors can be valuable reference values for the LADOTD engineers to design drilled shafts in Louisiana using the LRFD methodology.

RECOMMENDATIONS

1. LADOTD engineers need to start implementing the resistance factors (ϕ) recommended for the FHWA (O'Neill and Reese) design method based on the Louisiana drilled shaft load test database and soil conditions in the LRFD design of axially loaded drilled shafts for all future state projects.

2. It is recommended to select a few projects to demonstrate the comparison between the LRFD design and the traditional ASD design and conduct a cost benefit study.

3. It is recommended to hold a workshop to train LADOTD engineers in the LRFD design of deep foundations.

4. Since the co-PIs are from the geotechnical design section at LADOTD, they are already in the process of implementing previously mentioned recommendation items 1, 2, and 3 based on the findings of this research project.

5. It is recommended to continue collecting drilled shaft test data from new projects, especially for those cases in which the end bearing and side frictional capacities can be separated for possible future re-calibration of resistance factors. A database of a minimum 20 load tests is considered statistically reliable to perform LRFD calibration.

6. It should be noted that performing complete reliability analyses of deep foundations requires the inclusions of all risk factors. Scour is a critical factor in the selection of drilled shaft tip elevations. The risk associated with scour directly impacts the reliability of drilled shaft foundations. This is mainly due to expected changes on the in-situ stress state (overburden and stress history) of the subsurface soil that will affect the laboratory and in-situ test results. However, the scope of this study does not include the evaluation of scour and is recommended to be considered in the future.

7. Global resistance factors are recommended herein for the design of axially loaded drilled shafts in Louisiana. However, further research should be conducted to evaluate site variability and in-situ load tests' effect on the selection of resistance factor values.

8. Further research is needed to calibrate resistance factors for drilled shafts that are laterally loaded.

ACRONYMS, ABBREVIATIONS, AND SYMBOLS

AASHTO	American Association of Highway and Transportation Officials
ASD	Allowable Stress Design
CDF	Cumulative Distribution Function
COV	Coefficient of Variation
DOT	Department of Transportation
FHWA	Federal Highway Administration
IGM	Intermediate Geomaterial
LA	Louisiana
LADOTD	Louisiana Department of Transportation and Development
LRFD	Load and Resistance Factor Design
LTRC	Louisiana Transportation Research Center
MS	Mississippi
MSDOT	Mississippi Department of Transportation
NCHRP	National Cooperative Highway Research Program
PDF	Probability Density Function
SHAFT	Computer program for drilled shaft design
SLS	Serviceability Limit State
SPT	Standard Penetration Test
ULS	Ultimate Limit State

REFERENCES

1. Abu-Farsakh, Y. M., Yoon, S., and Tsai, C. *Calibration of Resistance Factors Needed in the LRFD Design of Driven Piles*. Report No. 449, Louisiana Transportation Research Center, May, 2009.
2. Misra, A., and Roberts, L.A. "Service Limit State Resistance Factors for Drilled Shafts." Geotechnique, Vol. 59, No. 1, 2009, pp. 53-61.
3. Yang, X., Han, J., Parsons, R., and Henthorne, R. "Resistance Factors for Drilled Shafts in Weak Rocks Based on O-Cell Test Data." In *Transportation Research Record 2045*. Transportation Research Board, National Research Council, Washington, D.C., 2008, pp. 62-67.
4. Paikowsky, S. G. *Load and Resistance Factor Design (LRFD) for Deep Foundations*, Publication NCHRP-507. Transportation Research Board, Washington D.C., 2004, 87 pp.
5. Allen, T. M. *Development of the WSDOT Pile Driving Formula and Its Calibration and Resistance Factor Design (LRFD)*, Publication FHWA-WA-RD 610.1. FHWA, Washington State Department of Transportation, 2005, 57 pp.
6. McVay, M., Birgisson, B., Zhang L., Perez, A., and Putcha, S. "Load and Resistance Factor Design (LRFD) for Driven Piles Using Dynamic Methods—A Florida Perspective." *Geotechnical Testing Journal*, Vol. 23, No. 1, 2000, pp. 55-66.
7. McVay, M., Birgisson, B., Nguyen, T., and Kuo, C. "Uncertainty in LRFD phi, ϕ, Factors for Driven Prestressed Concrete Piles." In *Transportation Research Record 1808*. Transportation Research Board, National Research Council, Washington, D.C., 2002, pp. 99-107.
8. Allen, T.M. "Development of a New Pile Driving Formula and Its Calibration for Load and Resistance Factor Design." Proceedings for the 86th TRB Annual Meeting, Washington, D.C., TRB, 2006.
9. Yang, L. and Liang, R. "Incorporating Setup into Load and Resistance Factor Design of Driven Piles in Sand." Proceedings for the 86th TRB Annual Meeting. Washington, D.C., TRB, 2006.
10. Nowak, A.S. *Calibration of LRFD Bridge Design Code*, Publication NCHRP-368, Transportation Research Board, Washington, D.C., 1999, 218 pp.
11. LRFD Highway Bridge Design Specifications. English Units, AASHTO, Washington, D.C., 1998.
12. Kuo, C. L., McVay, M., and Birgisson, B. "Calibration of Load and Resistance Factor Design." In *Transportation Research Record 1808*. Transportation Research Board, National Research Council, Washington, D.C., 2002, pp. 108-111.

13. Liang, R. and Li, J. "Resistance Factors Calibrated from FHWA Drilled Shafts Static Top-Down Test Data Base." GSP 186: *Contemporary Topics in In-Situ Testing, Analysis, and Reliability of Foundations*, 2009.
14. AASHTO. *LRFD Bridge Design Specifications*, 4th Edition, American Association of State Highway and Transportation Officials, Washington, D.C., 2007, 40 pp.
15. Barker, R. M., Duncan, J. M., Rojiani, K. B., Ooi, P. S. K., Tan, C. K., and Kim, S. G. *Manuals for the Design of Bridge Foundations*. NCHRP-343, Transportation Research Board, National Research Council, Washington, D.C., 1991, 306 pp.
16. O'Neill, M., Townsend, F., Hassan, K., Buller, A., and Chang, P. *Load Transfer for Drilled Shafts in Intermediate Geomaterials*. FHWA-RD-95-172, FHWA, 1996, 184 pp.
17. O'Neill, M.W. and Reese, L.C. *Drilled Shafts: Construction Procedures and Design Methods*, Publication FHWA-IF-99-025, FHWA, Washington, D.C., 1999, 758 pp.
18. AASHTO. *LRFD Bridge Design Specifications*, 3rd Edition, American Association of State Highway and Transportation Officials, Washington, D.C., USA, 2004, 582 pp.
19. Allen, T.M. *Development of Geotechnical Resistance Factors and Downdrag Load Factors for LRFD Foundation Strength Limit State Design*, Publication FHWA-NHI-05-052, FHWA, Washington, D.C., 2005, pp. 49
20. Yang, X.M., Han, J., Parsons, R.L., and Henthorne, R. "Resistance Factors for Drilled Shafts in Weak Rocks Based on O-cell Test Data." In *Transportation Research Record 2045*. Transportation Research Board, National Research Council, Washington, D.C., 2008, pp. 62-67.
21. DFI. *Guidelines for the Interpretation and Analysis of the Static Loading Test*, 1st Edition. Sparta, NJ: Deep Foundations Institute, 1990, 20 pp.
22. Reese, L.C., Wang, S.T., and Arrellaga, J.A. A Program for the Study of Drilled Shafts Under Axial Loads, SHAFT Version 5.0 for Windows, CD-ROM. Ensoft, Inc., Austin, Texas, 2001.
23. Schmertmann, J. H. and Hayes, J. A. "The Osterberg Cell and Bored Pile Testing – A Symbiosis." *3rd International Geotechnical Engineering Conference*, Cairo, Egypt; 1997, pp. 139-66.
24. Withiam, J., Voytko, E., Barker, R., Duncan, M., Kelly, B., Musser, S., and Elias, V. *Load and Resistance Factor Design (LRFD) of Highway Bridge Substructures*. FHWA-HI-98-032. FHWA, Washington, D.C., 1998.
25. Becker, D. E. "Eighteenth Canadian Geotechnical Colloquium: Limit States Design for Foundations. Parts I and II. An Overview of the Foundation Design Process." *Canadian Geotechnical Journal*, Vol. 33, 1996, pp. 956-1007.
26. Zhang, L., Tang, W. H., and Ng, C.W.W. "Reliability of Axially Loaded Driven pile Groups." *Journal of Geotechnical and Geoenvironmental Engineering*, ASCE, Vol. 127, No. 12, 2001, pp. 1051-1060.

27. Kim, J., Gao, X., and Srivatsan, T.S. "Modeling of Void Growth in Ductile Solids: Effects of Stress Triaxiality and Initial Porosity." *Engineering Fracture Mechanics*, Vol. 71, No. 3, 2004, pp. 379-400.
28. McVay, M., Ellis, Jr. R., Birgisson, B., Consolazio, G., Putcha, S., and Lee, S. "Load and Resistance Factor Design, Cost, and Risk: Designing a Drilled-Shaft Load Test Program in Florida Limestone." In *Transportation Research Record 1849.* Transportation Research Board, National Research Council, Washington, D.C., 2003, pp. 98-106.
29. Abu-Farsakh, M., and Titi, H. "Probabilistic CPT Method for Estimating the Ultimate Capacity of Friction Piles." *Geotechnical Testing Journal*, ASTM, Vol. 30, No. 5, 2007, pp. 387-398.
30. McVay, M.C. "Load and Resistance Factor Design, Cost, and Risk: Designing a Drilled Shaft Load Test in Florida Limestone." *Soil Mechanics*, 2003, pp. 98-106.
31. Hansell, W. C. and Viest, I. M. "Load Factor Design for Steel Highway Bridges." *AISC Engineering Journal*, Vol. 8, No. 4, 1971, pp. 113-123.
32. Zhang L.M., Li, D.Q., and Tang, W.H. "Reliability of Bored Pile Foundations Considering Bias in Failure Criteria." *Canadian Geotechnical Journal*, Vol. 42, 2005, pp. 1086-1093.
33. Abu-Farsakh, M., Yong, S., Yu, X., Tsai, C., and Zhang, Z. "Calibration of Resistance Factor for LRFD Design of Drilled Shafts in Louisiana." Proceedings for the 89th TRB Annual meeting, Washington, D.C., TRB, 2010, 12 pp.
34. Zhang, Z., and Tumay, M.T. "Statistical to Fuzzy Approach Toward CPT Soil Classification." *Journal of Geotechnical and Geoenvironmental Engineering,* ASCE, Vol. 125, No. 3, 1999, pp. 179-186.
35. Allen, T.M., Nowak, A., and Bathurst, R. *Calibration to Determine Load and Resistance Factors for Geotechnical and Structural Design*. Publication TRB Circular E-C079, Transportation Research Board, Washington, D.C., 2005. 93 pp.
36. Fishman, G. S. *Monte Carlo: Concepts, Algorithms, Applications*. Springer-Verlag, New York, 1995.
37. Harr, M. E. *Reliability-Based Design in Civil Engineering*. Dover Publications, Mineola, NY, 1996, 291 pp.
38. Baecher, G. B. and Christian, J. T. *Reliability and Statistics in Geotechnical Engineering*. Wiley, Chichester, England, 2003, 619 pp.
39. Reese, L.C. and O'Neill, M.W. *Drilled Shafts: Construction Procedures and Design Methods*. Report No. FHWA-HI-88-042, FHWA, Washington, DC, 1988, 564 pp.

APPENDIX A

Summary of Geotechnical Data for the Projects Investigated

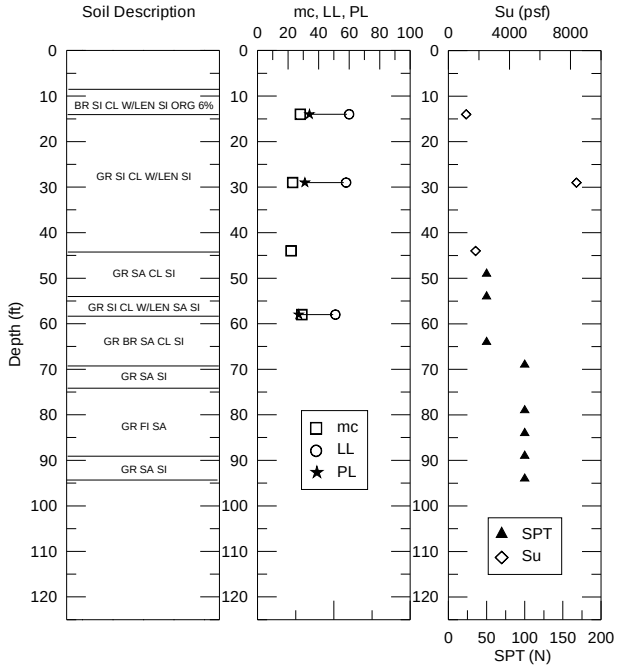

Figure 22
DS01

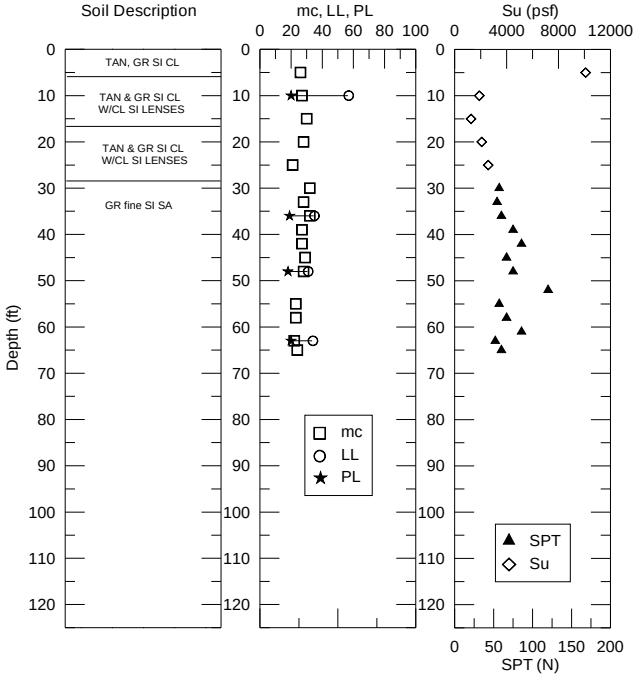

Figure 23
DS02

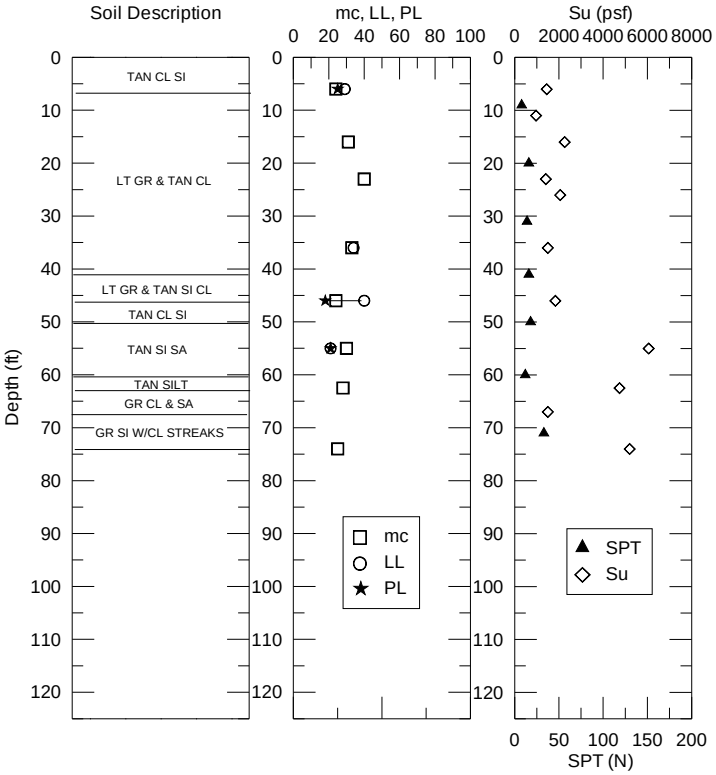

Figure 24
DS03

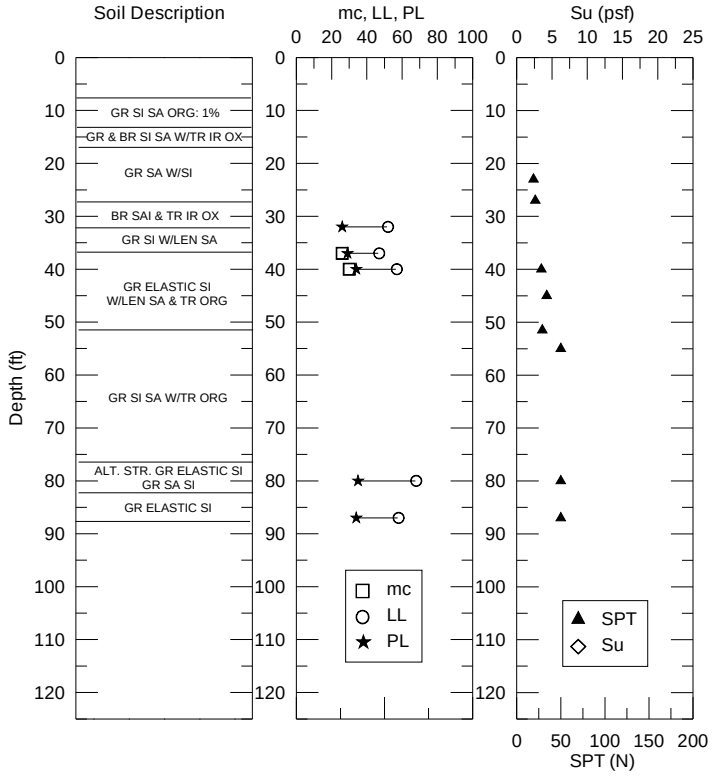

Figure 25
DS04

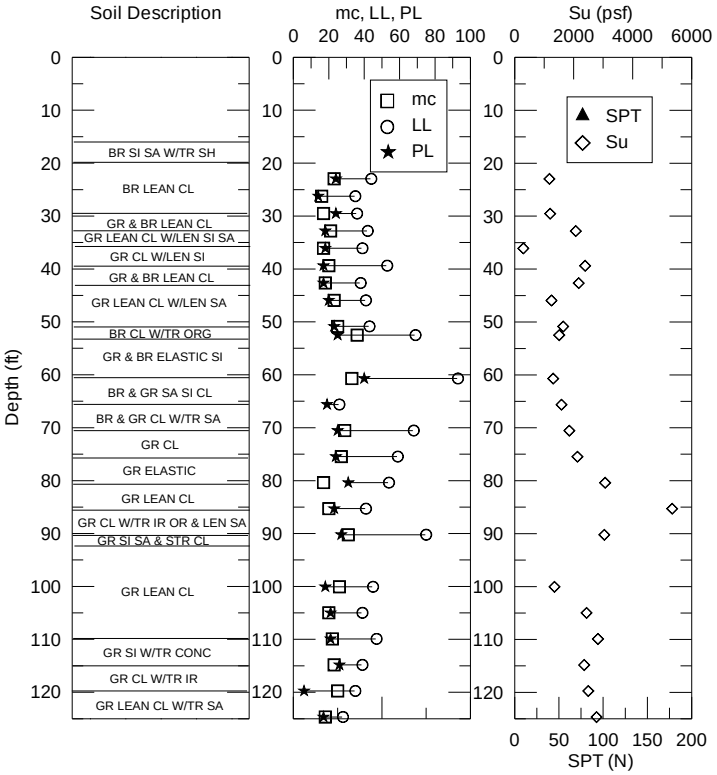

Figure 26
DS05

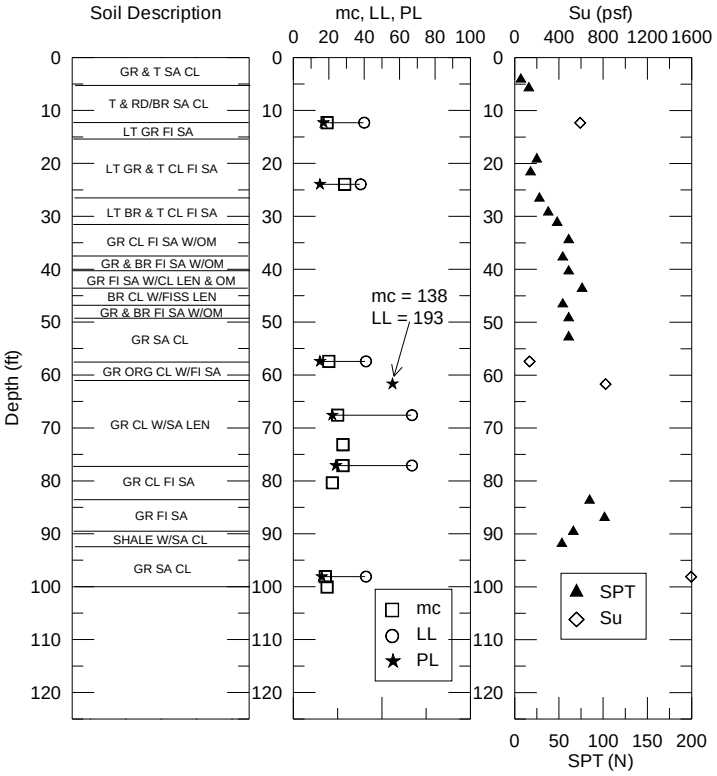

Figure 27
DS06

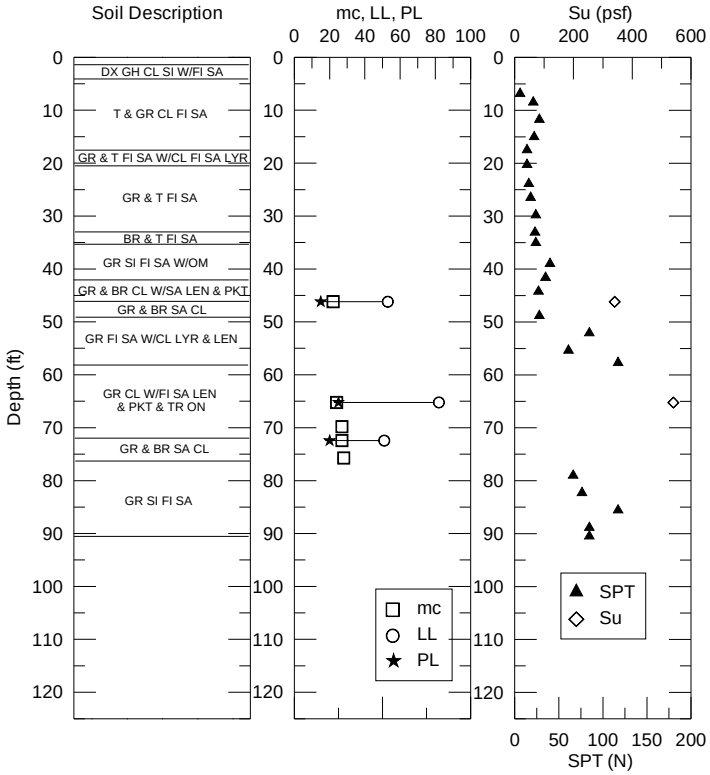

Figure 28
DS07

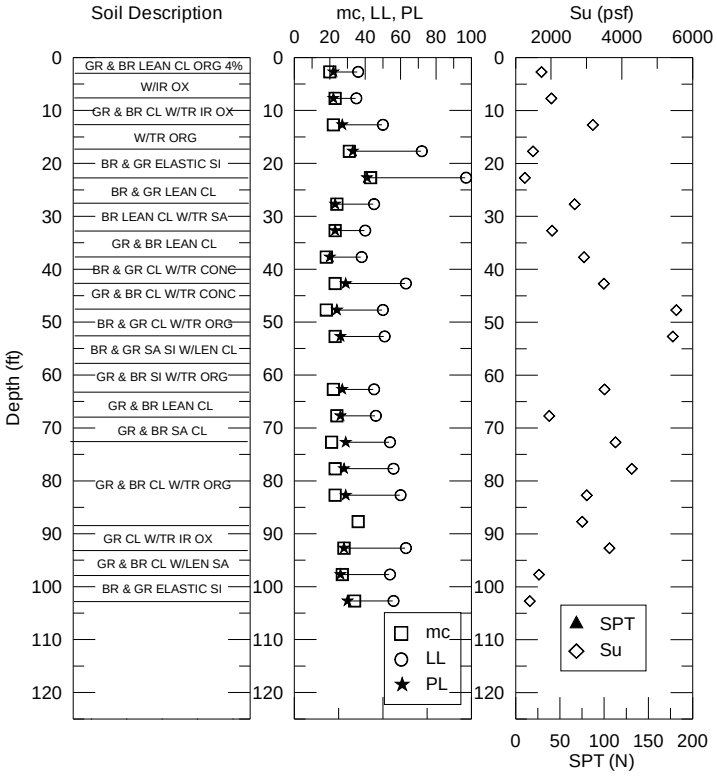

Figure 29
DS08

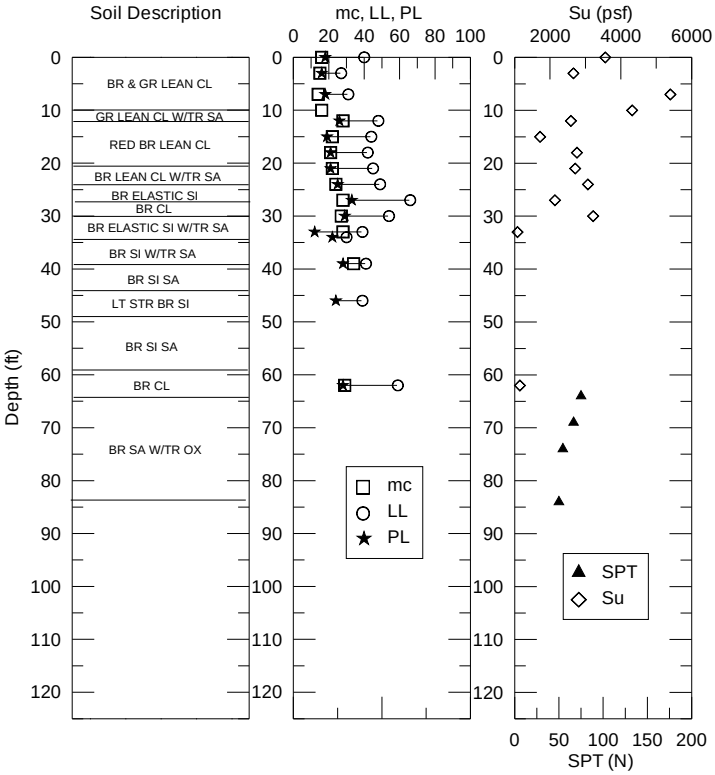

Figure 30
DS09

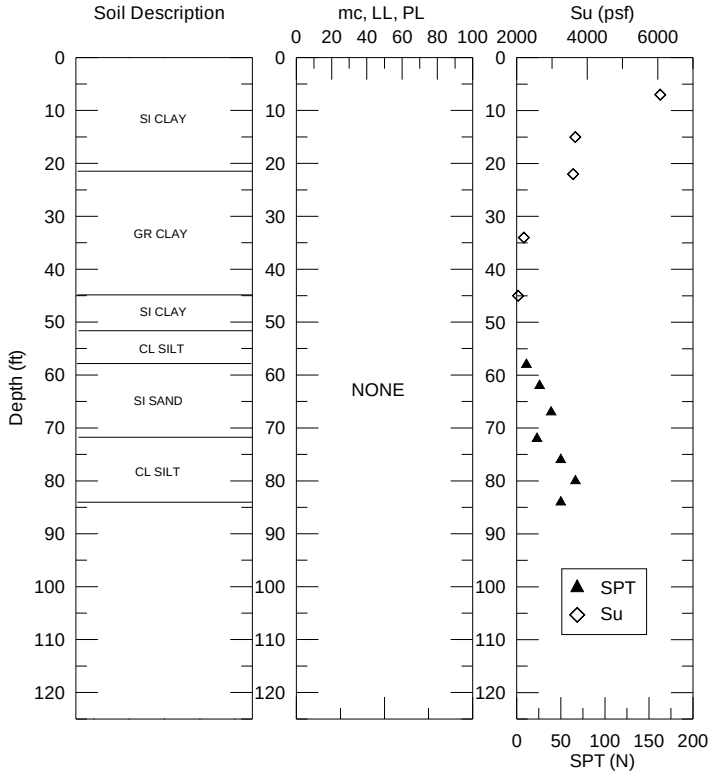

Figure 31
DS10 and DS11

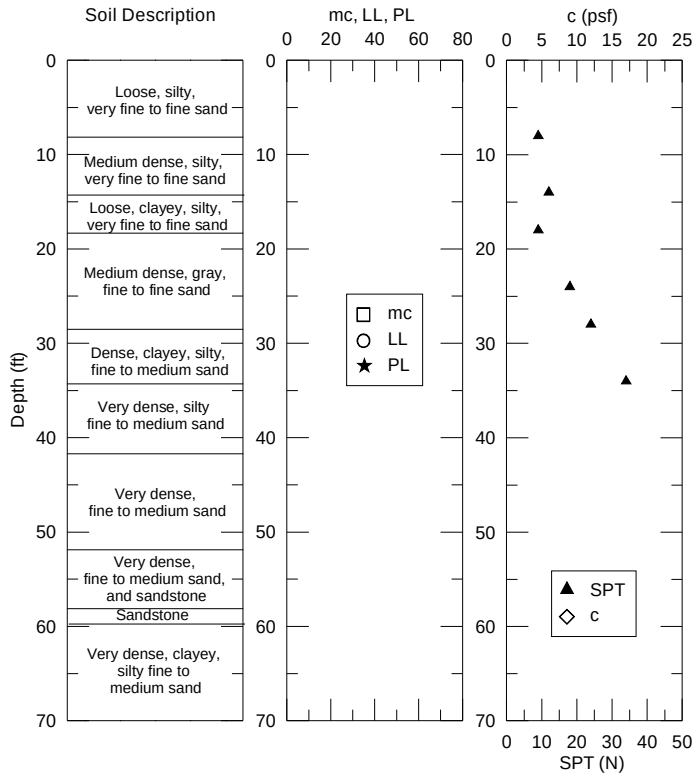

Figure 32
DS12

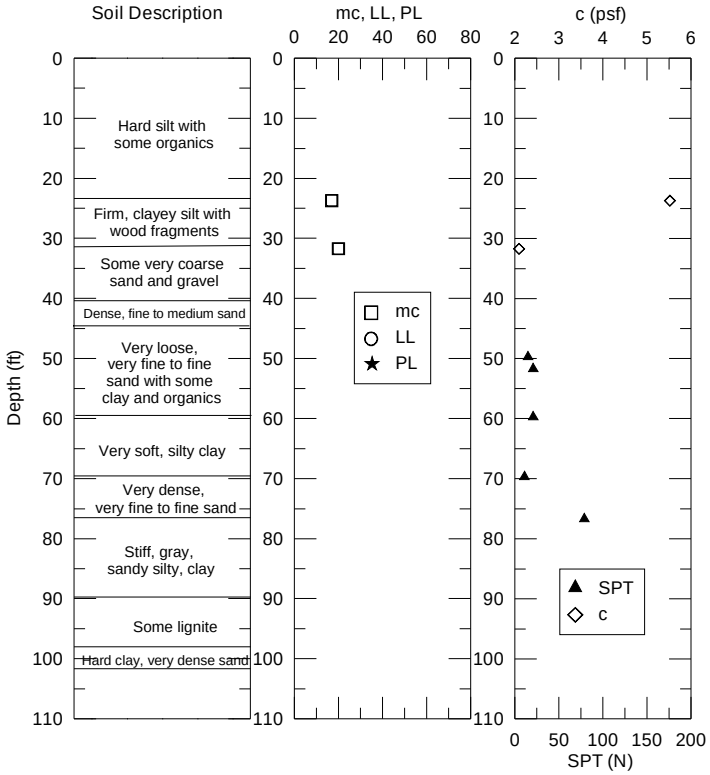

Figure 33
DS13

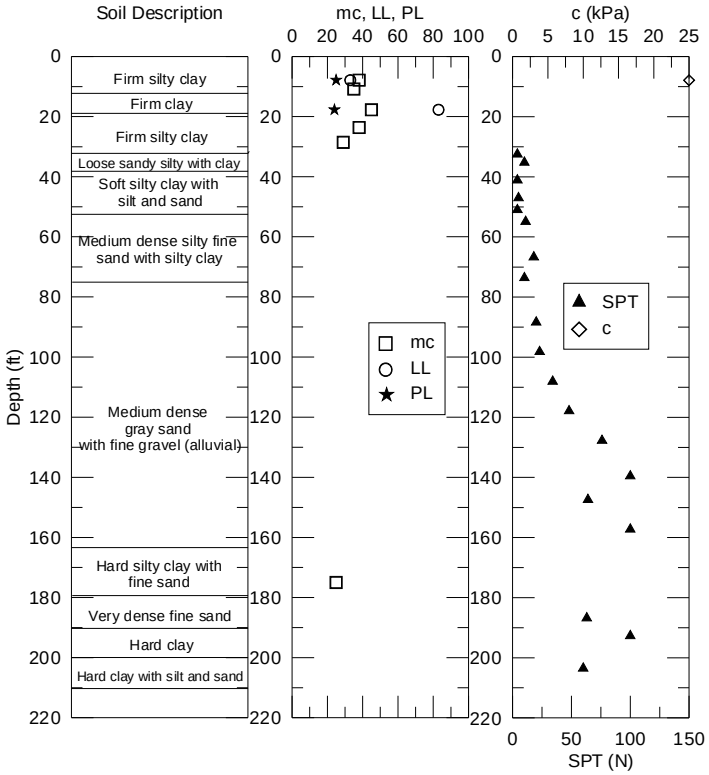

Figure 34
DS14

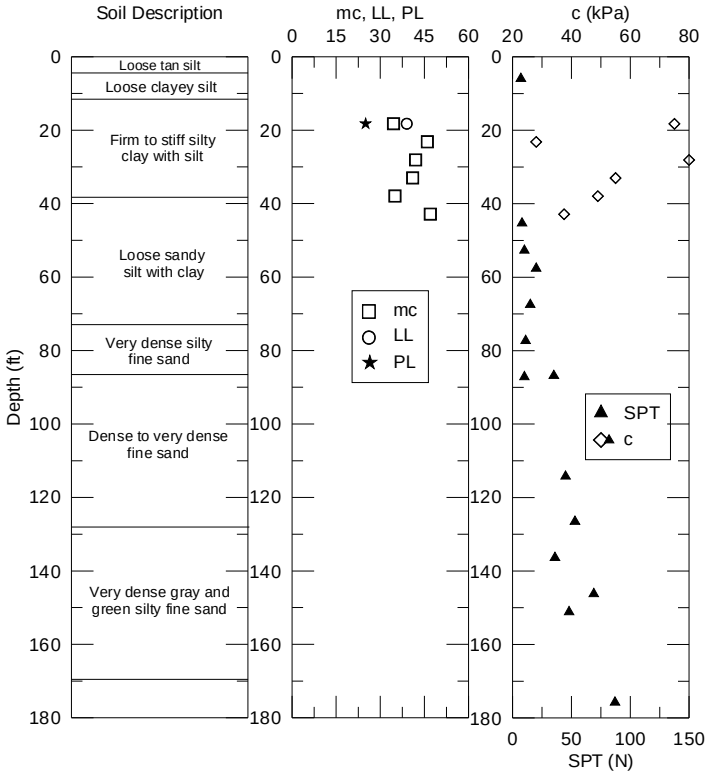

Figure 35
DS15

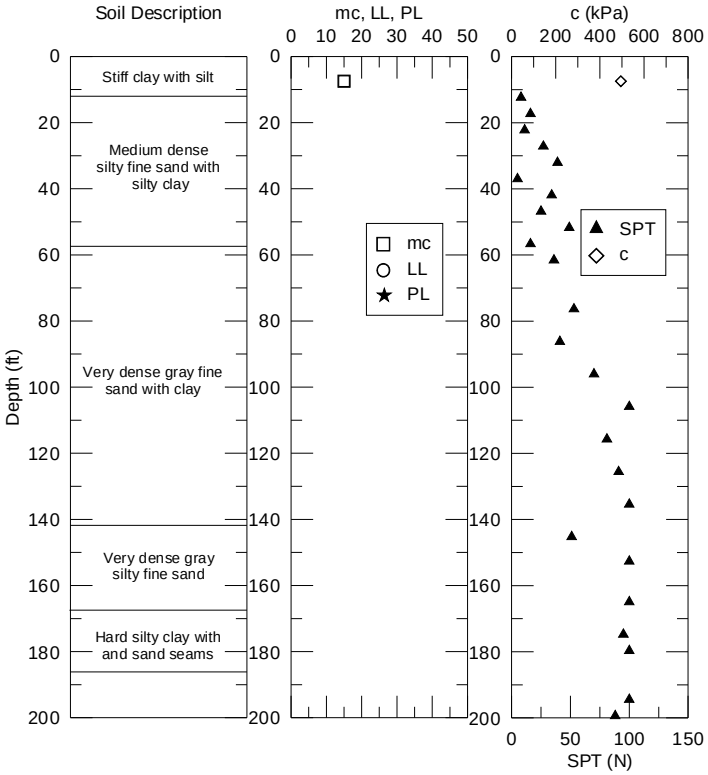

Figure 36
DS16

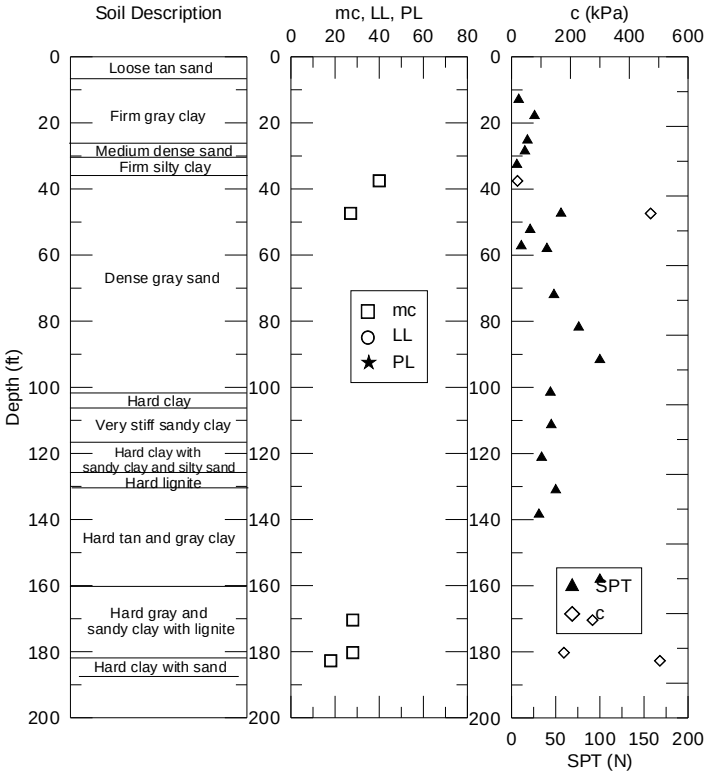

Figure 37
DS17

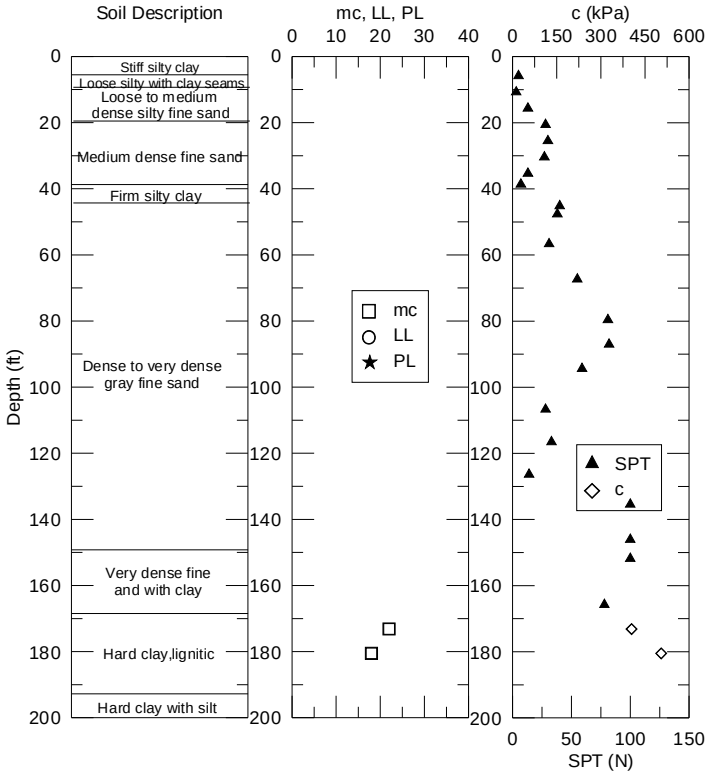

Figure 38
DS18

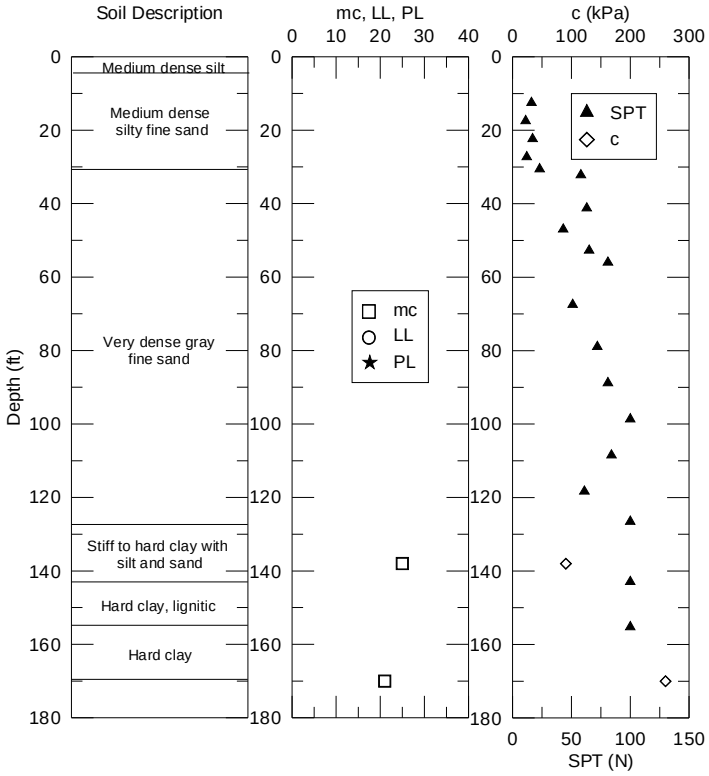

Figure 39
DS19

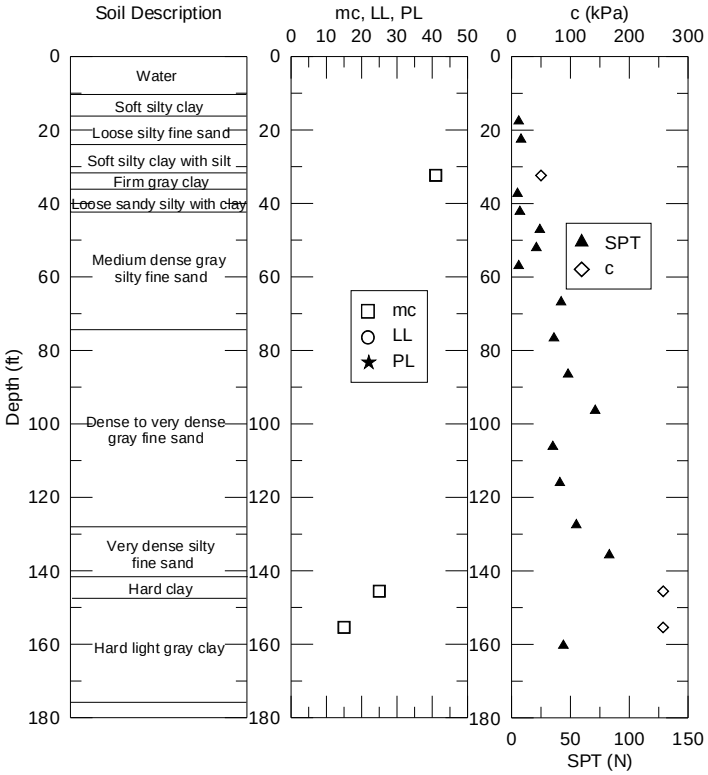

Figure 40
DS20

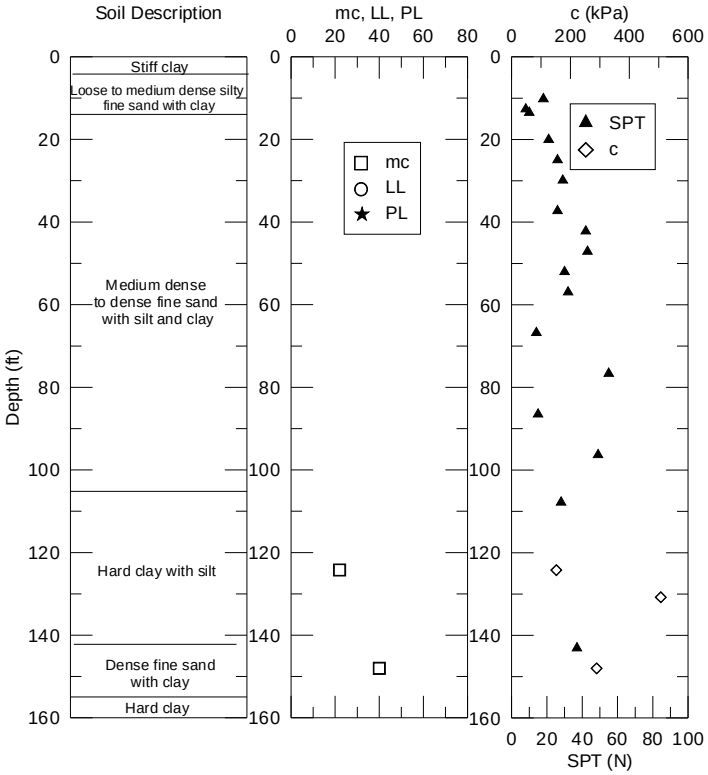

Figure 41
DS21

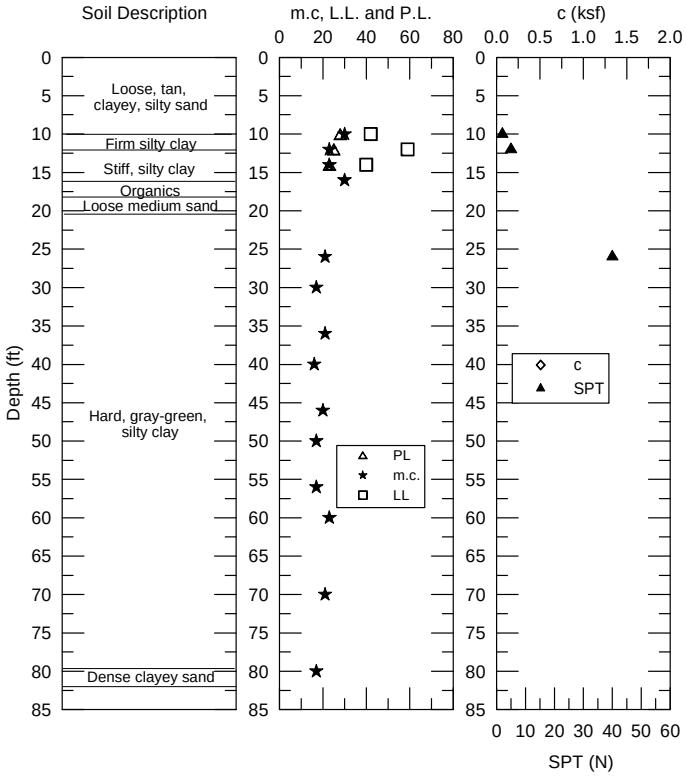

Figure 42
DS22

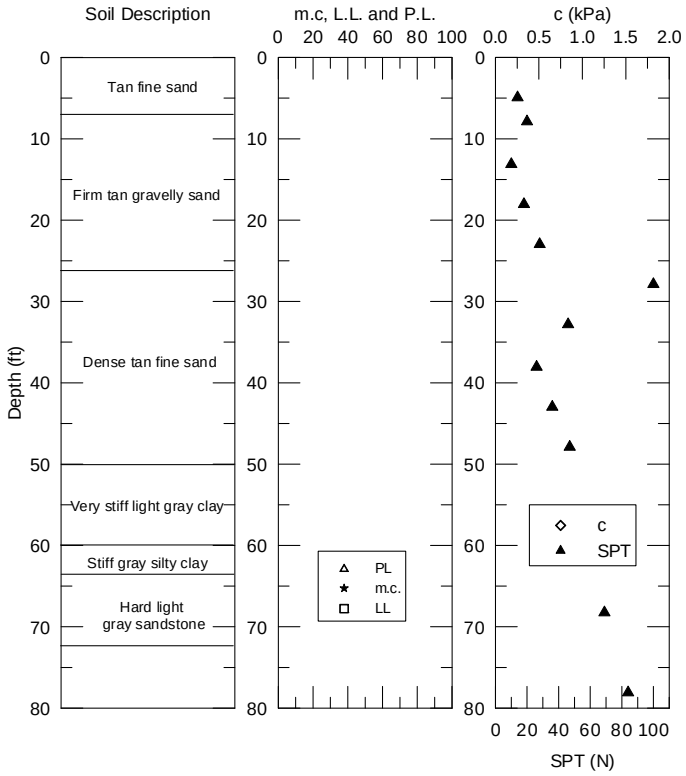

Figure 43
DS23

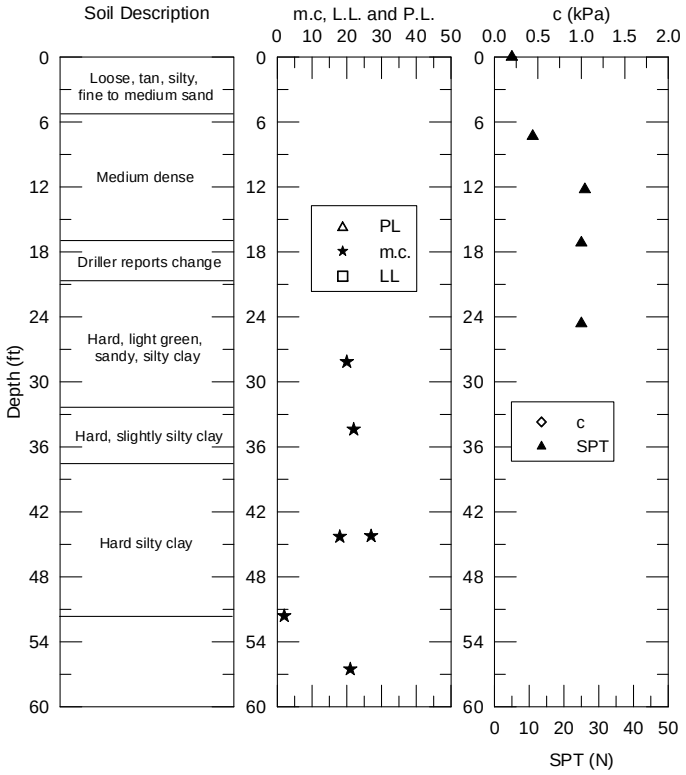

Figure 44
DS24

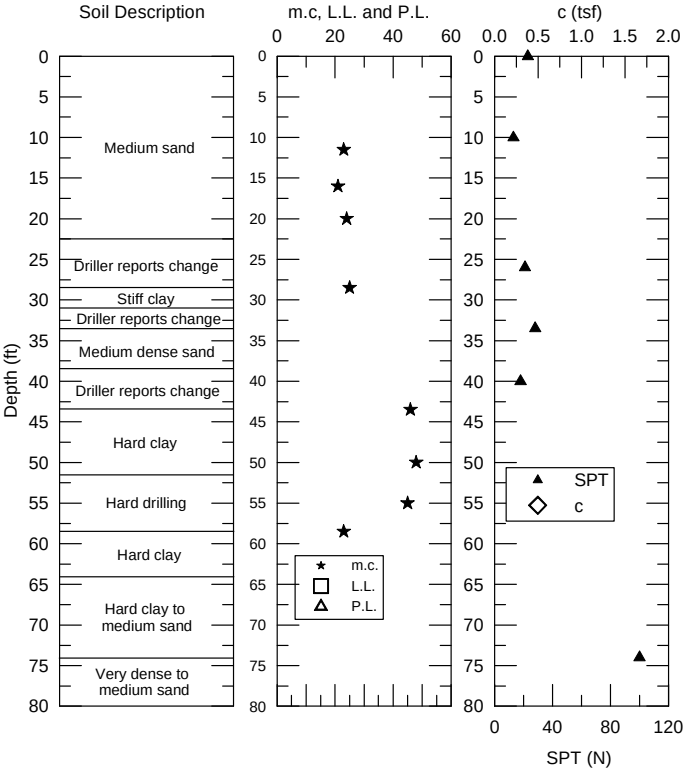

Figure 45
DS25

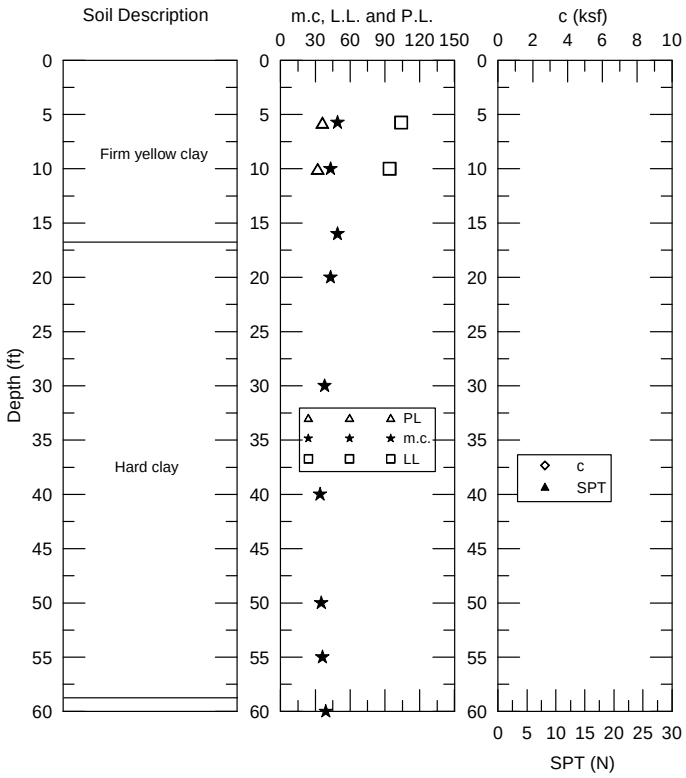

Figure 46
DS26

APPENDIX B

Measured Load-settlement Curves

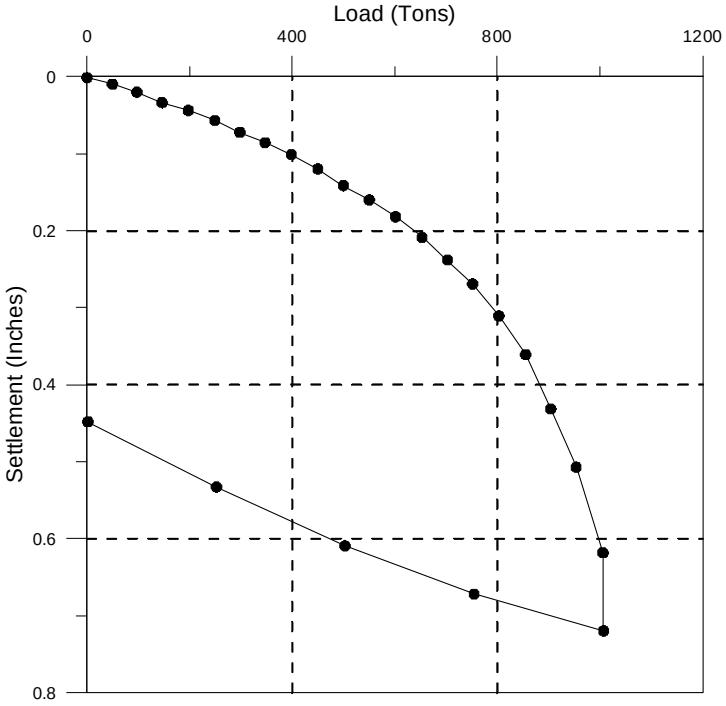

Figure 47
Top-down load settlement curve of DS01

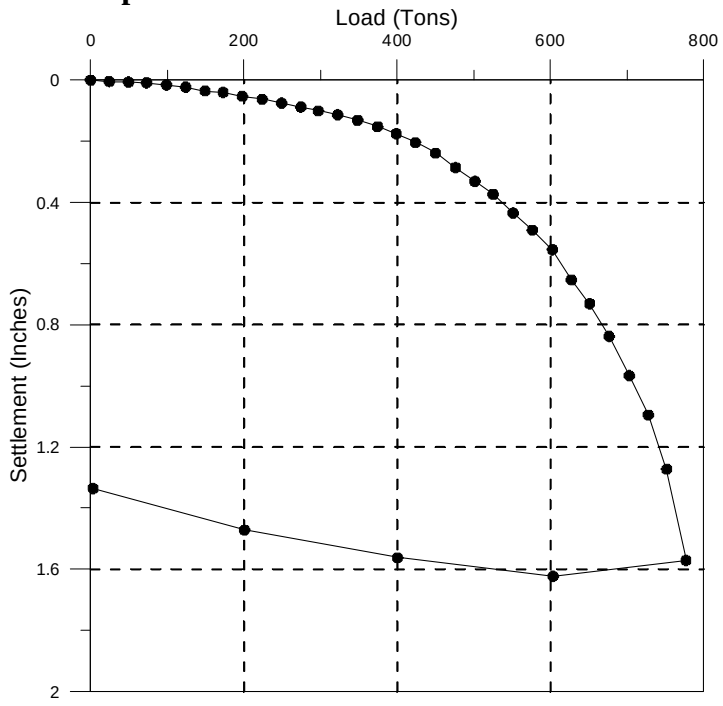

Figure 48
Top-down load settlement curve DS02

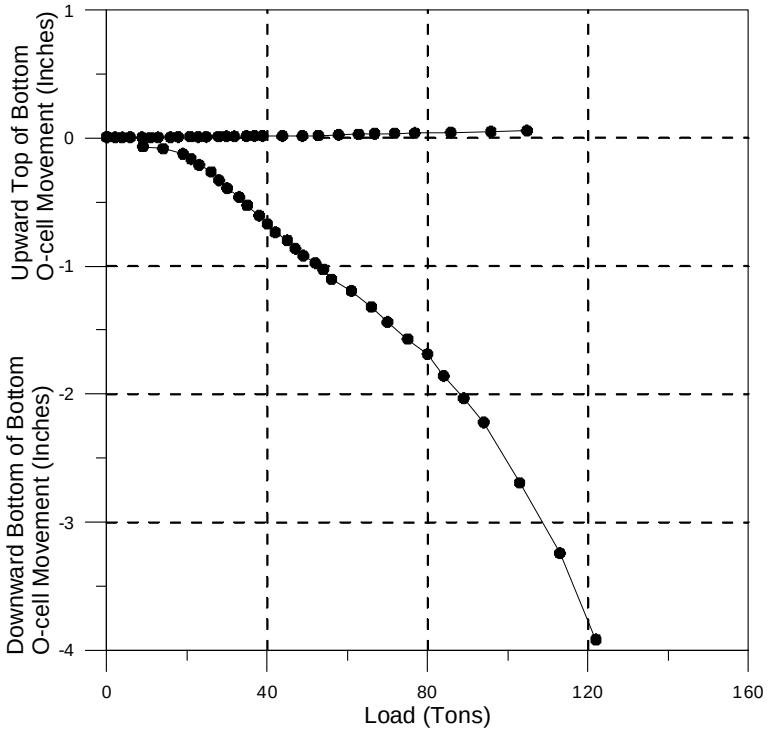

Figure 49
Lower O-cell load movement curves-stage 1 DS03

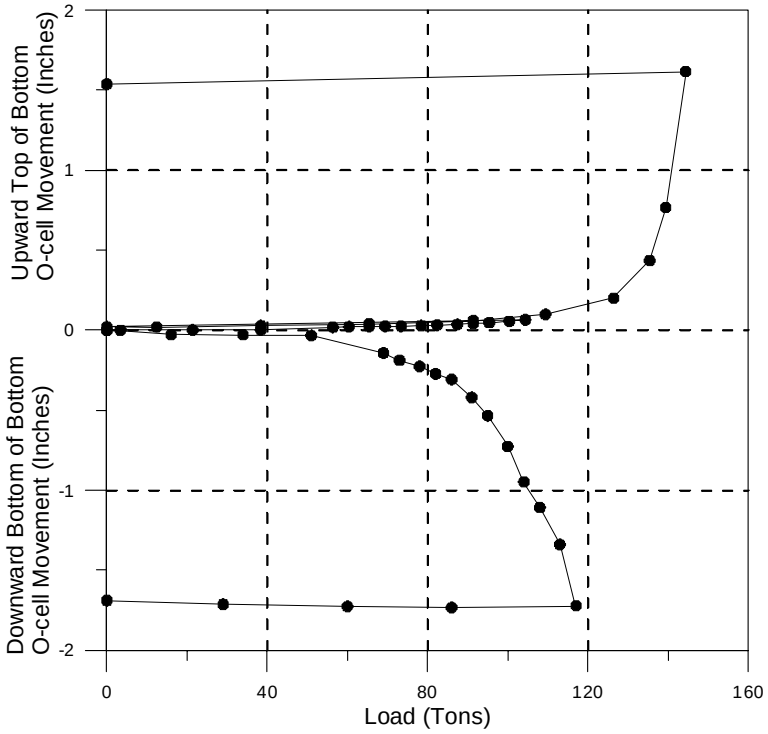

Figure 50
Upper O-cell load movement curves-stage 2 DS03

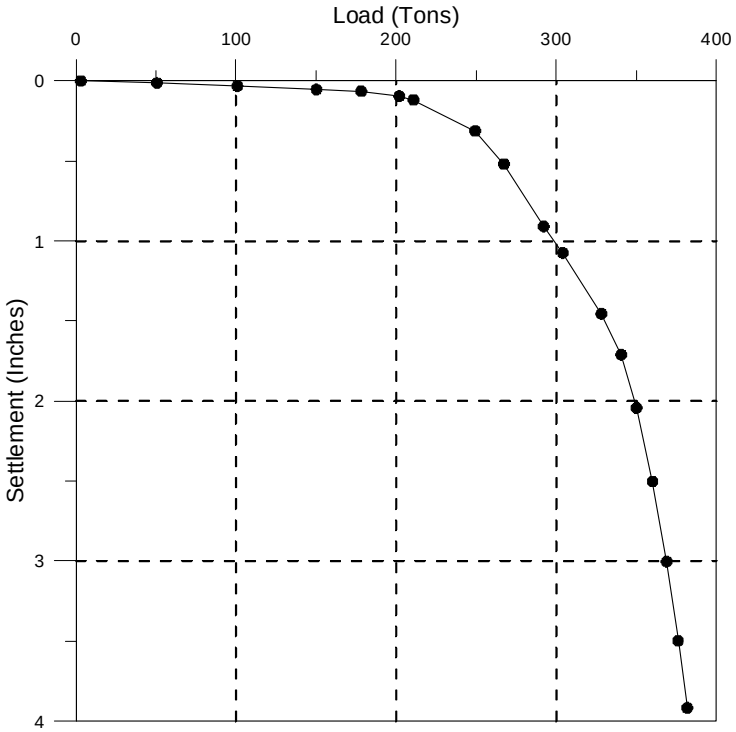

Figure 51
Equivalent top-down load settlement curve DS03

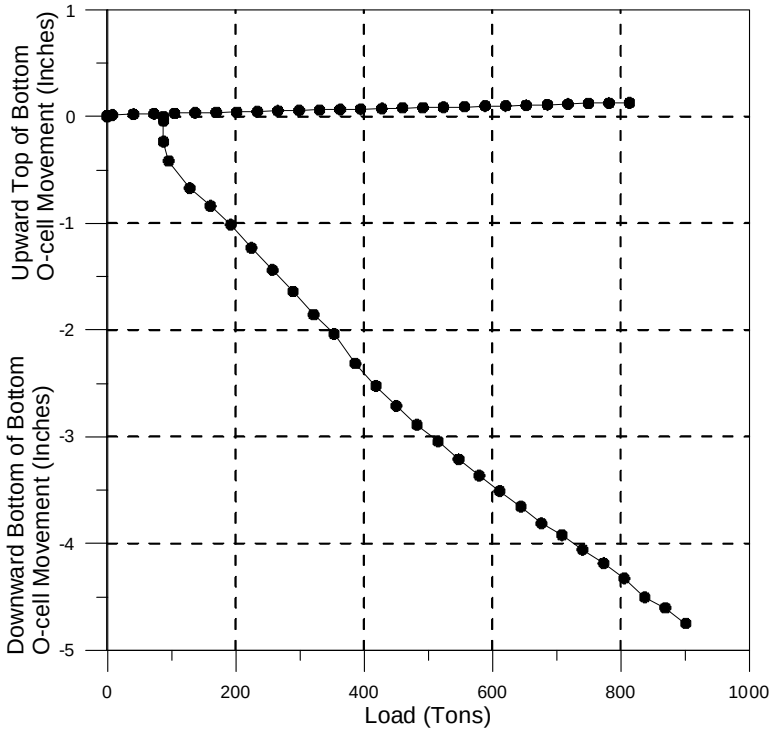

Figure 52
O-cell load settlement curve DS04

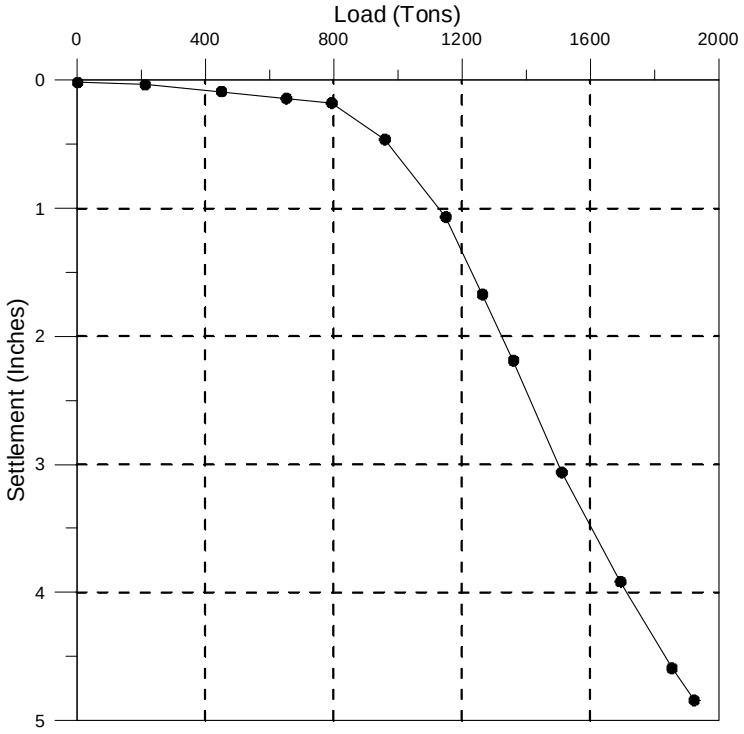

Figure 53
Equivalent top-down load settlement curve DS04

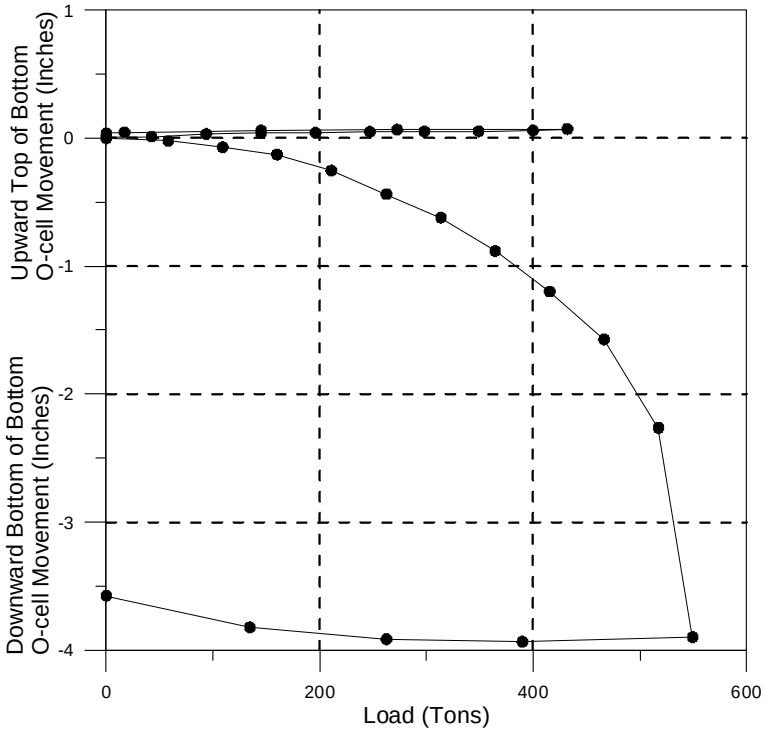

Figure 54

Lower O-cell load movement curves-stage 1 DS05

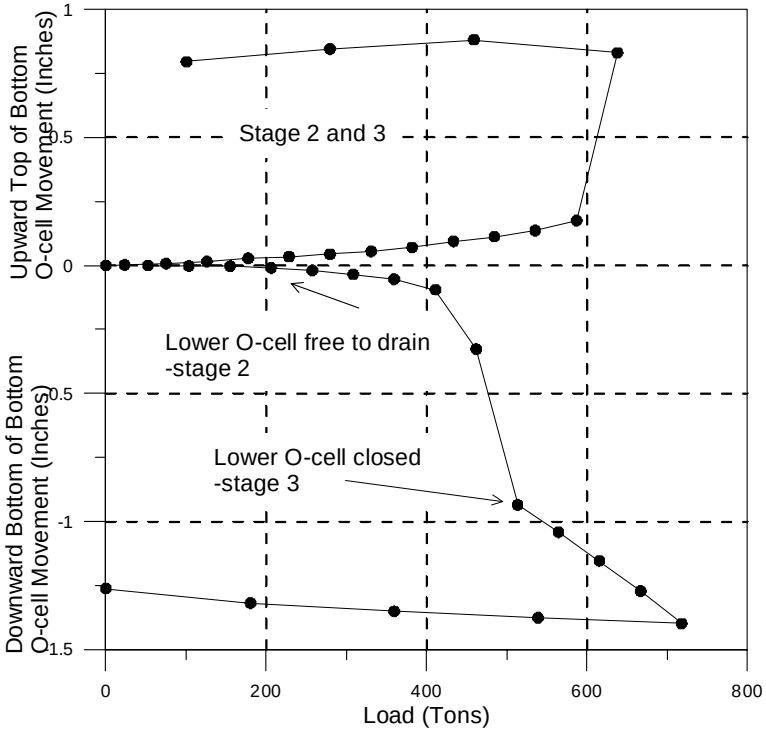

Figure 55

Upper O-cell load movement curves-stage 2 DS05

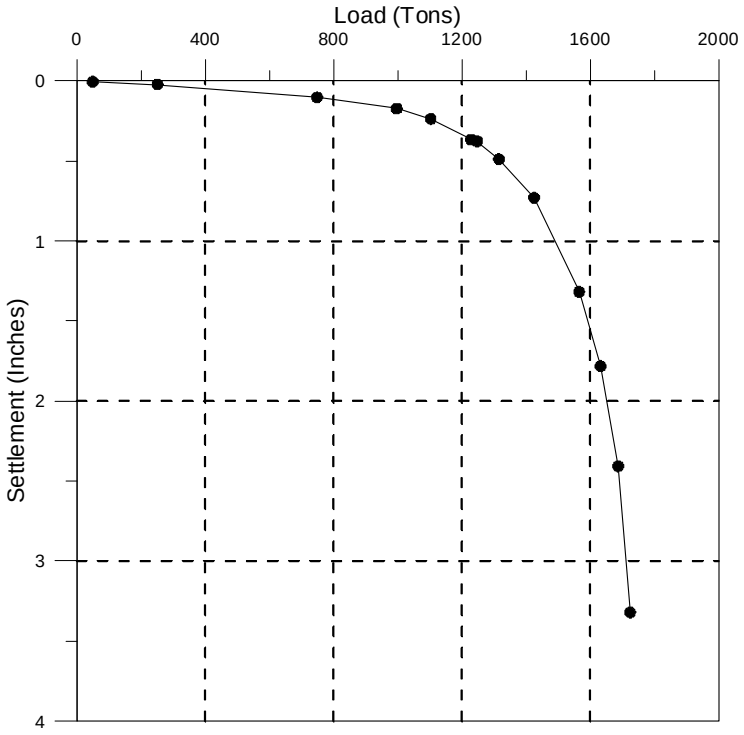

Figure 56
Equivalent top-down load settlement curve DS05

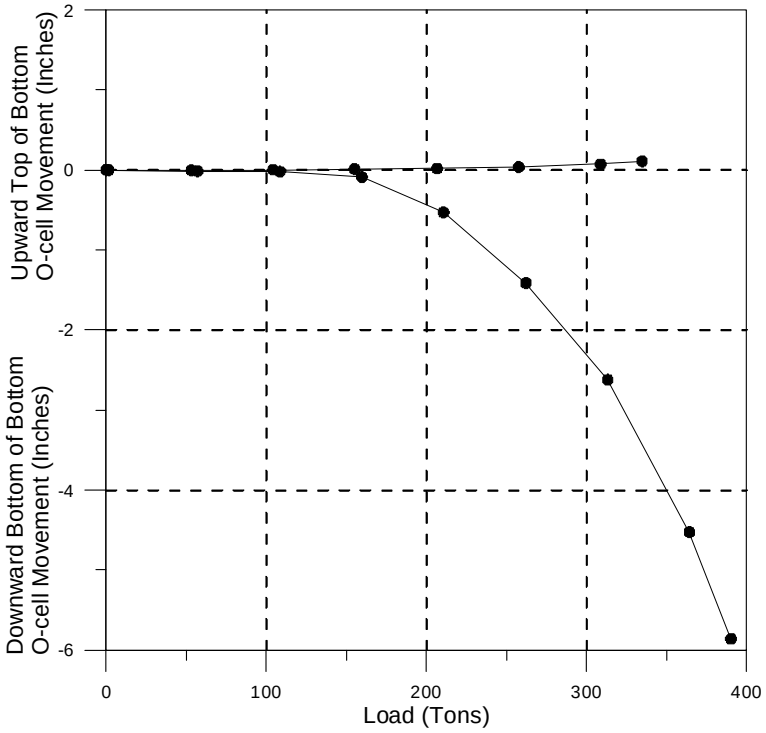

Figure 57
O-cell load settlement curve DS06

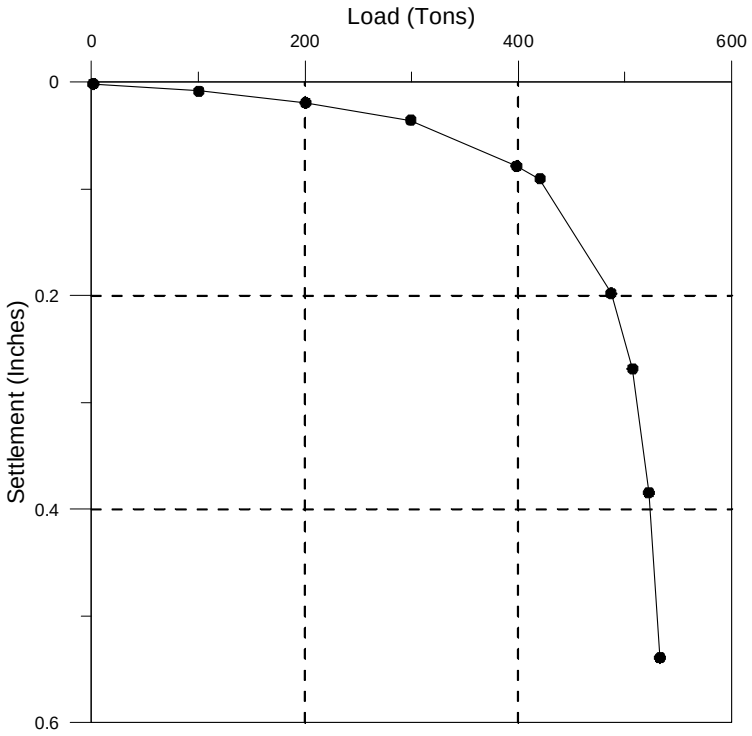

Figure 58
Equivalent top-down load settlement curve DS06

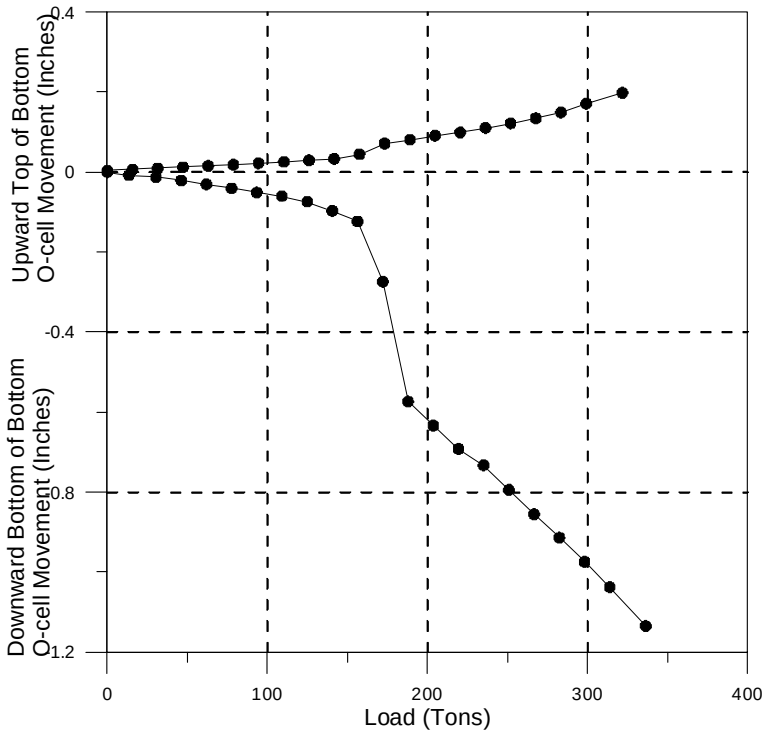

Figure 59
O-cell load settlement curve DS07

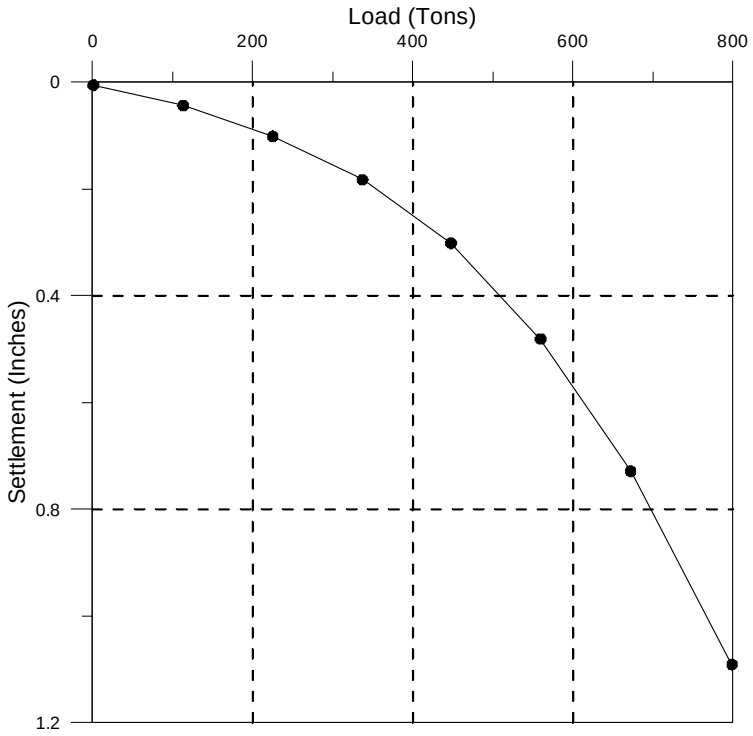

Figure 60
Equivalent top-down load settlement curve DS07

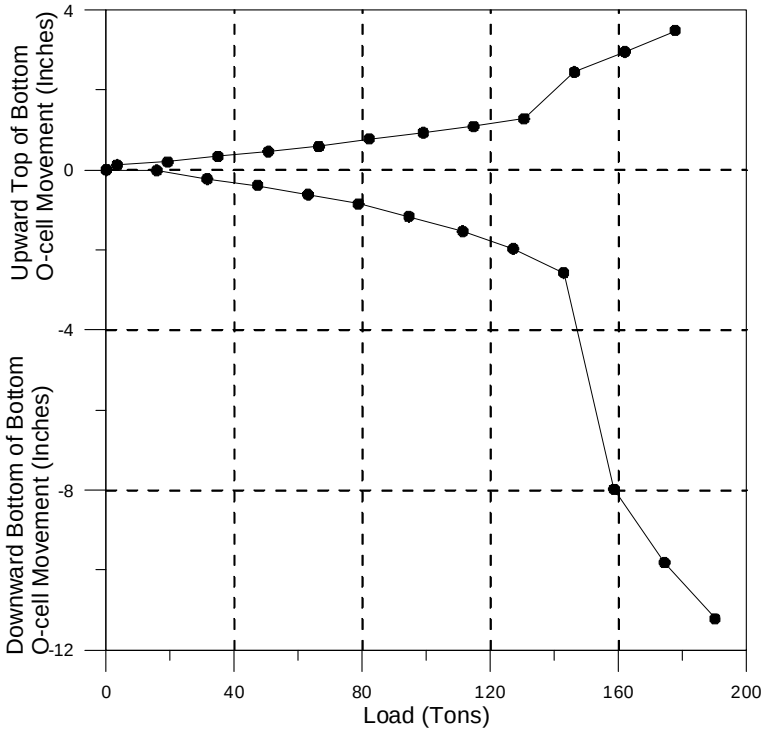

Figure 61
O-cell load settlement curve DS08

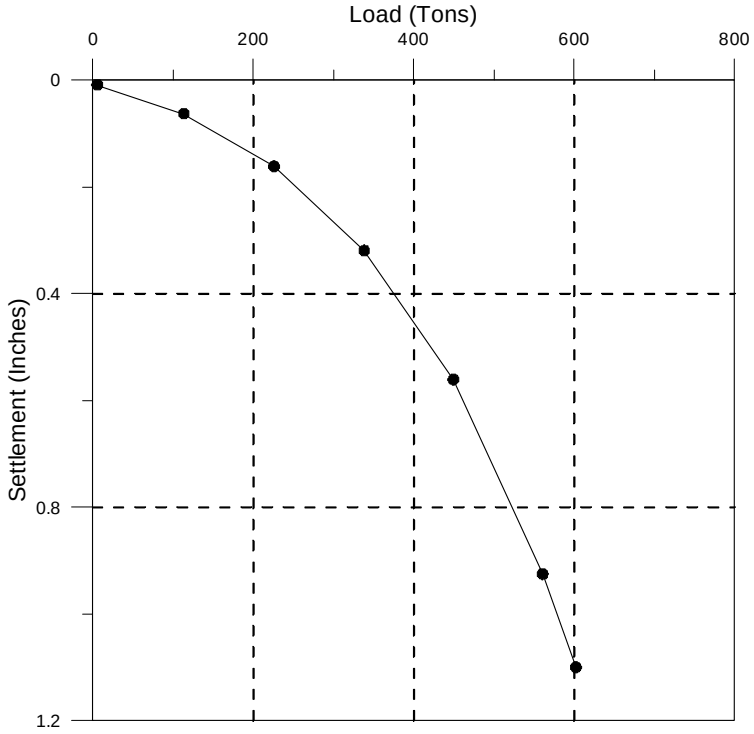

Figure 62
Equivalent top-down load settlement curve DS08

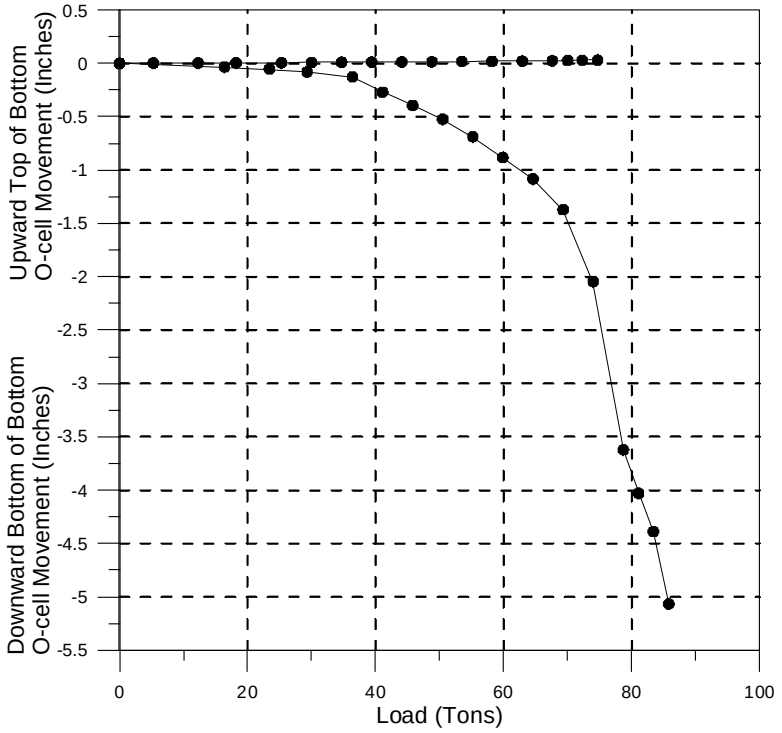

Figure 63

Lower O-cell load movement curves-stage 1 DS09

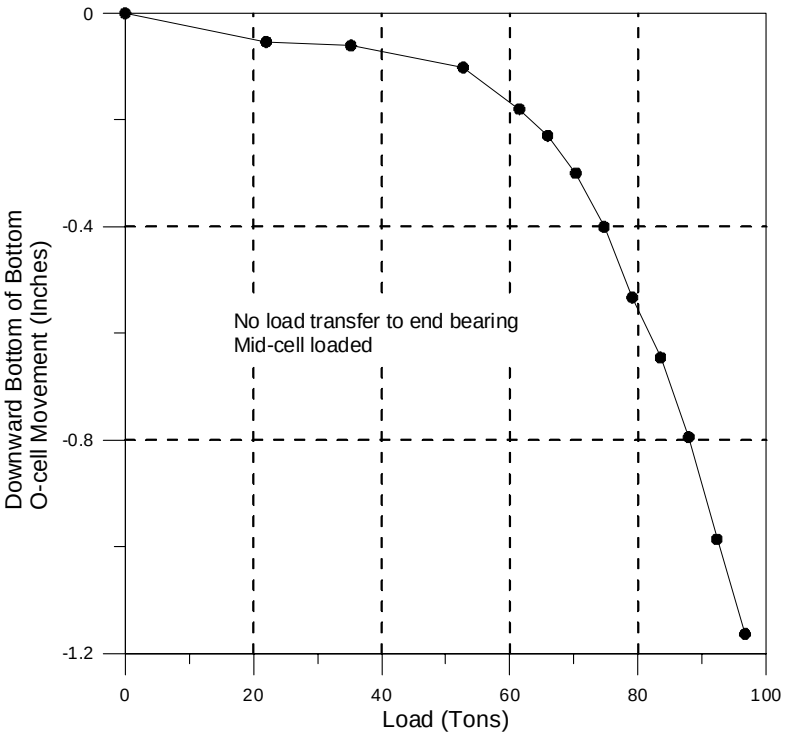

Figure 64

Upper O-cell load movement curves-stage 2 DS09

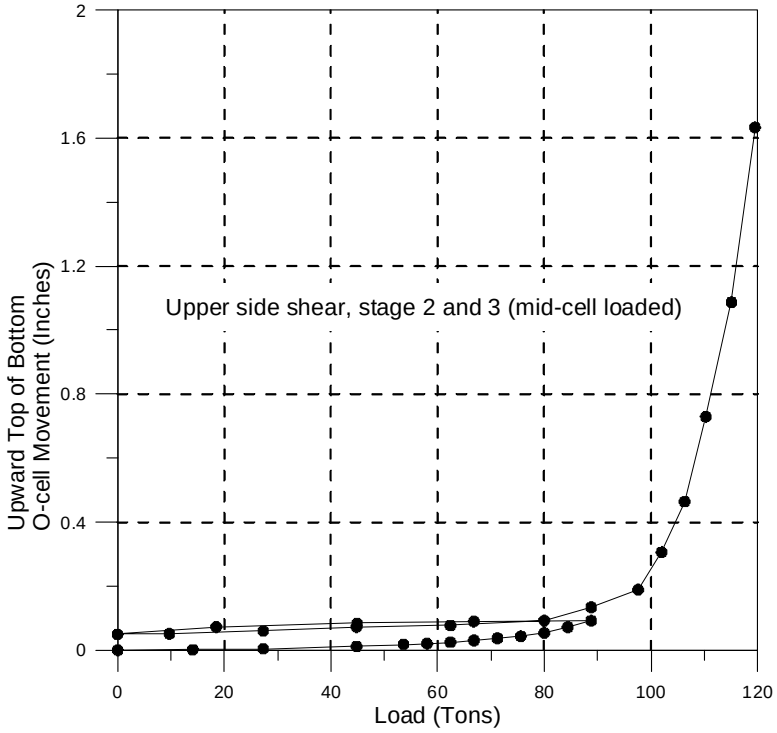

Figure 65
Upper O-cell load movement curves-stage 2 and3 DS09

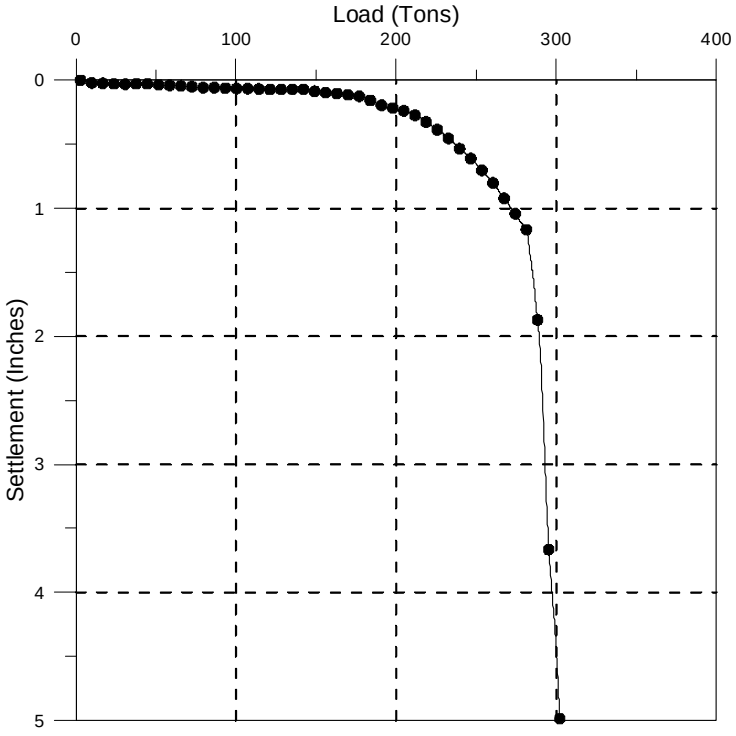

Figure 66
Equivalent top-down load settlement curve DS09

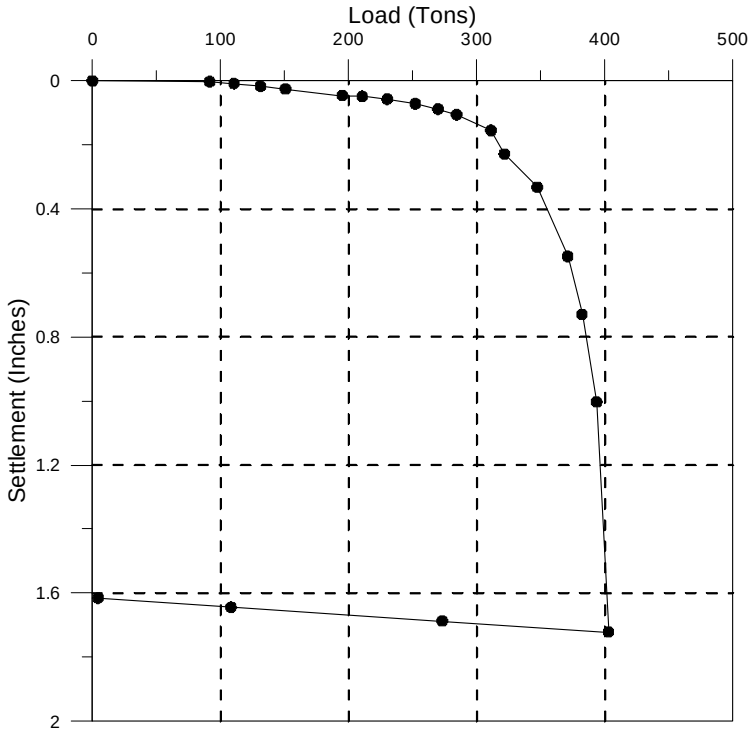

Figure 67
Top-down load settlement curve of DS10

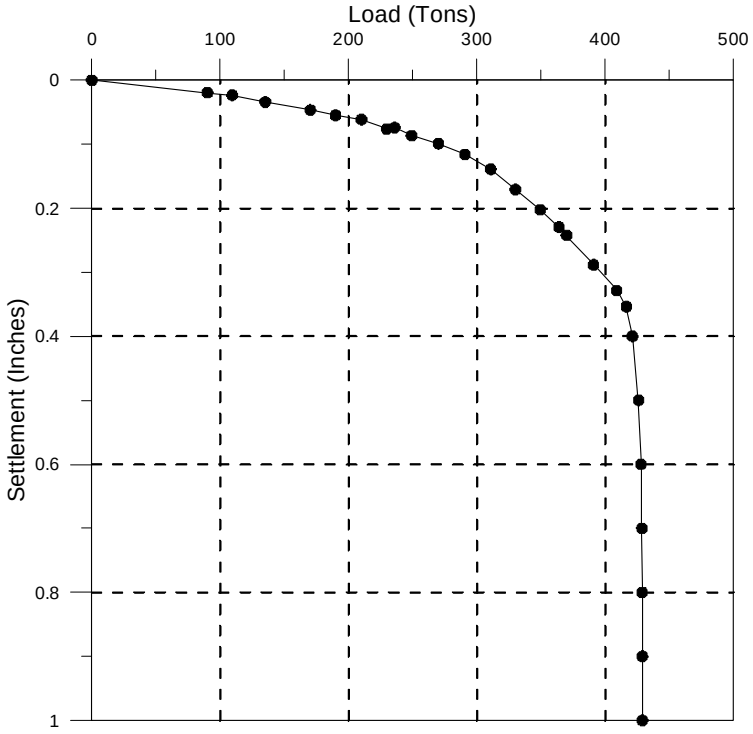

Figure 68
Top-down load settlement curve of DS11

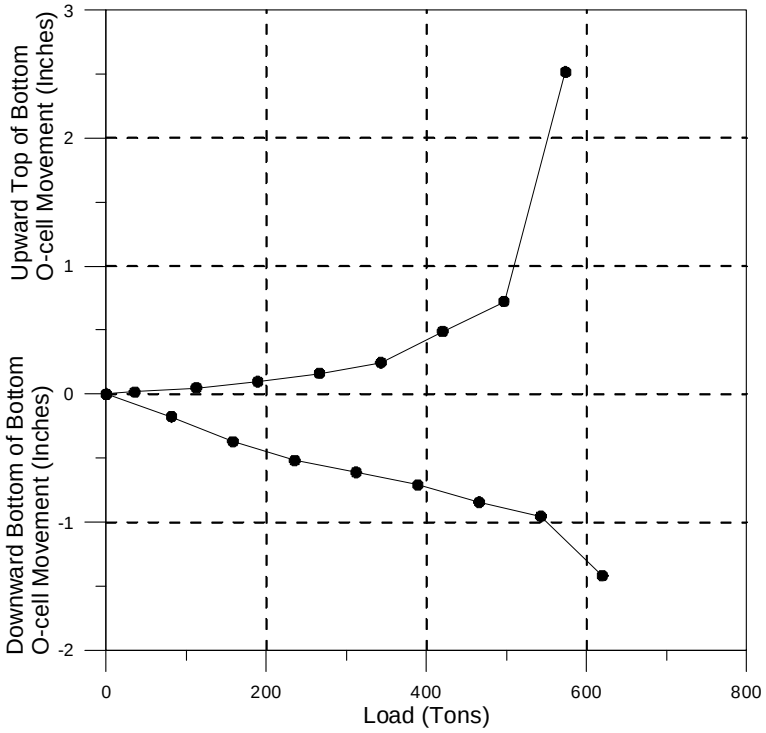

Figure 69
O-cell load settlement curve DS12

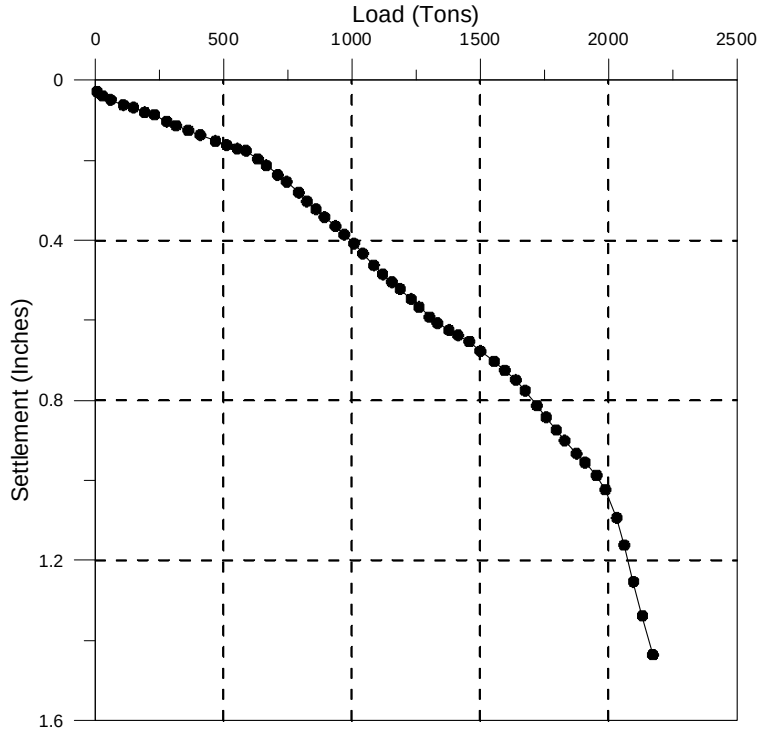

Figure 70
Equivalent top-down load settlement curve DS12

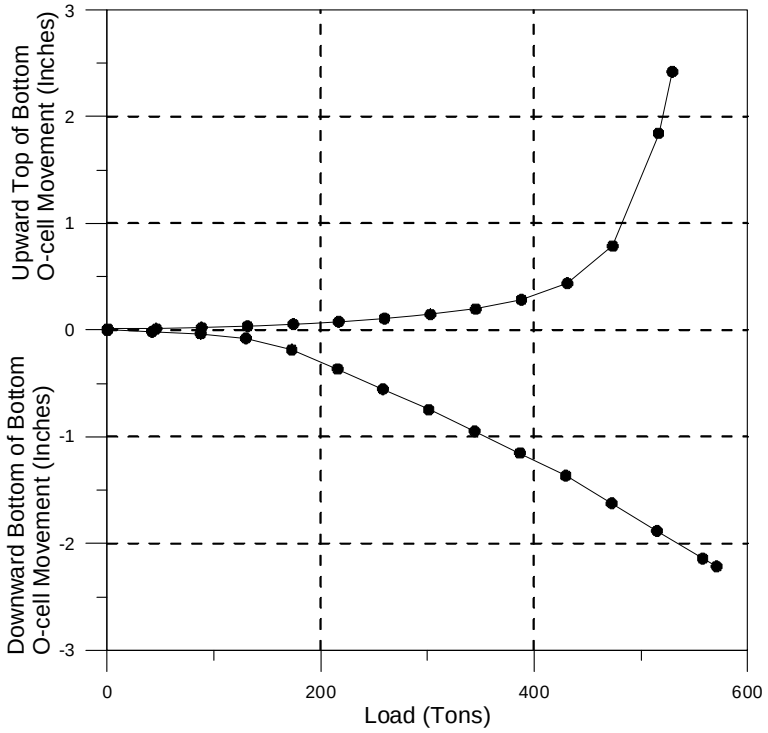

Figure 71
O-cell load settlement curve DS13

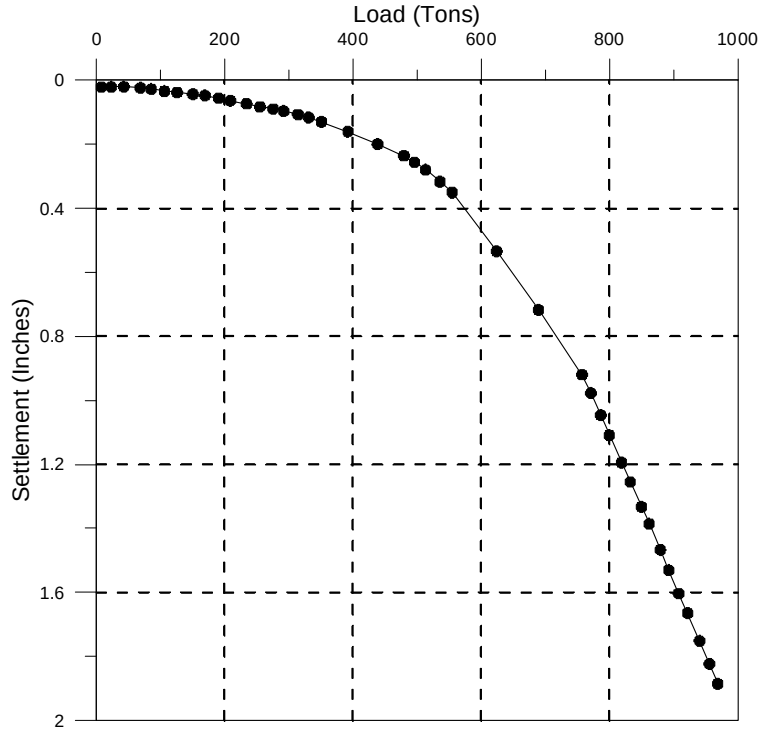

Figure 72
Equivalent top-down load settlement curve DS13

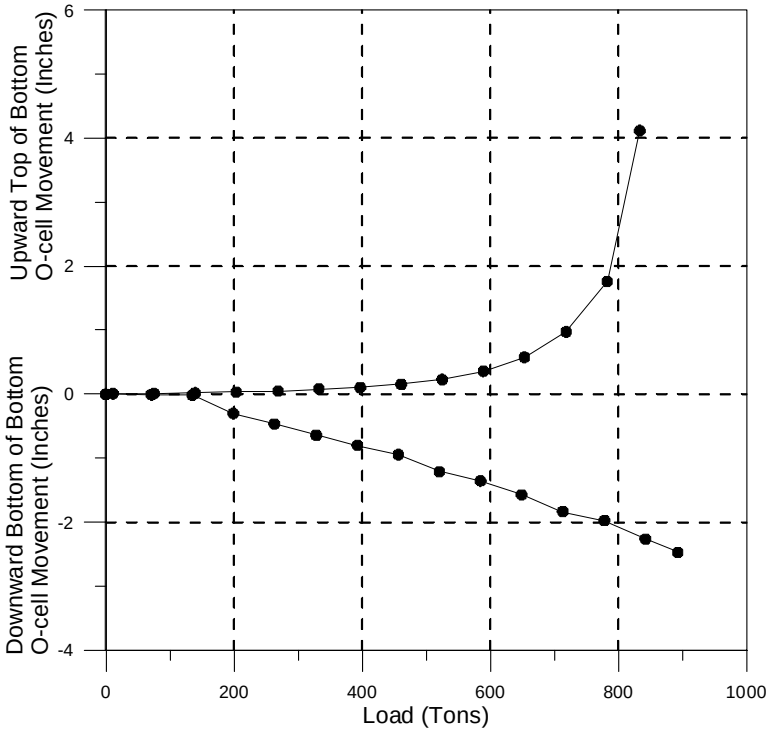

Figure 73
O-cell load settlement curve DS14

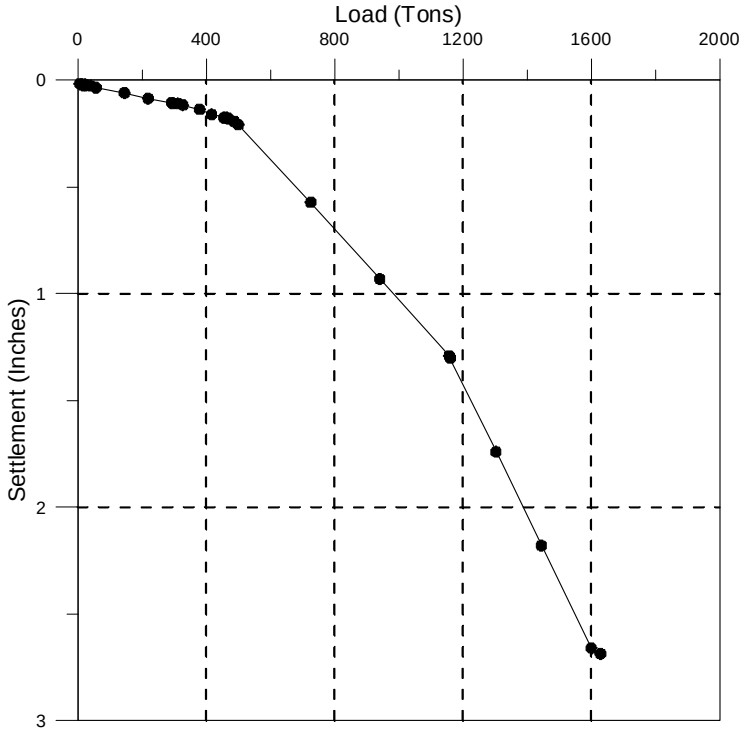

Figure 74
Equivalent top-down load settlement curve DS14

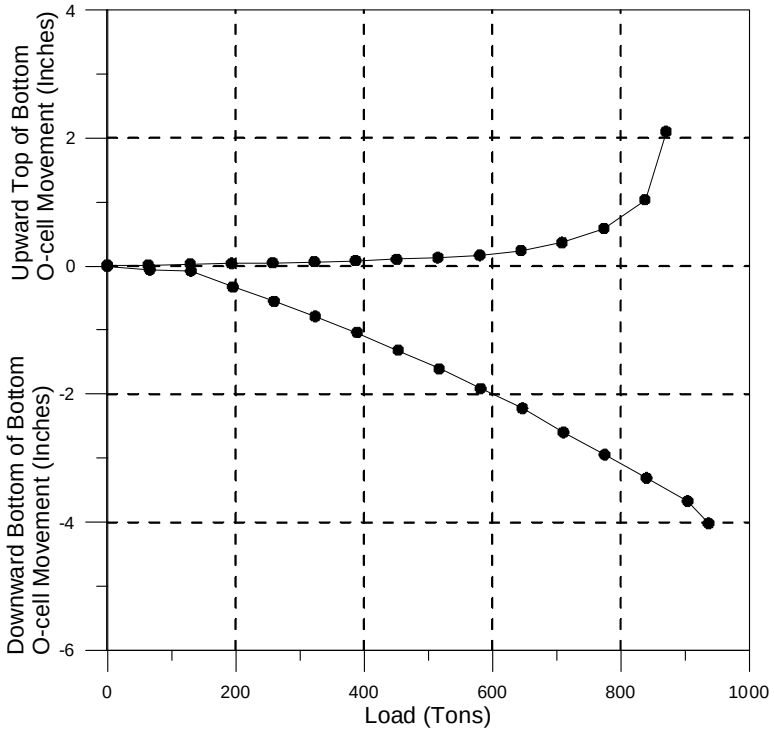

Figure 75
O-cell load settlement curve DS15

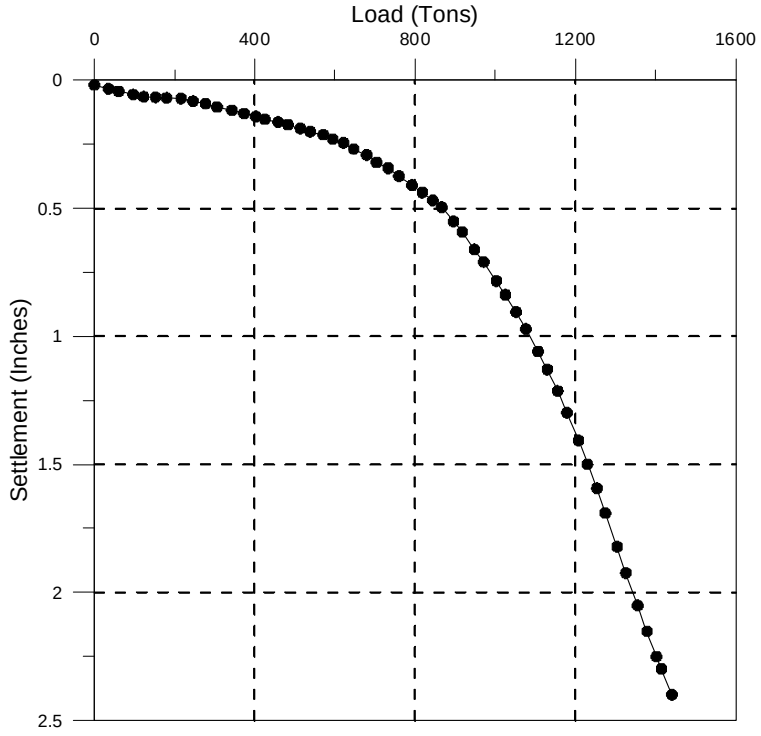

Figure 76
Equivalent top-down load settlement curve DS15

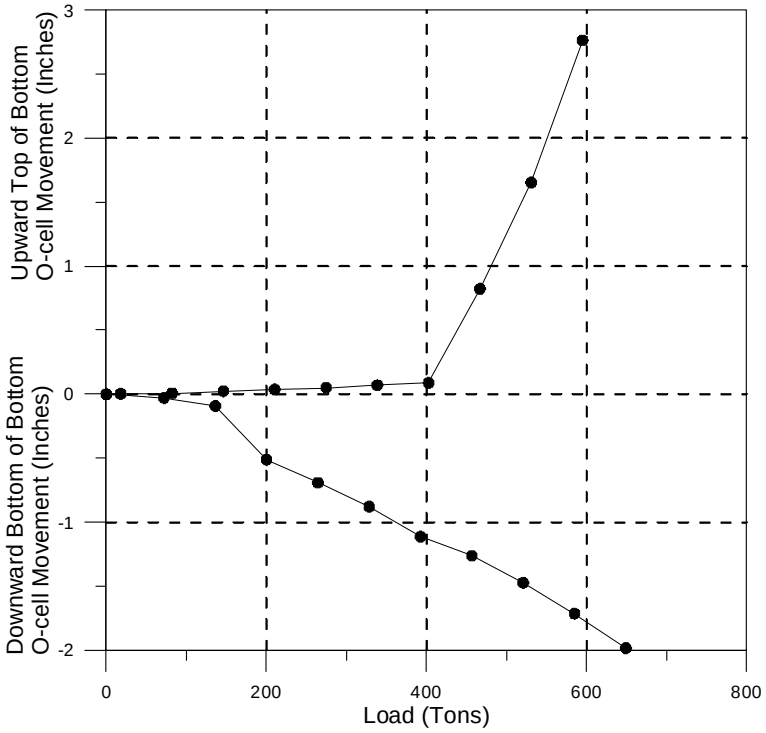

Figure 77
O-cell load settlement curve DS16

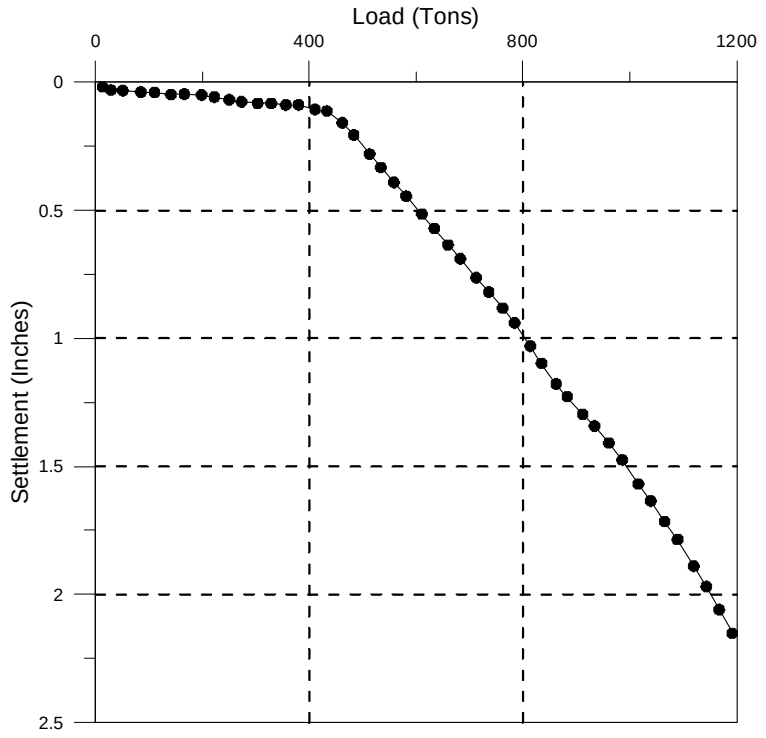

Figure 78
Equivalent top-down load settlement curve DS16

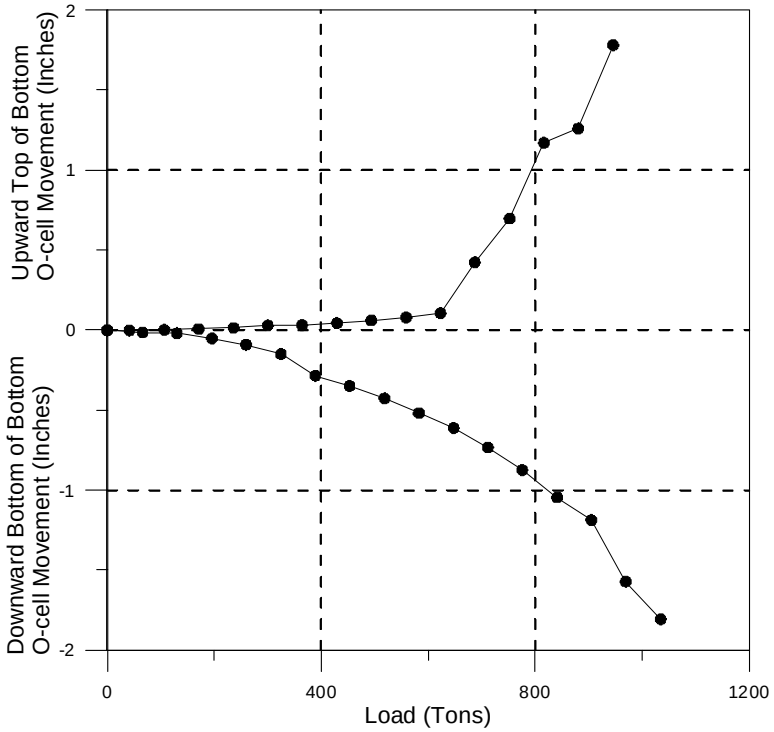

Figure 79
O-cell load settlement curve DS17

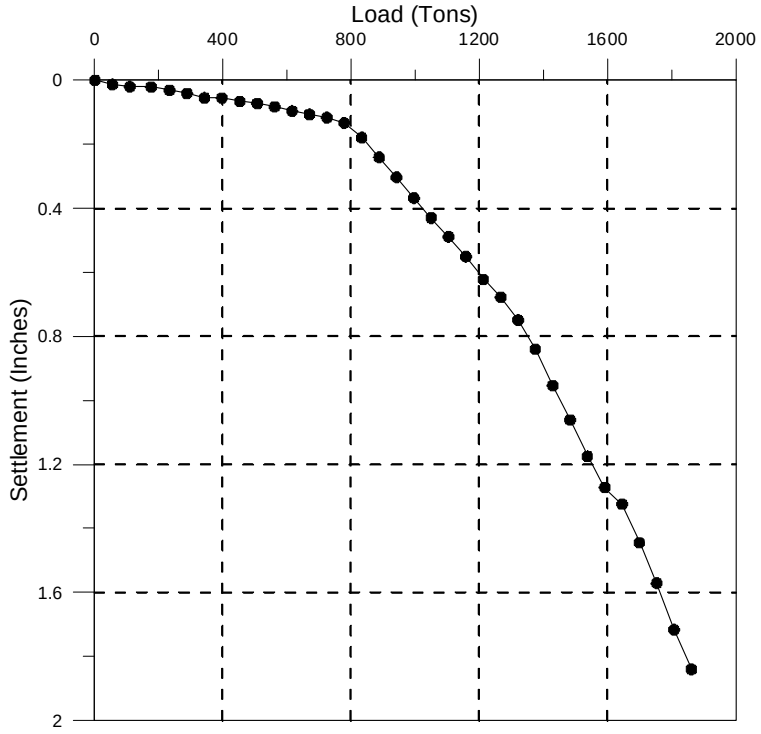

Figure 80
Equivalent top-down load settlement curve DS17

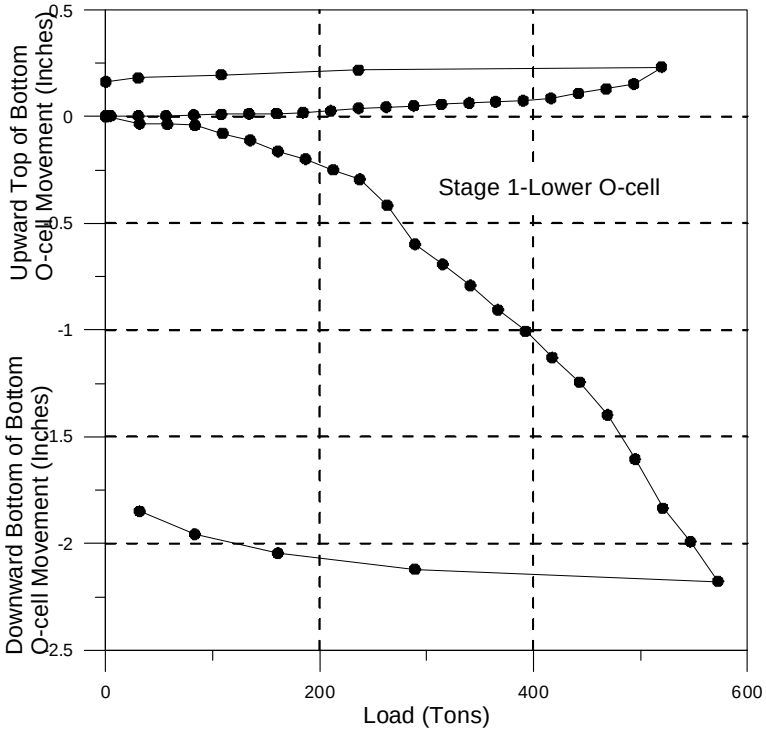

Figure 81

Lower O-cell load movement curves-stage 1 DS18

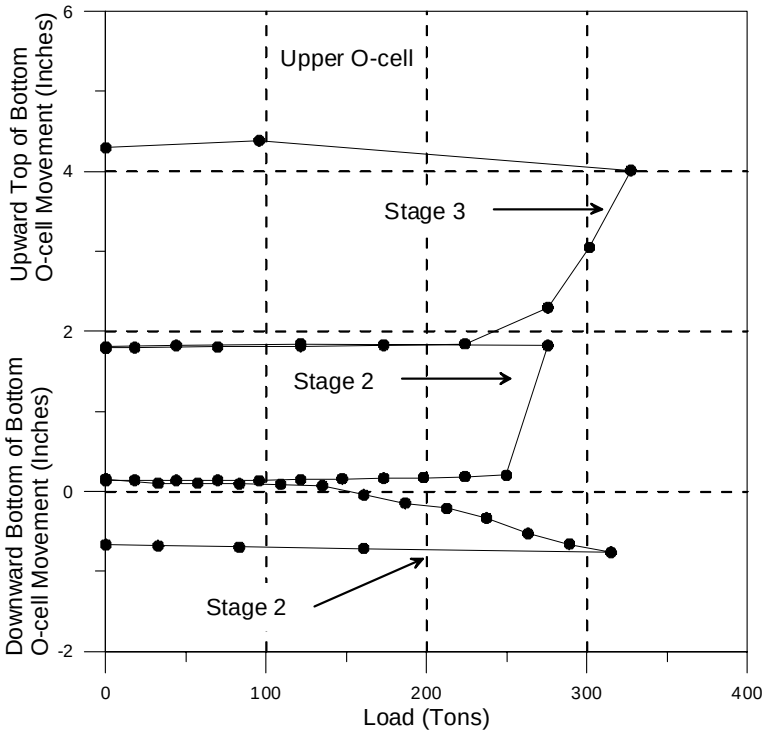

Figure 82

Upper O-cell load movement curves-stage 2 DS18

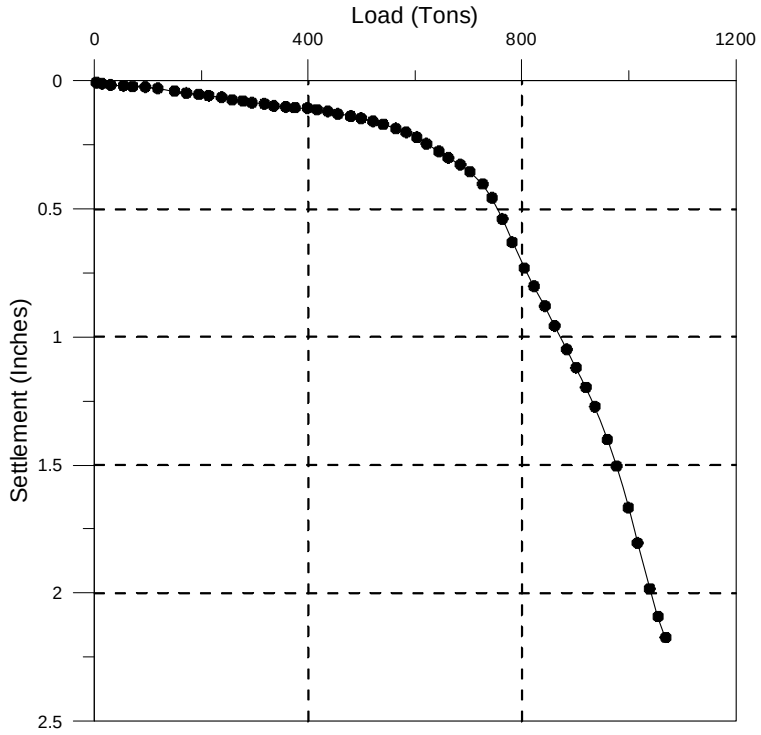

Figure 83
Equivalent top-down load settlement curve DS18

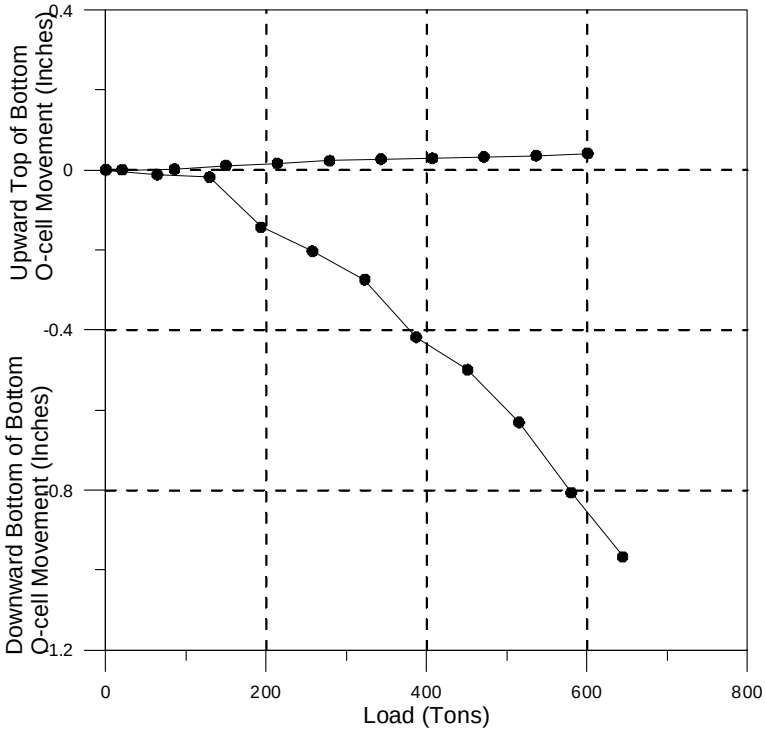

Figure 84
O-cell load settlement curve DS19

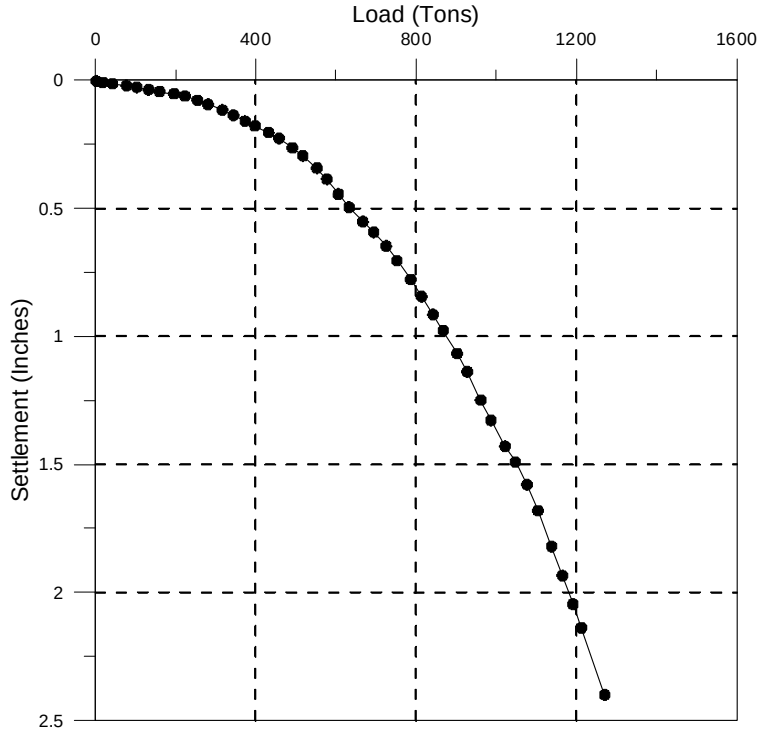

Figure 85
Equivalent top-down load settlement curve DS19

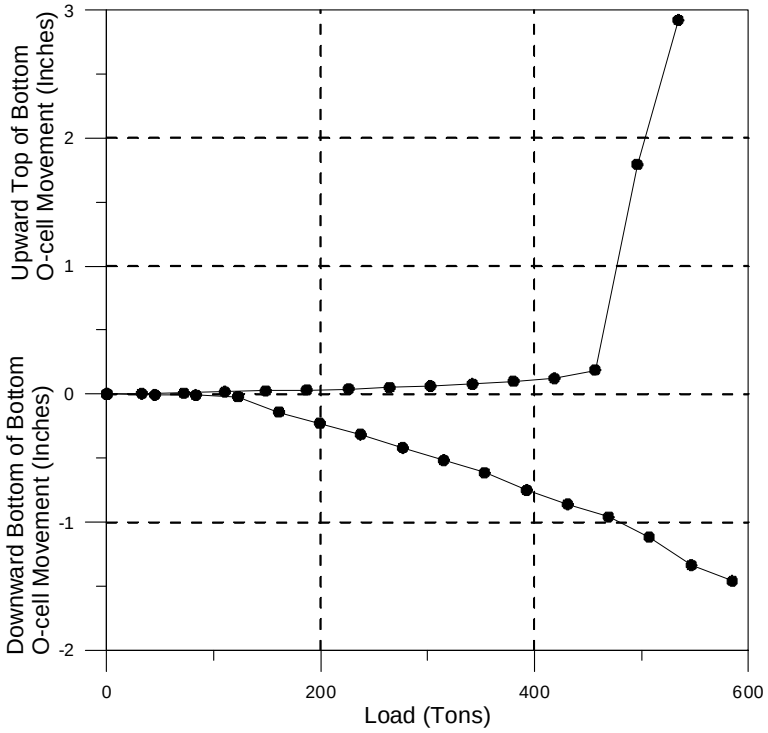

Figure 86
O-cell load settlement curve DS20

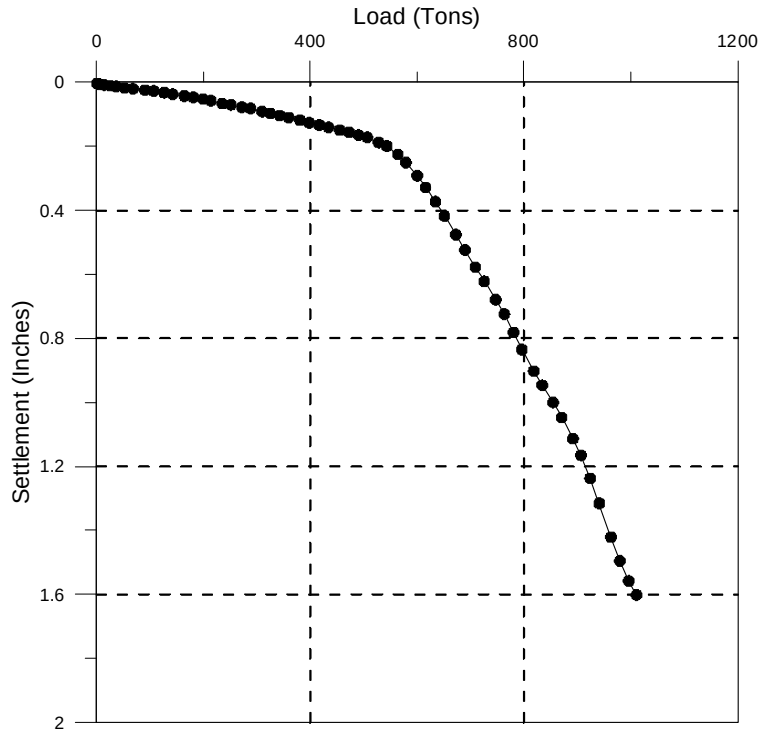

Figure 87
Equivalent top-down load settlement curve DS20

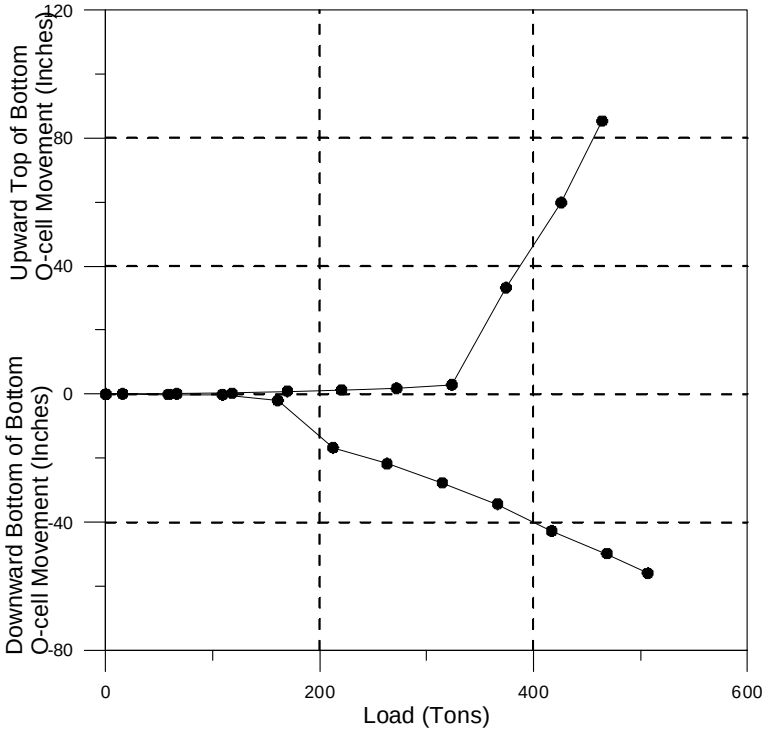

Figure 88
O-cell load settlement curve DS21

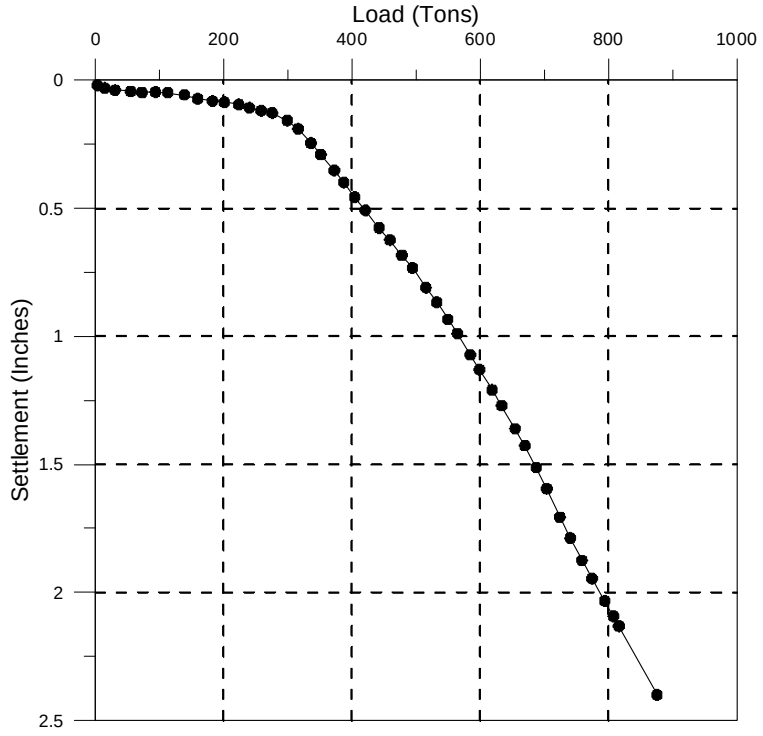

Figure 89
Equivalent top-down load settlement curve DS21

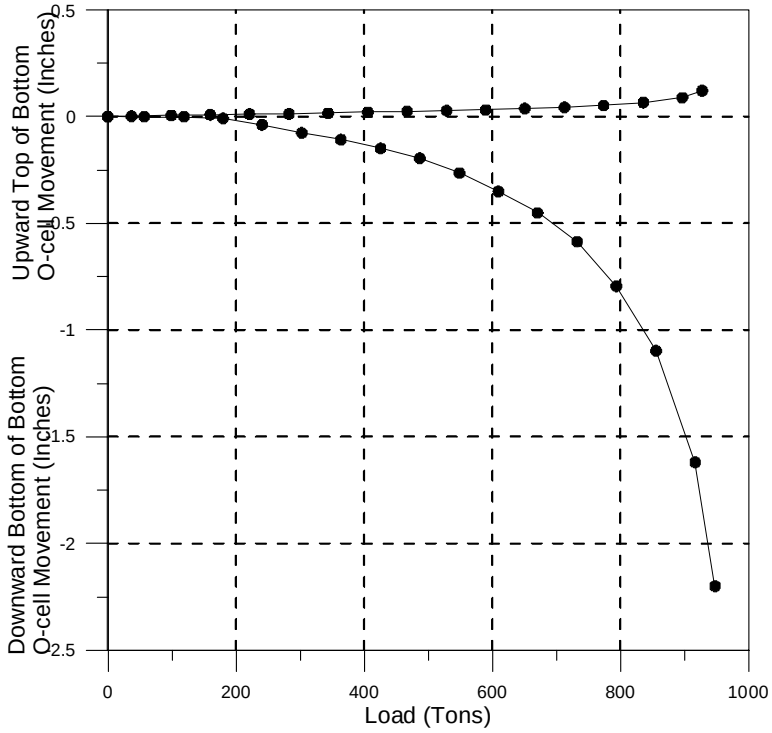

Figure 90
O-cell load settlement curve DS22

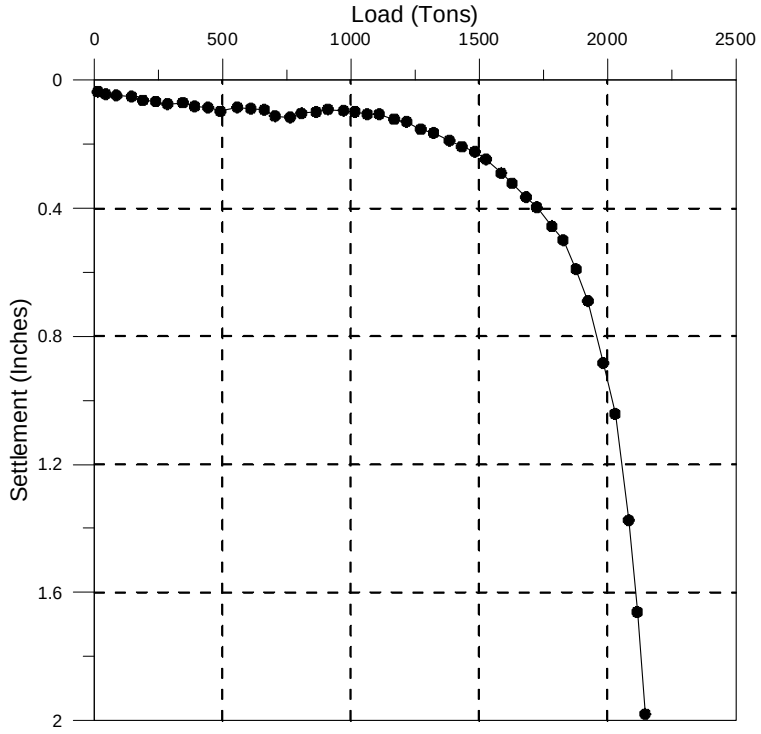

Figure 91
Equivalent top-down load settlement curve DS22

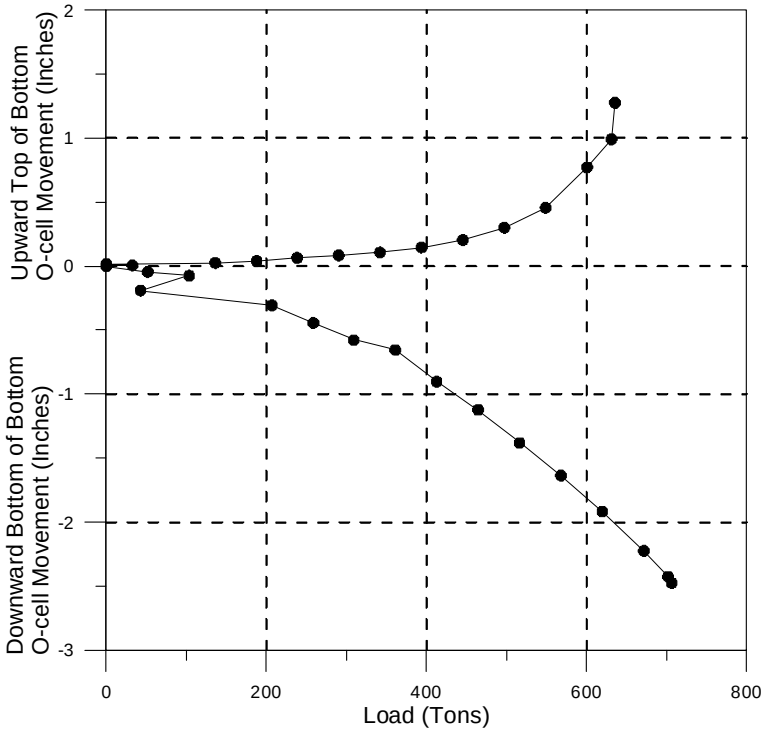

Figure 92
O-cell load settlement curve DS23

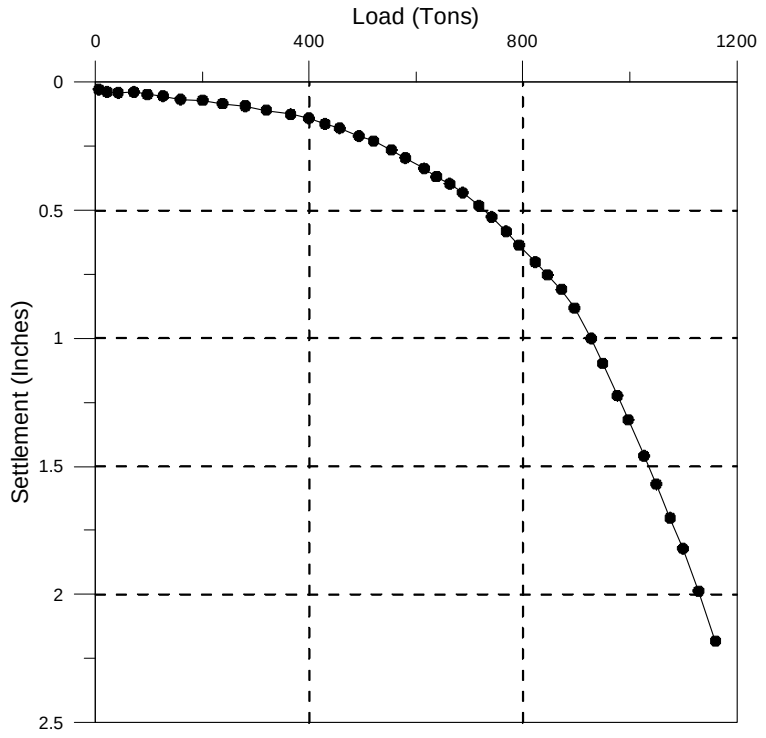

Figure 93
Equivalent top-down load settlement curve DS23

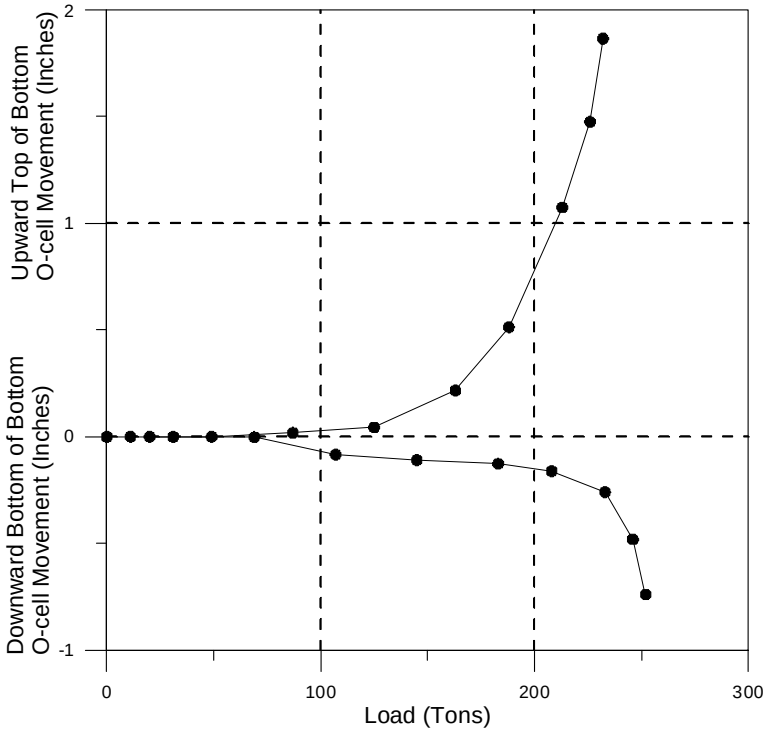

Figure 94
O-cell load settlement curve DS24

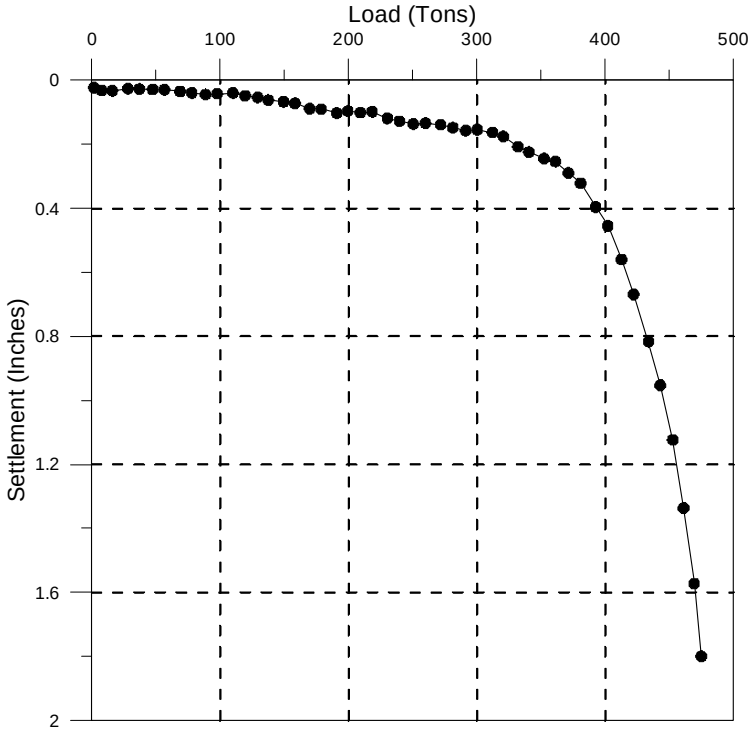

Figure 95
Equivalent top-down load settlement curve DS24

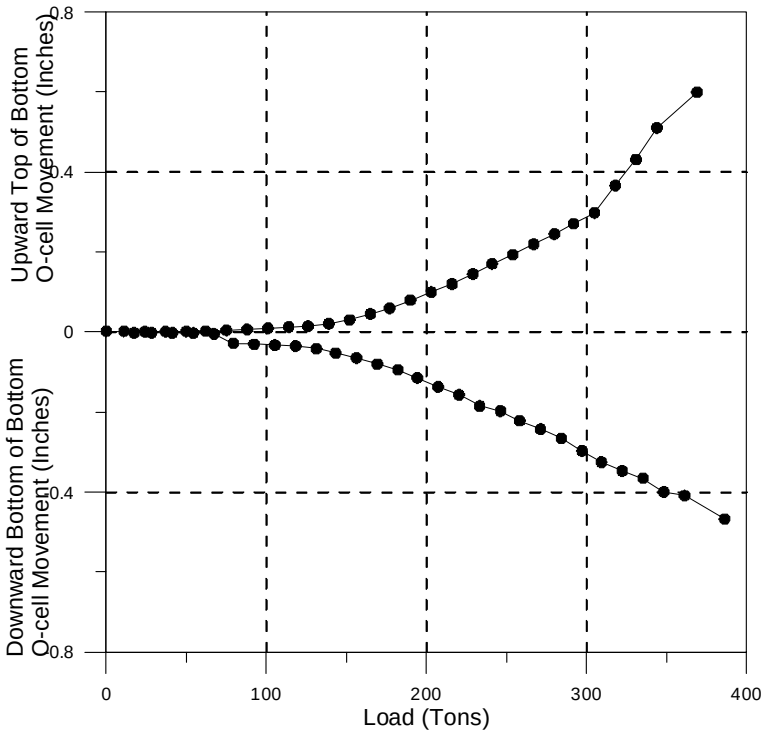

Figure 96
O-cell load settlement curve DS25

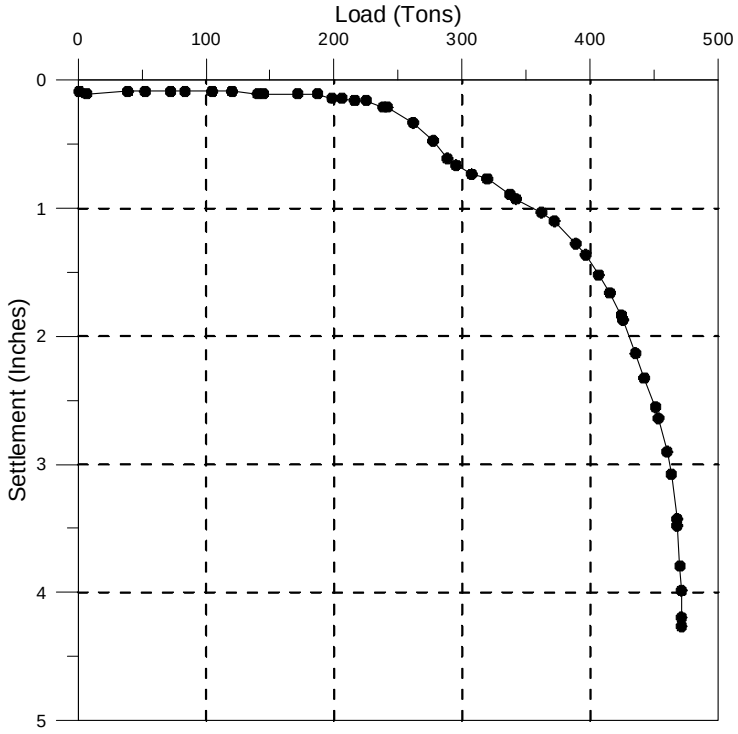

Figure 97
Equivalent top-down load settlement curve DS25

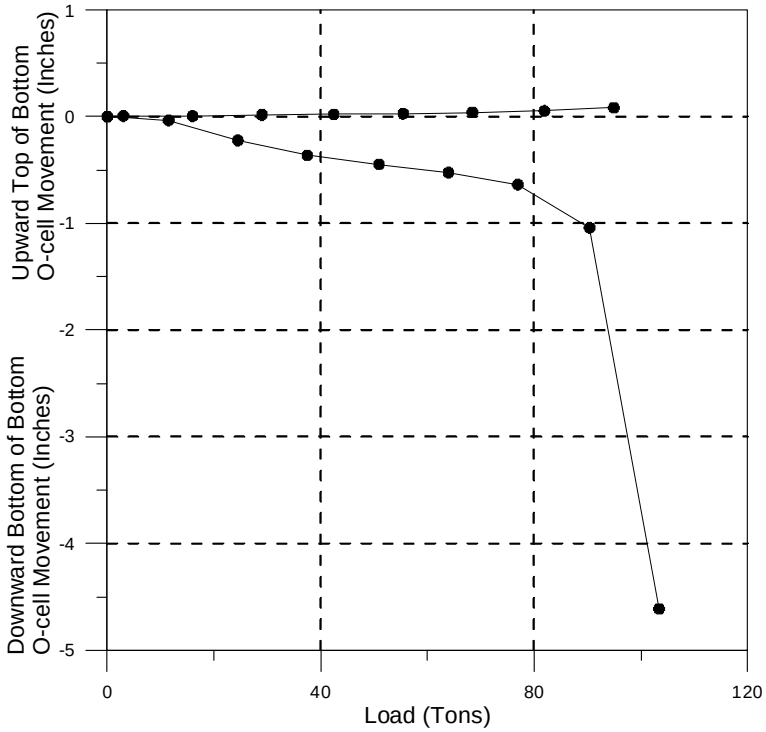

Figure 98
O-cell load settlement curve DS26

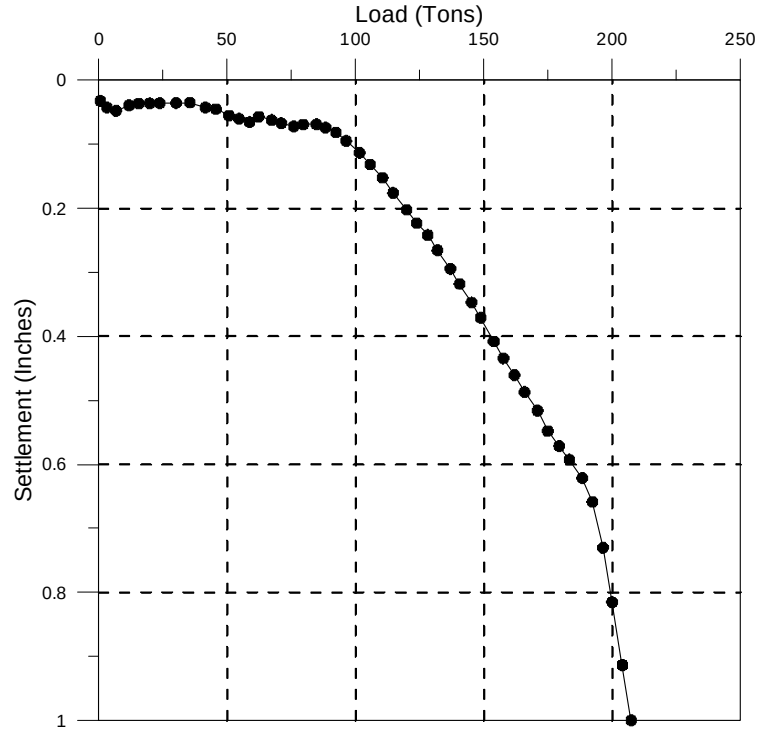

Figure 99
Equivalent top-down load settlement curve DS26